THE ROLE OF EXTRACELLULAR ADENOSINE IN REGULATION OF PARACELLULAR AND TRANSCELLULAR PERMEABILITY OF BLOOD BRAIN BARRIER

A Dissertation

Presented to the Faculty of the Graduate School

of Cornell University

In Partial Fulfillment of the Requirements for the Degree of

Doctor of Philosophy

by

Do-Geun Kim, D.V.M.

August 2015

THE ROLE OF EXTRACELLULAR ADENOSINE IN REGULATION OF PARACELLULAR AND TRANSCELLULAR PERMEABILITY OF BLOOD BRAIN BARRIER

Do-Geun Kim D.V.M. , Ph. D.

Cornell University 2015

The brain is the center of cognitive function and also regulates the physiology of the body. Due to its importance, it requires special vascular structure which separates itself from the peripheral circulation to maintain its electrical physiology and protect from insult from circulation. The vasculature of the brain is lined with a single layer of endothelial cells which is sealed with adherent and tight junction molecules. The endothelial cell lining is further insulated with pericytes and astrocytic endfeet. Also endothelial cells express varieties of transporters which selectively allow the entrance of molecules into the brain. This physicochemical vascular entity is called the blood brain barrier.

This structural barrier is, however, detrimental in the delivery of molecules to the brain. Many of drugs are dropped out from the pipelines because they cannot show the expected effect in the brain. To overcome this, many approaches were devised to increase the drug delivery to the brain, they were either invasive or ineffective.

In previous study, we have shown that adenosine receptor signaling can increase the permeability of large molecules to the brain. Adenosine receptor is the G-protein coupled receptor which is involved in numerous physiological reactions. Activation of

adenosine receptor showed potent and reversible increased permeability to the large molecules.

In this dissertation, we aimed to reveal if activation of adenosine receptor signaling can increase the permeability in the human primary brain endothelial cell monolayer. Indeed we observed robust and reversible permeability increase in human brain endothelial cells. This was mediated by increased Rho-GTPase activity and following stress fiber formation which subsequently disrupted the tight and adherens junctional molecules. Activation of AR also increased the permeability to chemotherapeutics Gemcitabine.

Also, we studied if adenosine receptor signaling can increase transcellular pathway which is mainly mediated by transporters highly expressed on the brain endothelial cells, especially P-glycoprotein. Indeed we observed that AR activation can increase the accumulation of the P-glycoprotein substrate in human primary brain endothelial cells by down regulating the expression and function of P-glycoprotein. Also, we could observe that it down-regulates the P-glycoprotein and thereby increase the accumulation of epirubicin, a P-glycoprotein substrate, in the brain of the mouse.

Collectively, we showed that AR activation can increase the permeability paracellular permeability of the human primary brain endothelial cells and also down regulate the P-glycoprotein function and enhance the transcellular permeability. These dual mechanism of regulating the permeability of the blood brain barrier might be beneficial in drug delivery in the brain which will benefit millions of patients suffering from the neurodegenerative disease or brain cancers.

BIOGRAPHICAL SKETCH

Do-Geun Kim was born in 1981 in Kyeonggi province, S. Korea which is suburban area of Seoul which is the capital of S. Korea to parents who were both elementary school teacher. He was so much interested in reading books and questioning everything around him which made his parents afraid of getting questions from him. He entered college of veterinary medicine in Konkuk University and was exposed and fascinated with the beauty of biology including genetics, physiology, and pharmacology. Nearing at the verge of graduation, he was debating whether he should pursue his career as a clinical veterinarian or researcher because he realized he loved doing research and asking more fundamental questions which will inevitably benefit larger number of people rather than making the animals and their owners happy. However, he realized the importance of broad experiences in pursuing biomedical research as his career. He was working as a clinical veterinarian in clinics, researcher in toxicology institute which became profound basis for his research while he was a Ph.D. student.

When he was college student, he constantly had curiosity in brain immunology and how molecules are delivered to the brain which he wanted to reveal the secret behind of those questions. Finally, he found Dr. Margaret Bynoe in College of Veterinary Medicine, Cornell University who was working on the fields of his interest as a pioneer. He decided to join her lab and put himself in the long journey of research to solve his long-time curiosity which possibly benefit millions of people suffering from brain diseases as he has always wished.

DEDICATION

Eunhye who is my dedicated wife and also the best friend in my life.

Ryan my lovely one and another me.

Father and mother who always believe in and support me in any circumstances.

Finally, my mentor Margaret. I will not forget every single word that you advised me.

I will love you all till the end of the world.

ACKNOWLEDGMENTS

First of all, I remember the saying from Deeqa who was a previous graduate student from our lab. "Once you blink your eyes, you are at the verge of graduation." Now I can understand what it meant. Time flew and now I am graduating. This makes me feel how little time I have in revealing truth behind of biological phenomena in my career as scientist and makes me humble.

There were so many people around me in the course of graduate program and this page is not long enough to list all of them. But I would like to thank to some special people in my graduate school life.

Margaret. You are the best and such a understanding mentor and a unbelievable philosopher. Your such encouraging comments and passions made me move forward and push the boundaries instead of staying where I feel comfortable and being satisfied with what I am doing. This made me see the real endeavor behind the discovery and findings and understand the reality of the science. Above all, I learned how to think and how to see as a scientist. I learned how to see the data critically and analyze them and see the unseen. This may have not been possible without your time commitment and such a caring guidance. Wherever I go, I can tell people for sure that everything that I know is coming from you. I respect you from the deepest bottom of myself.

Drs. August and Clark. I remember the sharp questions and clear guidances which were breakthrough for my research. Without that, I am sure that I would not be near at graduation. I learned how to look at my data more critically and objectively

which is always required as a good scientist.

Bynoe lab members, Jeff, Leah, Deeqa, Antje. You were always great friends and helpful. We shared the ups and downs in the course of graduate school. I could reach you all whenever I needed and shared all the emotional turmoil that we had. Wherever go, I would not be able to find such great lab mates.

Sudie. You are the best technician ever I met. I spent my last two years with you and that period was such a fruitful period due to your endless help and support. You were a great friend and scientific colleague. I hope the prosperity in your future.

Leon. You were always cheerful and friendly that made us always smile. You were always there when I ever I needed which was such a great help. Wish the best luck for your next move.

TABLE OF CONTENTS

LIST OF FIGURES

CHAPTER 1

CHAPTER 2

CHAPTER 3

APPENDICES

APPENDIX 1.

APPENDIX 2.

LIST OF TABLES

APPENDICES

APPENDIX 1.

APPENDIX 2.

Chapter 1

Introduction

The blood brain barrier (BBB).

BBB structure and function

The brain is the most highly vascularized organ in the body [1-2]. It is believed that if all the blood vessels and capillaries in the brain were attached, they would extend over 400 miles [1]. The immense vasculature of the brain is protected by the blood brain barrier (BBB), which is a tremendously tight-knit layer of endothelial cells that line the central nervous system and form the lumen of the brain microvasculature [1-3]. The BBB serves to ensure that the environment of the brain is constantly controlled [4]. Specifically, it works to maintain the brain's homeostatic environment, which is essential not only for the health of the brain, but for proper body functioning,[5-6]. The BBB carries out its function by disallowing the entry of toxins and preventing fluctuations in brain chemistry [7-8].

History of the BBB

The existence of the BBB was conceptually suggested by Dr. Paul Ehrlich in the 1880s [9]. When he injected a water soluble aniline dye into mice, he observed that no staining occurred in the brain [9]. At first, he thought that it might be attributed to the incapability of the dye to stain the brain. However, Dr. Edwin Goldmann, who was his assistant, showed that direct injection of the dye into the cerebro-spinal fluid induced the staining of the brain while other organs were not stained. This proved compartmentalization of the brain by the existence of some barrier structure separating peripheral blood circulation and the brain [10-11]. The term *blood brain barrier* was

first proposed by Lewandowsky as a symbolic term, since no such barrier structure could be visualized at the time due to technical limitations [12]. It wasn't until the 1960s that the actual structure of the BBB was observed, when scanning electro-microscopic techniques were developed. In 1967, Karnovsky showed that the endothelium of the mouse brain didn't allow the penetration of horse radish peroxidase (HRP) across the brain parenchyma [13]. A following seminal study by Reese and Karnovsky demonstrated for the first time that the mouse cerebral endothelium was the structural barrier to HRP. The barrier was composed of a plasma membrane of tightly-joined endothelial cells, forming what is called the zonula occludensa. Unlike the endothelium from peripheral organs, the cerebral endothelium had limited numbers of vesicles, indicating a reduced transport system [14]. Later studies using electro-microscopic analysis and immunohistochemical assay have revealed that the BBB is a multi-cellular complex comprising an endothelial monolayer, a pericyte, and astrocytic endfeet, all of which create tremendous resistance against molecular or cellular influx into the brain parenchyma [15].

The Neurovascular Unit

Endothelial cells, astrocytes, pericytes, microglial cells, neuronal cells, and the basement membrane work together to maintain proper BBB and brain function, and in total are referred to as the neurovascular unit (NVU) [7-8, 16] (Fig 1.1. A and B). In addition, transporters expressed on brain endothelial cells selectively regulate the influx of key molecules necessary for proper brain function, imposing additional restrictions on permeability [5-6, 17] (Fig 1.1. A). Although the BBB serves a

protective role, it also thwarts effective treatment of central nervous system (CNS) diseases by hindering the entry of therapeutic compounds into the brain [18]. For decades, researchers have focused on uncovering ways to manipulate the BBB to allow the entry of therapeutic drugs into the CNS [19]. Determining how to safely and effectively do this would have a major scientific and public health impact, affecting the treatment of a broad variety of neurological diseases, ranging from Alzheimer's disease to brain tumors [4, 6, 17, 20]. Promising therapies are available (or will become available) to treat many of these disorders; however, the efficacy of such therapies cannot be fully realized due to the tremendous hurdle posed by the BBB [21-22].

The BBB endothelium

Endothelial cells in brain capillaries are unique for their high resistance and expression of transporters, which are required to maintain the brain's physiology. The gaps of vascular endothelium in the brain are sealed with adherens and tight junction molecules that increase physical resistance, whereas other organs have fenestrations that facilitate delivery of molecules to the parenchyma [4, 7, 23]. Tightly-joined molecules are critically important to block the entry of toxic or unwanted substances into the brain. In brain vascular endothelial cells, transporters are highly expressed and selectively allow the entry of nutrients or ions [5-6]. Drug transporters such as P-glycoprotein are also highly expressed in brain vascular endothelial cells and block the entry of xenobiotics [17, 24].

A

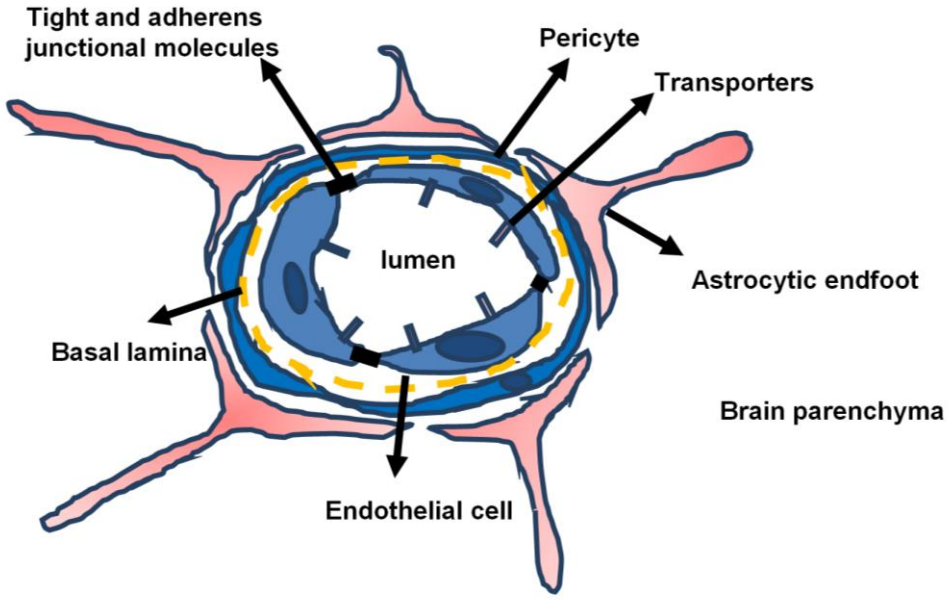
Tight and adherens junctional molecules
Pericyte
Transporters
lumen
Astrocytic endfoot
Basal lamina
Brain parenchyma
Endothelial cell

B

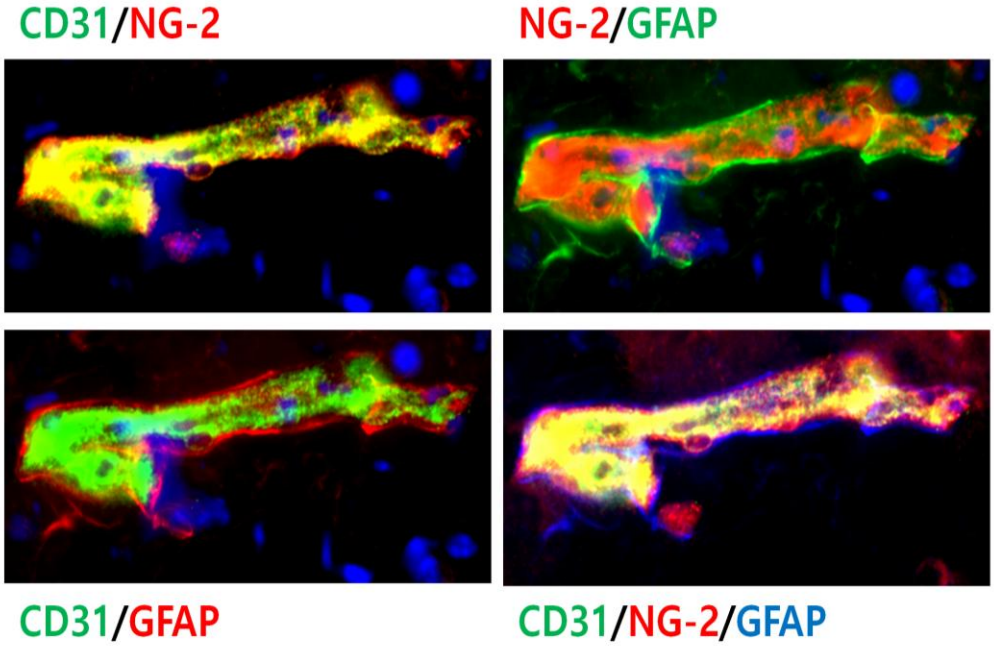
CD31/NG-2
NG-2/GFAP
CD31/GFAP
CD31/NG-2/GFAP

Figure 1.1. Structure of the BBB. (A) Schematic drawing of the BBB. The BBB consists of a single layer of endothelial cells sealed with tight junction and adherens molecules. Added to this monolayer of endothelial cells are pericytes and astrocytic endfeet, which further increase the resistance. Transporters are highly expressed on the endothelial cells and selectively allow the entry of nutrients or molecules into the brain. (B) Structure of the BBB was visualized using immunofluorescence assay. Endothelial cells, pericytes, and astrocytes were stained with CD31 (Green), NG2 (Red), GFAP (Blue), respectively.

Tight and adherens junctions

Resistance of the brain's endothelial monolayer is enhanced by tight junction molecules that seal the gaps between cell-to-cell junctions. Brain endothelial cells are well known to express a variety of tight junction molecules including Occludin 1 and 5, Claudin 1-5, and junctional adhesion molecules A-C (JAM-A-C)[25-27]. These molecules are tightly linked to F-actin by adaptor molecules such as ZO-1 [27]. As the outward tension applied to cell-to-cell contact increases, the expression level and membrane localization of tight junction molecules also increases, thereby enhancing the resistance of the brain's endothelial monolayer [27]. Along with tight junction molecules, adherens junction molecules represented by VE-Cadherin increase the cell-to-cell adherence, contributing to the increased resistance of the BBB [28]. When these molecules are knocked down by small interference RNA (siRNA), the permeability of the endothelial monolayer dramatically increases, indicating their importance in maintaining the impermeability of the brain's endothelial monolayer [29].

Basement membrane

Along with the cell component, the basement membrane also plays a critical role in the functioning of the BBB [8, 30]. The membrane fills the gaps between the endothelial cells and the astrocytic endfeet, forming a sheet-like structure and maintaining the integrity of the vasculature [30-31]. The basement membrane consists of structural elements (Collagen), specialized proteins (laminin, fibronenctin), and proteoglycans (heparan sulfate). The BBB actually consists of two basement

membranes, which are a vascular basement membrane and a parenchymal basement membrane. The parenchymal basement membrane covers the perivascular space and serves as the barrier for leuokocyte migration into the brain parenchyma. This results in the formation of perivascular cuffing [30, 32]. For several reasons, the basement membrane is critical to maintaining BBB permeability. First, it allows the proper positioning of the cell component, including endothelial cells and astrocytes. Second, it anchors the cells, thereby increasing the physical integrity of the barrier. Lastly, it regulates cellular processes and signaling between different cell types through interactions with integrin and other extracellular matrix receptors [30-31].

Transporters and carriers

Tight and selective regulation of the influx and efflux of molecules is essential for maintaining the brain's physiology and is mainly mediated by transporters highly expressed in the brain's endothelial cells. For example, Glut 1, a glucose transporter, maintains the glucose level of the brain by selectively allowing influx or efflux based on the need for glucose in the brain [5]. Drug transporters that block the entry of potentially harmful xenobiotics are also highly expressed in the brain's endothelial cells. Among these drug transporters are multi drug resistance (MDR) genes like P-glycoprotein (P-gp), which blocks the entrance of therapeutic agents into the brain [24, 33-36]. This protein was previously found on the surface of cancer cells that were resistant to chemotherapeutic agents and was thought to block the entry of drugs into cells [37-38]. P-gp consists of a non-specific drug binding domain, an ATPase domain, and 12 trans-membrane domains [39]. Its drug binding

pocket is large enough to attach to many types of substrates, including chemotherapeutic and anti-inflammatory agents [40]. When a drug attaches to a drug binding pocket, it utilizes ATP as its energy source to induce conformational changes that work to pump out the drug [40]. Mice lacking P-gp dramatically increase substrate accumulation in their brain compared to wild type [41-42]. This shows the importance of P-gp in the regulation of BBB permeability to the entry of drugs. Moreover, the influx of substrates into the brain increases when P-gp is pharmacologically inhibited [34, 36]. Because of the lack of specificity of its binding domain, it can hinder the entry of many promising drugs, including chemotherapeutic agents and drugs that can aid neurodegenerative disease [39, 43].

Paracellular and transcellular pathway of the BBB

The brain tightly regulates the entry of cells and molecules through the highly sophisticated machinery of the BBB [6, 44]. The mode of entry of substances into the brain is largely divided into paracellular and transcellular pathways [45]. In para-cellular transport, cells or molecules must move through the extremely small gaps between adjacent brain endothelial cells [3-4]. These gaps are normally sealed by tight and adherens junction molecules that hinder the influx of substances into the brain [3, 14]. A study performed using an *in vitro* model of the brain endothelial monolayer showed that the permeability coefficient of this monolayer is very low even to extremely small molecules[46]. This property is essential to protect the brain from insults from the blood circulation. In the trans-cellular pathway, cells or molecules directly pass through endothelial cells to enter the brain [17, 45, 47]. Most of the trans-

cellular pathway is mediated by active or passive transporters localized in the brain's endothelial layer, which regulates the selective influx of molecules into the brain. Some of these transporters selectively block the entry of xenobiotics into the brain, like P-glycoprotein [2, 17]. As these two major routes of entry are highly resistant to molecules, many approaches to increase BBB permeability aim to either increase gap junction space or downregulate the function of drug transporters.

Rho GTPases as the master regulator for paracellular permeability

Cells maintain their rigidity and morphology by their cytoskeletal molecules [48-49]. Morphological changes in cells are followed by the reorganization of filamentous actin [50-51]. Actins can be largely divided into cortical actin and stress fibers [51]. Cortical actin is localized on the cell membrane and maintains the shape and rigidity of cells [51]. Cortical actin induces the expansion of cell-to-cell contact, thereby increasing the resistance of the cell monolayer [51-52]. On the contrary, stress fibers create centripetal traction, inducing tension toward the center of the cell and thereby decreasing the cell-to-cell contact [53-54]. This decrease in cell-to-cell contact results in an increase in gaps between adjacent endothelial cells, thus increasing permeability [53].

Rho-GTPase is considered the master regulator of the actin-cytoskeleton [48]. It is a well-known small G-protein that regulates morphology, cell fate, and cell polarity[52]. Rho-GTPase is activated by the guanine exchange factor (GEF), which converts Rho-GDP into the GTP bound form, or the active form [48, 50]. Activation of GEF is mediated by changes in the second messenger signal, which is mainly

regulated by G-protein coupled receptor (GPCR) signaling [55]. It is well established that cell morphology is mediated by the Rho-GTPase dependent pathway, induced by the treatment of GPCR agonists or antagonists [55]. Activated Rho-GTPase triggers the Rho-GTPase associated kinase (ROCK) by attaching to the Rho binding domain (RBD), which helps the release of the coiled region of ROCK-1 [50]. Thereafter, ROCK-1 activation induces a downstream effector function, resulting in the modulation of filamentous actin formation and myosin light chain stabilization, resulting in changes in cell morphology (Fig 1.2. A) [50, 52]. Increased filamentous actin formation creates centripetal forces that stretch cells inwardly, boosting the permeability of the cell monolayer. ROCK-1 activation further stimulates the Ezrin-Radixin-Moesin (ERM) complex, which anchors actin on the cell membrane and enhances focal adhesion (Fig 1.2. B) [56-57]. Overall, an increase in the activity of Rho-GTPase disrupts the barrier by increasing stress fiber formation and disrupting tight junction molecules (Fig 1.2. C).

Current approaches for breaching the BBB

Traditionally, the brain has been considered a privileged organ that does not allow the entry of molecules or cells from the periphery by the BBB, thus impeding the development of drugs for CNS diseases.

A

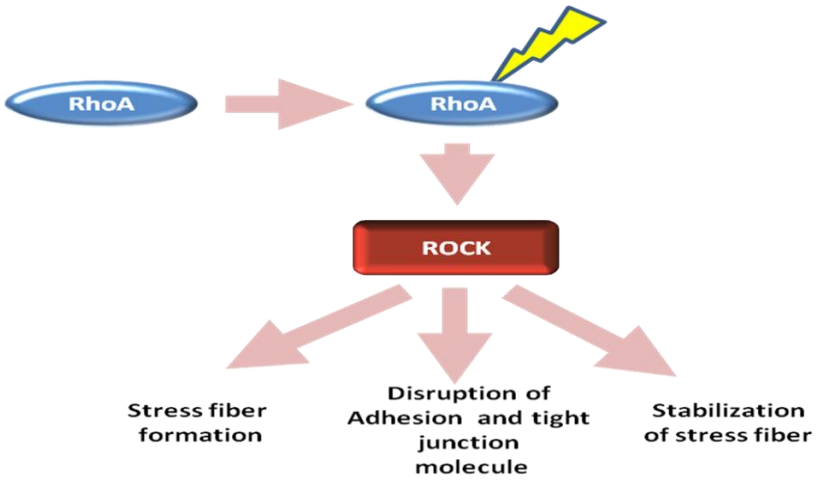
RhoA
RhoA
ROCK
Stress fiber formation
Disruption of Adhesion and tight junction molecule
Stabilization of stress fiber

B

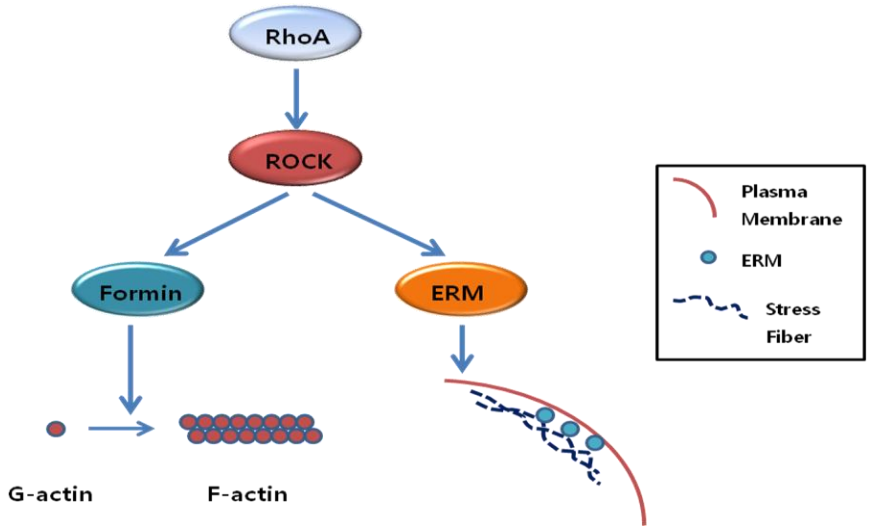
RhoA
ROCK
Formin
ERM
G-actin
F-actin
Plasma Membrane
ERM
Stress Fiber

C

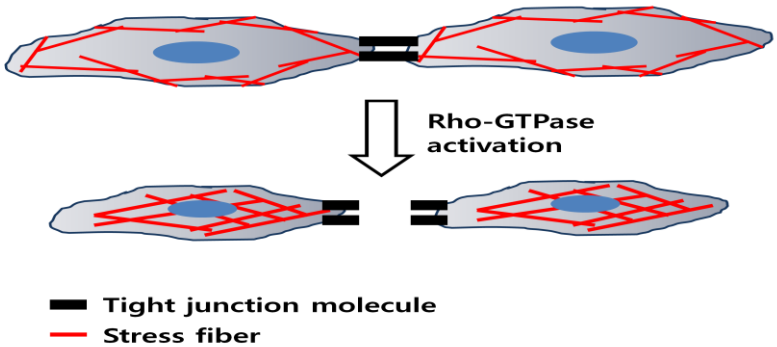
Rho-GTPase activation
Tight junction molecule
Stress fiber

Figure 1.2. Role of Rho-GTPase in disruption of endothelial barrier stability.

(A) Rho-GTPase activates Rho-GTPase associated kinase (ROCK), which induces both the formation and stabilization of stress fibers and the disruption of tight and adherens junction molecules. (B) The Rho-GTPase pathway induces the activation of Formin, which is an enzyme involved in the formation of F-actin from G-actin. This pathway causes activation of ERM, which helps link stress fibers to the plasma membrane. (C) Overall, activation of Rho-GTPase increases the formation of stress fibers, inducing centripetal forces and followed by shrinkage of cells. Also, it disrupts the tight junction molecules, which increases the permeability of the endothelial barrier.

However, there have been several attempts to manipulate BBB permeability in order to increase drug delivery to the brain. Nutwell *et al.* used a method for changing osmotic pressure in order to increase BBB permeability, but the clinical trial study showed disappointing results. [58-59]. Some groups have used direct intra-cerebral injections to increase drug delivery, but this approach is invasive and sometimes life-threatening [18, 47]. Similarly, focal ultrasound application has been attempted, but this method has also had limited success due to its invasiveness [60]. In addition, researchers have used hybrid antibodies that utilize receptor mediated transcytosis to increase drug delivery [19, 61]. Although this approach was shown to be successful in preclinical studies using primates, the efficiency was not optimal [61]. Recently, Carman *et al.* demonstrated that the A2A adenosine receptor mediated an increase in BBB permeability and enhanced the delivery of large molecules to the brain [20]. This method was shown to be very potent, reversible, and safe, and stands the possibility of being a promising alternative to current approaches to brain drug delivery.

Adenosine receptor signaling in the regulation of BBB permeability.

Adenosine, a signaling molecule.

Adenosine is a primordial molecule classified as purine. It is found in all life forms and is best known as the component of deoxyribonucleic acid (DNA) that carries genetic information. Due to its abundance and major function as a carrier of genetic material, its other biological roles, especially as signaling molecules, are easily

ignored. However, extracellular adenosine is indeed an important signaling molecule. Seminal studies by Drury and Gyorgi, which showed that *i.v.* injections of heart extract into rabbits slowed the heartbeat, found that the compound which induced the slowing of the heartbeat was adenosine [62]. It was the first evidence that adenosine is indeed the signaling molecule. Extracellular adenosine is mainly created by conversion of ATP into adenosine by Ecto-Apyrase (CD39) and 5'-ecto-nucleotidase (CD73) [63-65]. The conversion of ATP to adenosine is very rapid (1 ms). The concentration of extracellular adenosine is maintained at an extremely low range (25-250 nM), whereas the intracellular adenosine concentration is much higher [63-64]. However, in pathophysiological circumstances, its concentration increases up to 100 fold [66-67]. Because of rapid metabolism of extracellular adenosine, adenosine preferentially acts as a local signaling molecule rather than a systemic signaling molecule [67].

Adenosine Receptors

Extracellular adenosine exerts its action through the adenosine receptor (AR), which is a G-protein coupled receptor (GPCR) super-family [63, 67]. There are four different subtypes of adenosine receptors, including A1, A2A, A2B, and A3 [67-68]. A1 and A3 ARs are inhibitory, suppressing adenyl-cyclase and producing cAMP, while A2A and A2B ARs are stimulatory, activating cAMP [63-64]. Also, A1 and A2A have a high affinity to adenosine, whereas A2B and A3 have an extremely low affinity to adenosine [69]. This suggests that A1 and A2A are the major ARs activated at the physiological levels of extracellular adenosine [68].

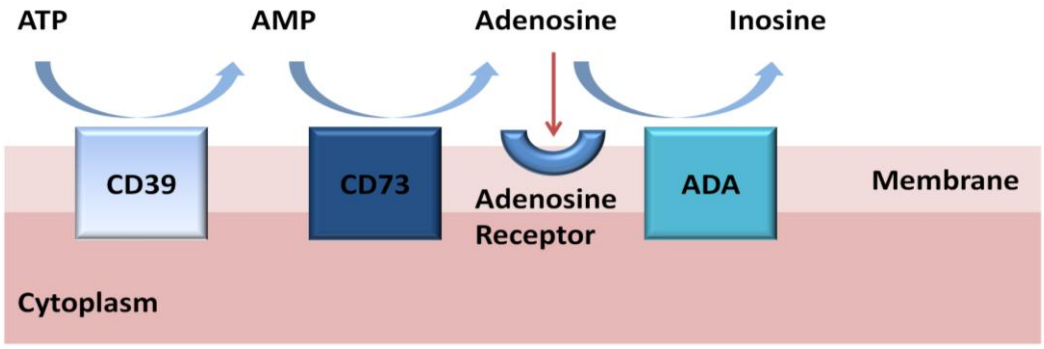

Figure 1.3. Cascade of enzymatic activity to create extracellular adenosine.

Extracellular ATP is converted into AMP by Ecto-apyrase (CD39), which is then converted into adenosine by 5'-Ecto-nucleotidase (CD73). Created adenosine is rapidly converted into inosine by the action of the adenosine deaminase (ADA).

The subtypes and expression levels of these receptors vary depending on the types of organs utilized in the development of organ specific drugs.[70-71]

Role of adenosine receptor signaling in maintaining general physiology of the body

Adenosine receptor signaling is the major signaling cascade required to maintain the physiological functioning of the body [71]. Notably, it has important roles in regulating cardiac pace, vascular permeability, immune response, metabolism, and neuronal conductance (Fig 1.4.) [64, 70, 72-75]. ARs are highly expressed in the cardiac muscles and vessels and are an excellent treatment target for abnormal heart rhythm [71]. Activation of A1 AR slows the heart rhythm and blood pressure, whereas A2A AR activation induces vasodilation in the aorta and coronary artery [71]. Also, activation of A2B AR induces vasodilation in many vessels, including the pulmonary artery, but causes vasoconstriction in other vessels, such as the chorionic artery [70]. Adenosine also regulates bronchoconstriction in the lung, which is the major symptom of asthma. A2B AR is closely related to hypoxia-induced endothelial permeability [71]. Activation of A2B AR induces bronchoconstriction and is related to the degranulation of mast cells, a major player in the development of asthma [69]. However, blockade of A2B AR alleviates asthma in animal models. Recent studies have shown that activation of A2A AR can delay asthma progression by dampening the immune response [71]. In a disease like type 2 diabetes, activation of A1 AR lowers the concentration of plasma-free fatty acids that control lipolysis. Blockade of A2B AR induces hypoglycemic activity in a type 2 diabetes animal model, suggesting a role in the glucose production of hepatocytes.

In many diseases, uncontrolled immune responses are the major drivers aggravating the severity of the pathology. Therefore, tight regulation of the immune response to minimize unwanted damage to host tissues is highly evolved. A2A AR receptor expression level is highest in the spleen and lymph-nodes, suggesting the receptor's possible role as immune regulator. Recent evidence of the role of adenosine as a major controller of host immunity came from the phenomenal study by Ohta, which demonstrated the importance of adenosine as master regulator of immune responses [67, 76]. The authors showed that liver pathology and proinflammatory cytokine production was increased in A2A AR deficient mice treated with endotoxin, demonstrating the importance of A2A AR signaling as the regulator for immune responses [76]. It is generally believed that AR signaling can downregulate the immune response through blocking neutrophil and macrophage activation, T cell differentiation and proliferation, and pro-inflammatory cytokines [69, 77-79]. Also, A2B activation decreases IL-6 and histamine production [69, 77].

Role of adenosine receptor signaling in the central nervous system.

Recent studies have shown that AR signaling is a major regulator of neuronal stimulation. Caffeine is a classic AR antagonist that enhances awareness and learning [80-81]. Studies have revealed that A1 AR is involved in the discriminative-stimulus effect of caffeine. A2A AR was shown to play

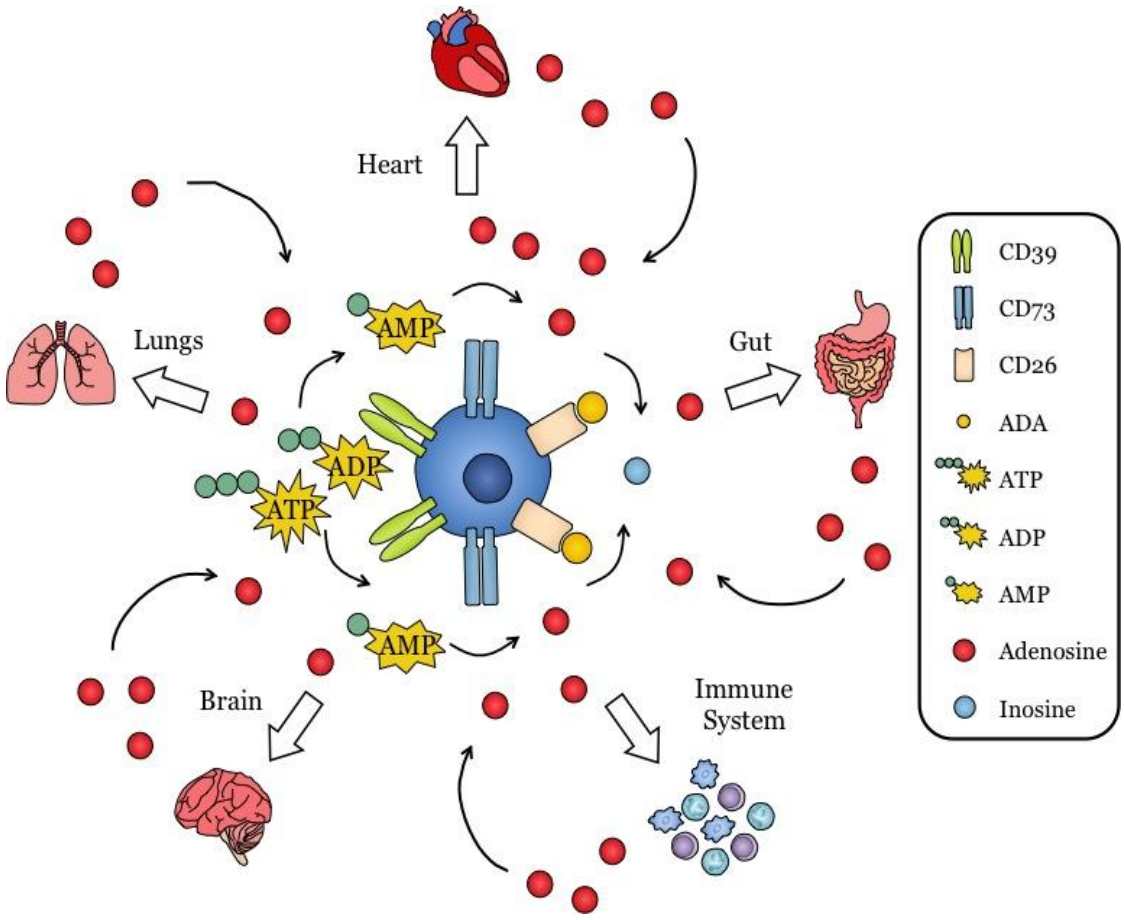

Figure 1.4. The role of adenosine receptor signaling in general physiology of the body. Adenosine receptor signaling is involved in regulation of cardiac pace, intestinal motility, the lung, neurotransmission, and immune responses.

a major role in the stimulatory effects of caffeine, mainly arousal. Later studies have shown that ARs play a significant role in controlling neurotransmission and cognitive functions. Still other studies demonstrate that A1 AR is involved in anxiety, pain, and sleep regulation. A2A AR interacts with dopamine D2 receptors (D2Rs) in striatum, which are mutually antagonistic. More specifically, when A2A AR is co-expressed with D2R in cell lines and exposed for long periods of time with the agonist of each receptor, they form heteromeric complexes, co-aggregate, and internalize.. This observation is closely related to Parkinson's disease (PD), which develops its symptoms when dopamine production declines, suggesting that constant activation of A2A AR may lead to neuronal degeneration. Also, large cohort studies have shown that high consumption of caffeine is inversely related to PD development, suggesting that antagonism of A2A AR decreases the clinical symptoms of PD. Finally, A2A AR plays a clear role in depression, whereby the blockage of this receptor induces the anti-depressant effect.

The history of adenosine role in BBB function

The initial findings that led to our current hypothesis that adenosine signaling regulates BBB function originated from work done by previous members of our lab showing that adenosine receptor signaling regulates lymphocyte migration into the CNS [82]. These previous findings showed that adenosine generated by CD73 expressed on either the infiltrating lymphocytes or on the choroid plexus epithelium is necessary for efficient lymphocyte migration into the CNS and EAE development [82]. CD73-generated extracellular adenosine signaling regulates lymphocyte migration into

the CNS by regulating adhesion molecule expression and chemokine secretion at the choroid plexus. We induced EAE in mice lacking CD73 ($CD73^{-/-}$) that are unable to synthesize extracellular adenosine. We anticipated an exacerbated immune response and hence more severe EAE. We instead found that $CD73^{-/-}$ mice were resistant to EAE [82], and analysis of CNS tissue demonstrated that there were very few T cells in the brains of $CD73^{-/-}$ mice immunized for EAE [82]. However, we could induce severe EAE when $CD4^{+}$ T cells from $CD73^{-/-}$ mice were transferred into C57BL/6-$TCR^{-/-}$ mice that lack endogenous T cells [82]. Although $CD4^{+}$ T cells from $CD73^{-/-}$ mice secrete more proinflammatory cytokines (IL-17, IL-1beta) than wild type mice, they were still unable to gain entry into the CNS [82]. These results suggest that adenosine's role in immune cell migration into the CNS is independent of its role in suppressing inflammation.

Adenosine function is mediated by its receptors expressed on a variety of cells, including immune cells and CNS resident cells[70, 74]. For adenosine to be bioactive, adenosine-generating enzymes and adenosine receptors must be present on the same cell or adjacent cells due to their short half-life [64, 83-84]. We investigated where in the CNS CD73 is expressed. Compared to other regions in the CNS, CD73 was most abundantly and constitutively expressed on choroid plexus ependymal cells[82]. We also found that two of the four ARs, A1 and A2A, are also expressed on choroid plexus cells [82]. Similar to CD73, the A2A AR is constitutively and abundantly expressed on choroid plexus ependymal cells [82]. We next investigated which adenosine receptor is responsible for mediating immune cell infiltration into the CNS by treating WT mice with A1 and A2A AR antagonists. Only A2A AR antagonism

blocked immune cell entry into the CNS and completely inhibited EAE [82].

Cell migration requires a cascade of events, including a chemokine gradient and adhesion to the endothelium [45]. We analyzed brains of wild type and $CD73^{-/-}$ mice over the course of EAE to identify potential chemokines, adhesion molecules, or integrins that are important for both EAE development and cell migration and that may be controlled by extracellular adenosine signaling [85]. We observed that extracellular adenosine triggered lymphocyte migration into the CNS by inducing the expression of the specialized chemokine/adhesion molecule CX3CL1 at the choroid plexus, which is the blood to cerebral spinal fluid barrier and a prime entry point into the CNS for immune cells [85]. In wild type mice, CX3CL1 is upregulated in the brain on day 10 post EAE induction, which corresponds with initial CNS lymphocyte infiltration and the acute stage of EAE [85]. Conversely, $CD73^{-/-}$ mice that cannot synthesize extracellular adenosine do not upregulate CX3CL1 in the brain following EAE induction and are protected from EAE development and associated lymphocyte infiltration [85]. Additionally, blockade of the A2A AR following EAE induction prevents disease development and the induction of brain CX3CL1 expression [85]. Blockade of CX3CL1 completely inhibited EAE development and lymphocyte entry into the CNS. From these findings, we conclude that extracellular adenosine is an endogenous modulator of neuroinflammation during EAE that induces CX3CL1 at the choroid plexus to trigger lymphocyte entry into the CNS parenchyma [85]. Similar findings using a spinal cord injury model were recently reported by Shechter *et al.* showing that M2 macrophages involved in resolving inflammation express high levels

of CX3CL1R and CD73 and trafficked through the ventricular choroid plexus barrier [86].

The A2A AR is highly expressed on lymphocytes and is a prime mediator of adenosine's anti-inflammatory effects [87-88]. We next determined the importance of A2A AR signaling during neuroinflammatory disease progression in EAE [89]. As noted above, A2A AR antagonist treatment protected mice from disease development and associated CNS lymphocyte infiltration [82]. Interestingly, A2A $AR^{-/-}$ mice developed a more severe acute EAE phenotype characterized by more proinflammatory lymphocytes and activated microglia/macrophages [89]. To delineate the contribution of A2A AR signaling to lymphocyte entry into the CNS during EAE, we generated bone marrow chimeric mice to generate mixed chimeras between A2A $AR^{-/-}$ and WT mice [89]. Remarkably, A2A $AR^{-/-}$ donor hematopoietic cells (immune cells) potentiated severe EAE, whereas lack of A2A AR expression on non-hematopoietic cells protected against disease development[89]. These results indicate that A2A AR expression on non-immune cells (such as the CNS) is required for efficient lymphocyte passage into the CNS and EAE development, whereas A2A AR expression on lymphocytes is essential for limiting the severity of the inflammatory response.

We next investigated whether AR signaling permeabilizes the BBB to entry of drugs [20]. Treatment of mice with AR agonists, including the FDA-approved selective A2A AR agonist Lexiscan, significantly increased BBB permeability [20]. These changes in BBB permeability are dose-dependent and temporally discrete. Most importantly, treatment with specific A2A AR agonists or a broad-spectrum AR agonist

facilitated both the entry of intravenously administered anti-beta-amyloid antibody into the CNS and the binding of the antibody to beta-amyloid plaques in a transgenic mouse model of Alzheimer's disease (AD) [20]. These results further proved that modulation of AR signaling has the potential to deliver therapeutic compounds into the CNS or to block harmful substances from entering the CNS.

Outline of the dissertation

This dissertation is composed of four chapters. The first chapter explains the structure of the BBB and the recent advances in methods to increase the permeability of the BBB. We also discuss the findings on the role of adenosine receptor signaling in the regulation of the permeability of the BBB from our laboratory.

The second chapter addresses the finding that the adenosine receptor mediated an increase of paracellular permeability in human primary brain endothelial cells, mainly through the Rho-GTPase pathway. A2A AR signaling increased Rho-GTPase activity, which increased stress fiber formation and induced the disruption of tight and adherens junction molecules. We also observed that AR signaling can indeed increase permeability to chemotherapeutics, which potentially can be applied to human medicine.

The third chapter discusses the role of AR signaling in regulating the trans-cellular pathway of the BBB, which is mediated by transporters, especially P-glycoprotein. P-glycoprotein is a well-known drug transporter highly expressed in drug-resistant cancer cells and on brain endothelial cells. P-glycoprotein blocks the entry of xenobiotics into the brain and acts as a bottleneck for drug delivery to the brain. In this chapter, we showed that AR signaling can downregulate the expression level and functionality of P-glycoprotein and increase drug delivery through the trans-cellular pathway.

The fourth chapter summarizes the findings of the first two chapters and discusses both the pitfalls of its conclusions and the future direction of my studies.

Lastly, results of additional research not strictly related to the theme of the

thesis but completed during my Ph.D. degree will be discussed in appendices. These include: 1) The role of Itk in the disease progression of experimental allergic encephalitis (EAE) and 2) The effect of a high fat diet in the progression of an Alzheimer's disease model. Although these were not studies strictly related to the BBB, we found that differences in the capacity of CD4 T cells to migrate by genetic mutation have critical roles in the disease progression of EAE, and that a high fat diet disrupts the integrity of brain vasculature, possibly harming the health of the brain. This research has directly and indirectly enhanced my understanding of the BBB, helping me to develop the themes included in my dissertation.

References

1. Adamson, C., et al., *Glioblastoma multiforme: a review of where we have been and where we are going.* Expert Opin Investig Drugs, 2009. **18**(8): p. 1061-83.
2. Deeken, J.F. and W. Loscher, *The blood-brain barrier and cancer: transporters, treatment, and Trojan horses.* Clin Cancer Res, 2007. **13**(6): p. 1663-74.
3. Abbott, N.J., L. Ronnback, and E. Hansson, *Astrocyte-endothelial interactions at the blood-brain barrier.* Nat Rev Neurosci, 2006. **7**(1): p. 41-53.
4. Ballabh, P., A. Braun, and M. Nedergaard, *The blood-brain barrier: an overview: structure, regulation, and clinical implications.* Neurobiology of disease, 2004. **16**(1): p. 1-13.
5. Devraj, K., et al., *GLUT-1 glucose transporters in the blood-brain barrier: differential phosphorylation.* Journal of neuroscience research, 2011. **89**(12): p. 1913-25.
6. Daneman, R. and A. Prat, *The Blood-Brain Barrier.* Cold Spring Harb Perspect Biol, 2015. **7**(1).
7. Abbott, N.J., *Blood-brain barrier structure and function and the challenges for CNS drug delivery.* Journal of inherited metabolic disease, 2013. **36**(3): p. 437-49.
8. Abbott, N.J., *Astrocyte-endothelial interactions and blood-brain barrier permeability.* Journal of anatomy, 2002. **200**(6): p. 629-38.

9. Ehrlich, P., *Das Sauerstoff-Bedurfnis des Organismus: eine farbenanalytische Studie.* Berlin: Hirschward, 1885.

10. Goldmann, E., *Die aussere und innere sekretion des gesunden und kranken Organismus im Licht der vitalen Farburg.* Beitr Klin Chir, 1909. **64**: p. 192-265.

11. Goldmann, E., *Vitalfarbung am Zentralnervensystem: beitrag zur Physiopathologie des plexus chorioideus der Hirnhaute.* Abh Preuss Akad Wiss Physik-Math, 1913. **1**: p. 1-60.

12. Lewandowsky, M., *Zur Lehre der Zerebrospinalflussigkeit.* Z Klin Med 1900. **40**: p. 480-484.

13. Karnovsky, M., *The ultratructural basis of capillary permeability studied with perxidase as a tracer.* J Cell Biol, 1967. **35**: p. 213-236.

14. Reese, T. and M. Karnovsky, *Fine structural localization of a blood-brain barrier to exogenouse peroxidase.* J Cell Biol, 1967. **34**: p. 207-217.

15. Ribatti, D., et al., *Development of the blood-brain barrier: A historical point of view.* The Anatomical Record Part B: The New Anatomist, 2006. **289B**(1): p. 3-8.

16. Bergers, G. and S. Song, *The role of pericytes in blood-vessel formation and maintenance.* Neuro-oncology, 2005. **7**(4): p. 452-64.

17. Begley, D.J., *ABC transporters and the blood-brain barrier.* Current pharmaceutical design, 2004. **10**(12): p. 1295-312.

18. Hossain, S., T. Akaike, and E.H. Chowdhury, *Current approaches for drug delivery to central nervous system.* Curr Drug Deliv, 2010. **7**(5): p. 389-97.

19. Rajadhyaksha, M., et al., *Current Advances in Delivery of Biotherapeutics across the Blood-Brain Barrier.* Curr Drug Discov Technol, 2011. **8**(2): p. 87-101.

20. Carman, A.J., et al., *Adenosine receptor signaling modulates permeability of the blood-brain barrier.* J Neurosci, 2011. **31**(37): p. 13272-80.

21. Pardridge, W.M., *The blood-brain barrier: bottleneck in brain drug development.* NeuroRx : the journal of the American Society for Experimental NeuroTherapeutics, 2005. **2**(1): p. 3-14.

22. Pardridge, W.M., *Drug transport across the blood-brain barrier.* Journal of cerebral blood flow and metabolism : official journal of the International Society of Cerebral Blood Flow and Metabolism, 2012. **32**(11): p. 1959-72.

23. Luissint, A.C., et al., *Tight junctions at the blood brain barrier: physiological architecture and disease-associated dysregulation.* Fluids Barriers CNS, 2012. **9**(1): p. 23.

24. Abuznait, A.H. and A. Kaddoumi, *Role of ABC transporters in the pathogenesis of Alzheimer's disease.* ACS Chem Neurosci, 2012. **3**(11): p. 820-31.

25. Stevenson, B.R. and B.H. Keon, *The tight junction: morphology to molecules.* Annu Rev Cell Dev Biol, 1998. **14**: p. 89-109.

26. Fujibe, M., et al., *Thr203 of claudin-1, a putative phosphorylation site for MAP kinase, is required to promote the barrier function of tight junctions.* Exp Cell Res, 2004. **295**(1): p. 36-47.

27. Aijaz, S., M.S. Balda, and K. Matter, *Tight junctions: molecular architecture and function.* Int Rev Cytol, 2006. **248**: p. 261-98.

28. Hordijk, P.L., et al., *Vascular-endothelial-cadherin modulates endothelial monolayer permeability.* J Cell Sci, 1999. **112 (Pt 12)**: p. 1915-23.

29. Dejana, E., E. Tournier-Lasserve, and B.M. Weinstein, *The control of vascular integrity by endothelial cell junctions: molecular basis and pathological implications.* Dev Cell, 2009. **16**(2): p. 209-21.

30. Baeten, K.M. and K. Akassoglou, *Extracellular matrix and matrix receptors in blood–brain barrier formation and stroke.* Developmental Neurobiology, 2011. **71**(11): p. 1018-1039.

31. Hallmann, R., et al., *Expression and Function of Laminins in the Embryonic and Mature Vasculature*. Vol. 85. 2005. 979-1000.

32. Kastrup, A., et al., *Early Disruption of the Blood–Brain Barrier After Thrombolytic Therapy Predicts Hemorrhage in Patients With Acute Stroke.* Stroke, 2008. **39**(8): p. 2385-2387.

33. Beaulieu, E., et al., *P-glycoprotein is strongly expressed in the luminal membranes of the endothelium of blood vessels in the brain.* Biochem J, 1997. **326 (Pt 2)**: p. 539-44.

34. Kusuhara, H., et al., *P-Glycoprotein mediates the efflux of quinidine across the blood-brain barrier.* J Pharmacol Exp Ther, 1997. **283**(2): p. 574-80.

35. Begley, D.J., et al., *Functional expression of P-glycoprotein in an immortalised cell line of rat brain endothelial cells, RBE4.* J Neurochem, 1996. **67**(3): p. 988-95.

36. van Asperen, J., et al., *The functional role of P-glycoprotein in the blood-brain barrier.* J Pharm Sci, 1997. **86**(8): p. 881-4.

37. Klein, E.A., *The multidrug resistance gene in renal cell carcinoma.* Semin Urol, 1989. **7**(4): p. 207-14.

38. Trambas, C.M., H.K. Muller, and G.M. Woods, *P-glycoprotein mediated multidrug resistance and its implications for pathology.* Pathology, 1997. **29**(2): p. 122-30.

39. Aller, S.G., et al., *Structure of P-glycoprotein reveals a molecular basis for poly-specific drug binding.* Science, 2009. **323**(5922): p. 1718-22.

40. Ueda, K., Y. Taguchi, and M. Morishima, *How does P-glycoprotein recognize its substrates?* Semin Cancer Biol, 1997. **8**(3): p. 151-9.

41. Schinkel, A.H., et al., *Normal viability and altered pharmacokinetics in mice lacking mdr1-type (drug-transporting) P-glycoproteins.* Proc Natl Acad Sci U S A, 1997. **94**(8): p. 4028-33.

42. Schinkel, A.H., *The physiological function of drug-transporting P-glycoproteins.* Semin Cancer Biol, 1997. **8**(3): p. 161-70.

43. Scala, S., et al., *P-glycoprotein substrates and antagonists cluster into two distinct groups.* Mol Pharmacol, 1997. **51**(6): p. 1024-33.

44. Zlokovic, B.V., *The blood-brain barrier in health and chronic neurodegenerative disorders.* Neuron, 2008. **57**(2): p. 178-201.

45. Carman, C.V. and T.A. Springer, *Trans-cellular migration: cell-cell contacts get intimate.* Curr Opin Cell Biol, 2008. **20**(5): p. 533-40.

46. Rubin, L.L. and J.M. Staddon, *The cell biology of the blood-brain barrier.* Annu Rev Neurosci, 1999. **22**: p. 11-28.

47. Pardridge, W.M., *The blood-brain barrier: bottleneck in brain drug development.* NeuroRx, 2005. **2**(1): p. 3-14.

48. Wojciak-Stothard, B. and A.J. Ridley, *Rho GTPases and the regulation of endothelial permeability.* Vascul Pharmacol, 2002. **39**(4-5): p. 187-99.

49. Wojciak-Stothard, B., et al., *Rho and Rac but not Cdc42 regulate endothelial cell permeability.* Journal of cell science, 2001. **114**(Pt 7): p. 1343-55.

50. Riento, K. and A.J. Ridley, *Rocks: multifunctional kinases in cell behaviour.* Nat Rev Mol Cell Biol, 2003. **4**(6): p. 446-56.

51. Pollard, T.D. and J.A. Cooper, *Actin, a central player in cell shape and movement.* Science, 2009. **326**(5957): p. 1208-12.

52. Jaffe, A.B. and A. Hall, *Rho GTPases: biochemistry and biology.* Annu Rev Cell Dev Biol, 2005. **21**: p. 247-69.

53. Hirao, M., et al., *Regulation mechanism of ERM (ezrin/radixin/moesin) protein/plasma membrane association: possible involvement of phosphatidylinositol turnover and Rho-dependent signaling pathway.* J Cell Biol, 1996. **135**(1): p. 37-51.

54. Fehon, R.G., A.I. McClatchey, and A. Bretscher, *Organizing the cell cortex: the role of ERM proteins.* Nat Rev Mol Cell Biol, 2010. **11**(4): p. 276-87.

55. Rex, C.S., et al., *Different Rho GTPase-dependent signaling pathways initiate sequential steps in the consolidation of long-term potentiation.* J Cell Biol, 2009. **186**(1): p. 85-97.

56. Hall, A., *Rho GTPases and the actin cytoskeleton.* Science, 1998. **279**(5350): p. 509-14.

57. Bretscher, A., K. Edwards, and R.G. Fehon, *ERM proteins and merlin: integrators at the cell cortex.* Nat Rev Mol Cell Biol, 2002. **3**(8): p. 586-99.

58. Neuwelt, E.A., et al., *Osmotic blood-brain barrier modification: clinical documentation by enhanced CT scanning and/or radionuclide brain scanning.* AJR Am J Roentgenol, 1983. **141**(4): p. 829-35.

59. Neuwelt, E.A., et al., *Osmotic blood-brain barrier disruption. Computerized tomographic monitoring of chemotherapeutic agent delivery.* J Clin Invest, 1979. **64**(2): p. 684-8.

60. Bradley, W.G., Jr., *MR-guided focused ultrasound: a potentially disruptive technology.* J Am Coll Radiol, 2009. **6**(7): p. 510-3.

61. Yu, Y.J., et al., *Therapeutic bispecific antibodies cross the blood-brain barrier in nonhuman primates.* Science translational medicine, 2014. **6**(261): p. 261ra154.

62. Drury, A. and A. Szent-Gyorgi, *The pyhsiological activity of adenine compounds with especial reference to their action upon the mammalian heart.* 1929. **9**: p. 214-237.

63. Fredholm, B.B., et al., *International Union of Pharmacology. XXV. Nomenclature and classification of adenosine receptors.* Pharmacol Rev, 2001. **53**(4): p. 527-52.

64. Fredholm, B.B., et al., *International Union of Basic and Clinical Pharmacology. LXXXI. Nomenclature and classification of adenosine receptors--an update.* Pharmacol Rev, 2011. **63**(1): p. 1-34.

65. Yegutkin, G.G., *Nucleotide- and nucleoside-converting ectoenzymes: Important modulators of purinergic signalling cascade.* Biochim Biophys Acta, 2008. **1783**(5): p. 673-94.

66. Hasko, G., et al., *Adenosine receptor signaling in the brain immune system.* Trends in pharmacological sciences, 2005. **26**(10): p. 511-6.

67. Hasko, G., et al., *Adenosine receptors: therapeutic aspects for inflammatory and immune diseases.* Nat Rev Drug Discov, 2008. **7**(9): p. 759-70.

68. Fredholm, B.B., et al., *Structure and function of adenosine receptors and their genes.* Naunyn-Schmiedeberg's archives of pharmacology, 2000. **362**(4-5): p. 364-74.

69. Blackburn, M.R., et al., *Adenosine receptors and inflammation.* Handb Exp Pharmacol, 2009(193): p. 215-69.

70. Sheth, S., et al., *Adenosine receptors: expression, function and regulation.* International journal of molecular sciences, 2014. **15**(2): p. 2024-52.

71. Jacobson, K.A. and Z.G. Gao, *Adenosine receptors as therapeutic targets.* Nat Rev Drug Discov, 2006. **5**(3): p. 247-64.

72. Stone, T.W., S. Ceruti, and M.P. Abbracchio, *Adenosine receptors and neurological disease: neuroprotection and neurodegeneration.* Handb Exp Pharmacol, 2009(193): p. 535-87.

73. Linden, J., *Cell biology. Purinergic chemotaxis.* Science, 2006. **314**(5806): p. 1689-90.

74. Sebastiao, A.M. and J.A. Ribeiro, *Adenosine receptors and the central nervous system.* Handb Exp Pharmacol, 2009(193): p. 471-534.

75. Burnstock, G. and J.M. Boeynaems, *Purinergic signalling and immune cells.* Purinergic signalling, 2014. **10**(4): p. 529-64.

76. Ohta, A. and M. Sitkovsky, *Role of G-protein-coupled adenosine receptors in downregulation of inflammation and protection from tissue damage.* Nature, 2001. **414**(6866): p. 916-920.

77. Ernst, P.B., J.C. Garrison, and L.F. Thompson, *Much Ado about Adenosine: Adenosine Synthesis and Function in Regulatory T Cell Biology.* The Journal of Immunology, 2010. **185**(4): p. 1993-1998.

78. Takedachi, M., et al., *CD73-generated adenosine restricts lymphocyte migration into draining lymph nodes.* Journal of immunology, 2008. **180**(9): p. 6288-96.

79. Tsutsui, S., et al., *A1 adenosine receptor upregulation and activation attenuates neuroinflammation and demyelination in a model of multiple sclerosis.* The Journal of neuroscience : the official journal of the Society for Neuroscience, 2004. **24**(6): p. 1521-9.

80. Chen, X., et al., *Caffeine protects against MPTP-induced blood-brain barrier dysfunction in mouse striatum.* Journal of neurochemistry, 2008. **107**(4): p. 1147-57.

81. Stevens, B., et al., *Adenosine: a neuron-glial transmitter promoting myelination in the CNS in response to action potentials.* Neuron, 2002. **36**(5): p. 855-68.

82. Mills, J.H., et al., *CD73 is required for efficient entry of lymphocytes into the central nervous system during experimental autoimmune encephalomyelitis.* Proc Natl Acad Sci U S A, 2008. **105**(27): p. 9325-30.

83. Svenningsson, P., et al., *Distribution of adenosine receptors in the postmortem human brain: an extended autoradiographic study.* Synapse, 1997. **27**(4): p. 322-35.

84. Thompson, L.F., et al., *Regulation of leukocyte migration across endothelial barriers by ECTO-5'-nucleotidase-generated adenosine.* Nucleosides, nucleotides & nucleic acids, 2008. **27**(6): p. 755-60.

85. Mills, J.H., et al., *Extracellular adenosine signaling induces CX3CL1 expression in the brain to promote experimental autoimmune encephalomyelitis.* Journal of neuroinflammation, 2012. **9**: p. 193.

86. Shechter, R., et al., *Recruitment of Beneficial M2 Macrophages to Injured Spinal Cord Is Orchestrated by Remote Brain Choroid Plexus.* Immunity, 2013. **38**(3): p. 555-569.

87. Hasko, G. and P. Pacher, *A2A receptors in inflammation and injury: lessons learned from transgenic animals.* J Leukoc Biol, 2008. **83**(3): p. 447-55.

88. Csoka, B., et al., *Adenosine A2A receptor activation inhibits T helper 1 and T helper 2 cell development and effector function.* FASEB J, 2008. **22**(10): p. 3491-9.

89. Mills, J.H., et al., *A2A adenosine receptor signaling in lymphocytes and the central nervous system regulates inflammation during experimental autoimmune encephalomyelitis.* Journal of immunology, 2012. **188**(11): p. 5713-22.

Chapter 2

A2A adenosine receptor regulates the human blood brain barrier permeability*

*Originally published in Molecular Neurobiology

Kim *et al* Mol Neurobiol 2014 Sep 28. [Epub ahead of print]

2.1. Abstract:

The blood brain barrier (BBB) symbolically represents the gateway to the central nervous system. It is a single layer of specialized endothelial cells that coats the central nervous system (CNS) vasculature and physically separates the brain environment from the blood constituents, to maintain the homeostasis of the CNS. However, this protective measure is a hindrance to the delivery of therapeutics to treat neurological diseases. Here, we show that activation of A2A adenosine receptor (AR) with an FDA-approved agonist potently permeabilizes an in vitro primary human brain endothelial barrier (hBBB) to the passage of chemotherapeutic drugs and T cells. T cell migration under AR signaling occurs primarily by paracellular transendothelial route. Permeabilization of the hBBB is rapid, time-dependent and reversible and is mediated by morphological changes in actin-cytoskeletal reorganization induced by RhoA signaling and a potent down-regulation of Claudin-5 and VE-Cadherin. Moreover, the kinetics of BBB peing in mice closely overlaps with the permeability kinetics of the hBBB. These data suggest that activation of A2A AR is an endogenous mechanism that may be used for CNS drug delivery in human.

2.2. Introduction

The brain is the most vascularized organ in the body [1]. It is estimated that the brain has more than 100 billion capillaries [1]. If all the capillaries and blood vessels in the brain are strung together they will extend over 400 miles long [1]. The brain vasculature is lined by a single layer of endothelial cells that forms a tight barrier against unwanted substances from the blood circulation [2]. In addition, the gaps between adjacent endothelial cells are sealed with tight and adherens junction molecules to further increase the brain endothelial barrier resistance [1-2]. Extracellular matrix proteins, pericytes and astrocytic endfoot processes (referred to as the neurovascular unit), insulate the endothelial lining, making this structure impermeable even to very small molecules (less than 450 Da) and polar and ionic substances [1]. In addition, transporters expressed on brain endothelial cells selectively regulate the influx of key molecules necessary for proper brain function, and thus, imposes additional restrictions on permeability [1-4]. The characteristic physico-chemical entity of the brain-blood vasculature is called the blood brain barrier (BBB) [2, 5]. However, this inherent high-impermeability of the BBB impedes drug delivery to the brain that could treat myriad of neurodegenerative diseases such as brain cancers and multiple sclerosis [1]. There is a tremendous need to be able to modulate the permeability of the BBB to enhance the deliverability of therapeutics into the brain [6].

Adenosine is a purine nucleoside that mediates its function through its 7-transmembrane G-protein coupled receptors. Adenosine is produced both

extracellularly and intracellularly. Extracellular adenosine is produced from the conversion of extracellular adenosine triphosphate (ATP) into adenosine diphosphate (ADP) and adenosine monophosphate (AMP) by the extracellular enzyme CD39; and AMP is further converted to adenosine by the extracellular enzyme, CD73 [7-9]. Adenosine receptors (ARs) are of four different subtypes, A1, A2A, A2B and A3 [10]. ARs, and extracellular enzymes are expressed on brain endothelial cells in mice and human [11-12]. Previously, we have shown that blockade of CD73 or inhibition of the A2A AR signaling inhibits the migration of leukocytes into the central nervous system (CNS) [13]. Further, we showed that activation of ARs with a broad spectrum AR agonist increases BBB permeability and allow the entry of macro-molecules into the brain [11]. These studies strongly indicate that signaling via the ARs represents a *bone fide* pathway that controls the entry of cells and molecules into the CNS. Because extracellular adenosine mediates many of its functions around inflammation or injury [9], we hypothesize that signaling via adenosine receptors on BBB endothelial cells signals the recruitment of cells and/or molecules into the CNS to sites of damage or inflammation. Based on these studies we now focus our attention on determining how we can exploit adenosine modulation of BBB permeability to deliver drugs into the CNS to treat neurological diseases ranging from Alzheimer's to brain tumors. To do this we need to first determine whether AR signaling regulates human BBB permeability, and second, understand the mechanisms that regulate brain endothelial barrier permeability and determine where in the pathway AR signaling functions.

Recent studies demonstrated that AR activation regulates RhoA activity in various cell types mediated by second messenger signals including cyclic AMP [14].

RhoA is a small GTPase that is the master regulator of actin-cytoskeletal re-organization. The actin-cytoskeleton maintains the structure and morphology of cells [15]. Factors that modulate actin-cytoskeletal rearrangement have been shown to increase or decrease endothelial barrier permeability [16].

In this study, we will determine a) whether AR modulates human brain endothelial barrier, b) determine its potential clinical application in drug delivery to the brain in treatment of neurological diseases and c) unravel/reveal the mechanism underlying the increased permeability imposed upon brain endothelial cells by activation of AR. To accomplish this, 1) we studied these processes in human primary brain endothelial cells and a well established human brain endothelial cell line as human BBB model as we cannot perform these studies in humans. 2) We used an FDA-approved A2A AR agonist, Lexiscan (used in humans for cardiac perfusion imaging), to determine its potential as a BBB permeabilizing (or brain)-drug delivery tool. Here, we report that activation of the A2A AR on primary human brain endothelial cells triggers a rapid increase in RhoA activity, re-organization of the actin cytoskeleton and consequently disruption of the endothelial cell-to-cell junctions, leading to the increased paracellular permeability. These processes promote transendothelial migration (TEM) of T cells through paracellular routes. These studies make use of an endogenous mechanism for BBB control. They demonstrate the potential for precise time dependent control of BBB permeability. Moreover, we would show that the process is reversible and there is the potential to tremendously improve the retention of therapeutics into the brain by targeting adenosine receptors on brain endothelial cells.

2.3. Materials and Methods

Cells and reagents

The hCMEC-D3 cell was a kind gift from Dr. Babette Weksler (Weill Cornell Medical Center) and bEnd3 cell was purchased from ATCC. Primary human brain microvascular endothelial cell (ACBRI 376 V), attachment factor, and growth media were purchased from Cell Systems (Kirkland, WA). RhoA specific antibody and RhoA pulldown assay kit were purchased from Cytoskeleton (Denver, CO). Anti ROCK-1 antibody, Phycoerythrin (PE) conjugated anti-human CD73 antibody, human Collagen IV were purchased from BD bioscience (Carlsbad, CA). Rabbit anti Ezrin-Radixin-Moesin (ERM), phospo-ERM, VE-Cadherin, GAPDH were purchased from Cell Signaling (Danvers, MA). Alexa-Fluor 568 conjugated-Phalloidin, rabbit-anti-Claudin-5 antibody, anti rabbit and mouse Alexa Fluor 488, Texas Red conjugated secondary antibody, Fluorescein isothiocyanate (FITC) conjugated 10 kDa Dextran, Prolong Gold with DAPI, and cAMP-screening-kit were purchased from Life Technologies (Carlsbad, CA). Allophycocyanin (APC) conjugated anti-human CD39 antibody was purchased from ebioscience (San Diego, CA). Anti-phospo-focal adhesion kinase (FAK) was purhcased from Millipore (Billerica, MA). Mouse human CD31 antibody was purchased from R&D systems (Minneapolis, MN). Rabbit anti-A2A adenosine receptor antibody was purchased from Alomone labs (Jerusalem, Israel). EBM-2 media and supplementary bullet kit were purchased from Lonza (Allendale, NJ). 5'-*N*-(Ethylcarboxamido)adenosine (NECA) was purchased from Tocris (Bristol, UK) and 2-[4-[(Methylamino)carbonyl]-1H-pyrazol-1-yl]adenosine

(Lexiscan) was purchased from Toronto Research Chemicals (Ontario, Canada). Adenosine was purchased from Sigma Aldrich (St. Louis, MO).

Flow Cytometry

HCMEC-D3 and HBMVEC cells were stained with PE anti-human CD73 and APC anti-human CD39 and the frequencies of positive cells were analyzed with BD Canto flow cytometer (BD Bioscience, Carlsbad, CA).

Immunofluorescence Assay (IFA)

Cells were treated with adenosine receptor agonists which was grown on coverslips, fixed with 4% Paraformaldehyde and permeablized with 0.2% Triton X and washed twice. Subsequently, it was blocked with 5% goat serum in 0.5 % BSA-PBS solution for 45 minutes. Primary antibodies (1:200) were incubated at room-temperature for 2 hrs and washed twice. Fluorchrome conjugated secondary antibody (1:1000) was incubated at room-temperature for 1 hr followed by two washes. For stress fiber staining, cells were additionally counter stained with AF568 conjugated phalloidin. Coverslip was washed with double distilled water and placed on the slide-glass with anti-fade mounting medium, Prolong Gold-DAPI. Samples were analyzed with Axiovision flurorescent microscope and images were recorded and analyzed with Axiovision (Carl Zeiss, Thornwood, NY).

Rho-GTPase pull down assay

HCMEC-D3 and HBMVEC were plated on collagen IV or attachment factor coated 10 cm petri dish and grown to 100 % confluency then treated with Lexiscan or NECA (1uM) over multiple time points: the reaction was halted by placing them on ice. Plates were washed with ice cold PBS and lysed with 250 ul of lysis buffer. The lysate was preserved at -80 ℃ until further analysis. Rho-GTPase pull down assay was performed according to the manufacturers' protocol (Cytoskeleton, Denver, CO). The intensity of Active-RhoA was divided by that of total RhoA for densitometric analysis and to measure its activity at different time point.

Measurement of intracellular cyclic AMP (cAMP)

Primary human brain endothelial cells were plated on the 48 well plates until it reached confluency and treated with 1 uM of Lexiscan and NECA for 1, 5, 15 minutes (n=3). 1 uM of Forsklon (FSK) was used as positive control. Cells were lysed with lysis buffer at 37 ℃ for 30 minutes. Samples were processed following the protocols provided from manufacturer (cAMP-Screen System, Life Technologies) and the levels of cAMP were analyzed using luminometer function in Synergy 4 (Biotek, Winooski, VT).

Western Blot Analysis

Adenosine receptor agonist treated cells were lysed with lysis buffer containing protease inhibitor and mixed with 5X laemaeli buffer. Samples were loaded and separated by the 10 % SDS-PAGE gel and transferred to nitrocellulose paper. Subsequently, membranes were blocked by 1 % bovine serum albumin (BSA) in

TBST buffer for 30 minutes at 4 ℃. Primary antibody (1:2000) was incubated in 1% or 5 % BSA (p-ERM) for overnight at 4 ℃ and blot was washed three times with TBST. Subsequently, membranes were incubated with secondary mouse or rabbit antibody in non-fat dry milk (1:2000) for 1 hr at room temperature and washed three times with TBST. Membrane was visualized by West Pico enhanced chemiluminescence (ECL) solution which was exposed to X-ray film.

Transendothelial electrical resistance (TEER) assay.

Mouse brain endothelial cells (bEnd 3) or primary human brain endothelial cells (HBMVEC) were plated ($1X10^5$) on the collagen IV (BD bioscience, Car) coated 8.0 um porous membrane insert (BD bioscience). When the confluency reached 100%, growth media was replaced with serum deprived media for overnight. Subsequently, 1 uM of Lexiscan, NECA which are A2A specific and broad spectrum adenosine receptor agonists, respectively, were applied into the insert along with DMSO control. The changes in the resistance were measured using Ohm voltmetry (World Precision Instrument, Sarasota, FL) at different time point. The TEER of different time points were subtracted by that of vacant porous membrane and the value was normalized by that of 0 time point.

FITC Dextran Permeability assay.

Mouse and human brain endothelial cells were plated ($1X10^5$) on the collagen IV or attachment factor coated 3.0 um porous membrane insert (BD bioscience, San Jose, CA). Experiments initiated when its confluency reached 100%. Subsequently,

media in insert and bottom well was replaced by pre-warmed HBSS and incubated at 37 ℃ for 2 hrs as acclimatization. 100 ug/ml of 10 kDa FITC-Dextran with or without 1 uM of Lexiscan and 1uM of NECA was applied into the insert. 50 ul of HBSS at the bottom well was collected at each time point (n=3). The concentration of FITC-Dextran was measured using fluometry (BioTek) with excitation at 488 nm, and emission at 523 nm. Acquired values were normalized by that of DMSO control.

Mice.

C57BL/6 mice (Jackson Laboratories) aged 7–9 weeks and weighed between 20 and 25 g were used for experiments. Animals were bred and housed under specific pathogen-free conditions at Cornell University, Ithaca, NY. All procedures were done in accordance with approved Institutional Animal Care and Use Committee protocols.

Administration of drugs and tissue collection.

Lexiscan was dissolved in DMSO and further diluted in the PBS. For vehicle controls, DMSO was diluted in PBS to the same concentration. Dextrans labeled with FITC were suspended in PBS to 10 mg/ml. Experiments involving dextran injection used 1.0 mg of dextran in PBS. When drug and dextran were injected concomitantly, 1.0 mg of dextran was mixed with the drug to the desired concentration in a final volume of 200 µl. Lexiscan was administered retro-orbitally and at indicated times mice were anesthetized and perfused with cold PBS through the left ventricle of the heart. Brains were weighed and frozen for later analysis.

Fluorimetric analysis of FITC-Dextran in the brain.

Tris-Cl, 50mM, pH7.6, was added to brains (100 µl per 100 mg brain). Brains were homogenized with a Dounce homogenizer and centrifuged at 16.1 X g for 30 min. Supernatants were transferred to new tubes and an equal volume absolute methanol was added. Samples were centrifuged at 16.1 X g for 30 min. Supernatant (200 µl) was transferred to a Corning Costar 96 well black polystyrene assay plate (clear bottom). Fluorimetric analysis was performed on a BioTek Synergy 4.

Chemotherapeutics extravasation assay.

Primary human brain endothelial cells were plated ($1X10^5$) on the attachment factor coated 0.4 um porous membrane insert (BD bioscience, San Jose, CA). Experiments initiated when its confluency reached 100%. Subsequently, media in insert and bottom well was replaced the day before experiment. At the receiver well, $2.5X10^5$ of YFP transfected human gliobliostoma cells (U251, NCI cell repository, Frederick, MD) were plated. On donor well, 10 ug/ml of Gemzar (Eli Lilly, Indianapolis, IN) with or without 1 uM of Lexiscan or NECA (n=3) was administered. Also, 1 uM of Lexiscan or NECA without Gemzar was administered to further test the effect of these molecules on glioma viability. At 5, 15, 30, 60 minutes post treatment, donor well was removed and glioblastoma cells were further incubated for 4 days at 37 ℃ with 5 % CO2. Viability of glioblastoma compared to untreated group was measured using fluometry (BioTek) with excitation at 488 nm, and emission at 523 nm.

Jurkat Cell migration assay

To test the effect of adenosine receptor signaling in promoting the migration of immune cells, we performed migration assay of Jurkat Cell through *in vitro* blood brain barrier model using primary brain endothelial monolayer. Primary brain endothelial cell was cultured on the porous membrane insert (BD bioscience, San Jose, CA) which was pre-coated with attachment factor. When the confluency reached 100 %, media in both donor and reciever chamber was replaced with fresh media and acclimatized for overnight. 2.5 X 10^5 of Jurkat cells with or without 0.1 and 1 uM Lexiscan or NECA were placed on the upper chamber and the number of Jurkat cells migrated to the bottom well was counted at 1 and 24 hrs by hemocytometer.

To test if the effect of adenosine receptor signaling on migratory process of Jurkat cell is mediated by paracellular or transcellular pathway, primary brain endothelial cells were plated on the cover slip until it reached 100 % confluency. Cells were treated with 1 uM of Lexiscan and NECA for 2 hrs and washed with PBS. Jurkat cells were added and incubated for 5 minutes. Cells were fixed with 4% PFA and permeabilized with 0.1 % Triton X and blocked with 5 % Goat serum. Endothelial cell was stained with anti VE-Cadherin antibody which was subsequently stained with AF 647 conjugated 2ndary anti-Rabbit antibody. F-Actin was counterstained with AF568 conjugated phalloidin. Cells were visualized with Leica Confocal Microscope (Leica Microsystems, Buffalo Grove, IL) and images were recorded and analyzed by Leica Application Suite software. The route of transmigration of cells were classified as paracellular (cells on the borderline of endothelial cell to cell junction), transcellular

(cells on the top of cytoplasmic area of endothelial cells), ambiguous depending on the localization of migrating Jurkat cells on the endothelial monolayer and quantified.

Statistical analysis

All statistical analysis was carried out using GraphPad 5.0 software. Statistical significances were assessed using either unpaired two tailed Student's t-test or two-way analysis of variance (ANOVA) with Bonferroni multiple comparison test. P values less than 0.05 were considered to be statistically significant.

2.4. Results

Adenosine receptors and enzymes that produce it are abundantly expressed on primary human brain endothelial cells.

Adenosine mediates its function through its four G-protein coupled receptors (A1, A2A, A2B, and A3) [7]. Here, we showed that the A2A adenosine receptor (AR) that we have previously shown increases brain endothelial barrier permeability upon activation in mice is highly expressed on primary human brain endothelial cells (HBMVEC) and an established human brain endothelial cell line (HCMEC-D3) (Fig 2.1.A and B). Extracellular adenosine acts locally due to its short half-life (approximately ten seconds) [8, 10]. Hence, to mediate its function, adenosine receptors and the enzymes that generate it must also be present on the same cell or on adjacent cells. We confirmed that both CD39 and CD73 (ecto-enzymes responsible for generating extracellular adenosine), are highly expressed on both primary human brain endothelial cells and the human brain endothelial cell line HCMEC-D3 (Fig 2.1.C). Taken together, these results suggest that human brain endothelial cells have the capacity to respond to AR-mediated signaling both *in vivo* and *in vitro.*

A2A AR activation increases paracellular permeability in primary human brain endothelial cell monolayers.

To begin to evaluate the role of the A2A AR in human brain endothelial cell permeability, HBMVEC cells were cultured on a porous membrane to form a

Figure 2.1.

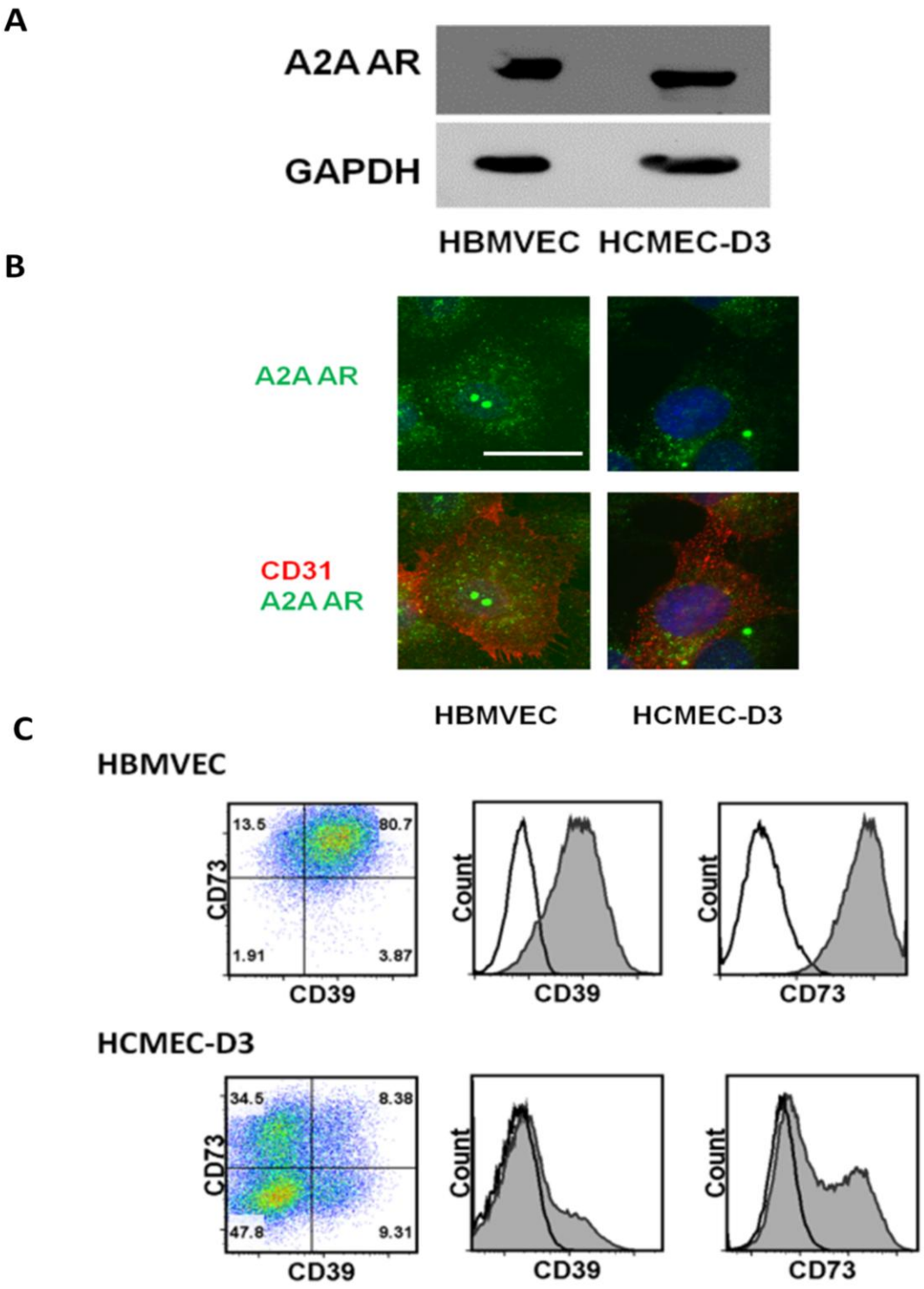
A
A2A AR
GAPDH
HBMVEC HCMEC-D3
B
A2A AR
CD31
A2A AR
HBMVEC HCMEC-D3
C
HBMVEC
13.5
80.7
1.91
3.87
CD73
CD39
Count
CD39
Count
CD73
HCMEC-D3
34.5
8.38
47.8
9.31
CD73
CD39
Count
CD39
Count
CD73

Figure 2.1. A2A AR is expressed in primary human brain endothelial cells and human brain endothelial cell line.

Western blot (A) and immunofluoresecence assay (IFA) (B) show the presence of A2A adenosine receptor (AR) expression on human primary brain endothelial cells (HBMVEC) and human brain endothelial cell line (HCMEC-D3). For IFA, cells were stained with anti-A2A AR antibody (Green) and anti-human CD31 as endothelial cell marker (Red). Nucleus was counter stained with DAPI (Blue). Scale bar indicates 25 um. (C) FACS analysis (Dot-plot and histogram) shows expression of the extracellular enzymes, CD39 and CD73, in HBMVEC and HCMEC-D3.

monolayer to measure transendothelial resistance (TEER), which is a measure of endothelial cell monolayer permeability. Decrease in TEER correlates with increased paracellular space between adjacent endothelial cells and hence with increased permeability [17]. We next treated monolayers with an FDA-approved A2A AR agonist Lexiscan or a broad spectrum agonist NECA. Both Lexiscan and NECA induced rapid decrease in TEER by ten minutes after treatment with AR agonists, consistent with increase in paracellular permeability (Fig 2.2.A). This was compared to vehicle, which showed no change, and S1P and VEGF controls which increased and decreased TEER, respectively[16]. Subsequently, TEER values gradually declined post-treatment in HBMVEC monolayers. A similar trend in TEER was observed in the mouse brain endothelial cell line, bEnd 3, although the kinetics was somewhat different (Fig 2.2.B). These studies clearly indicate that human brain endothelial cells are capable of responding to AR modulation and that activation of the A2A receptor decreases brain endothelial paracellular permeability.

To further evaluate the effects of AR activation on human brain endothelial cell permeability, we generated an *in vitro* human BBB (hBBB) model, to examine the passage of high molecular weight Dextrans. 10 kDa FITC-Dextran concentration in bottom chamber increased in a time dependent manner up to 90 minutes after NECA treatment in hBBB (Fig 2.2.C). NECA's effect on increased permeability was significantly abrogated at 60 and 90 minutes when SCH58261 was concomitantly treated which is an A2A AR specific antagonist. This suggested that the A2A AR activation has an important role in increase the permeability of hBBB. However, Lexiscan did not increase permeability to FITC-Dextran over the 30-90 minutes time

Figure 2.2.

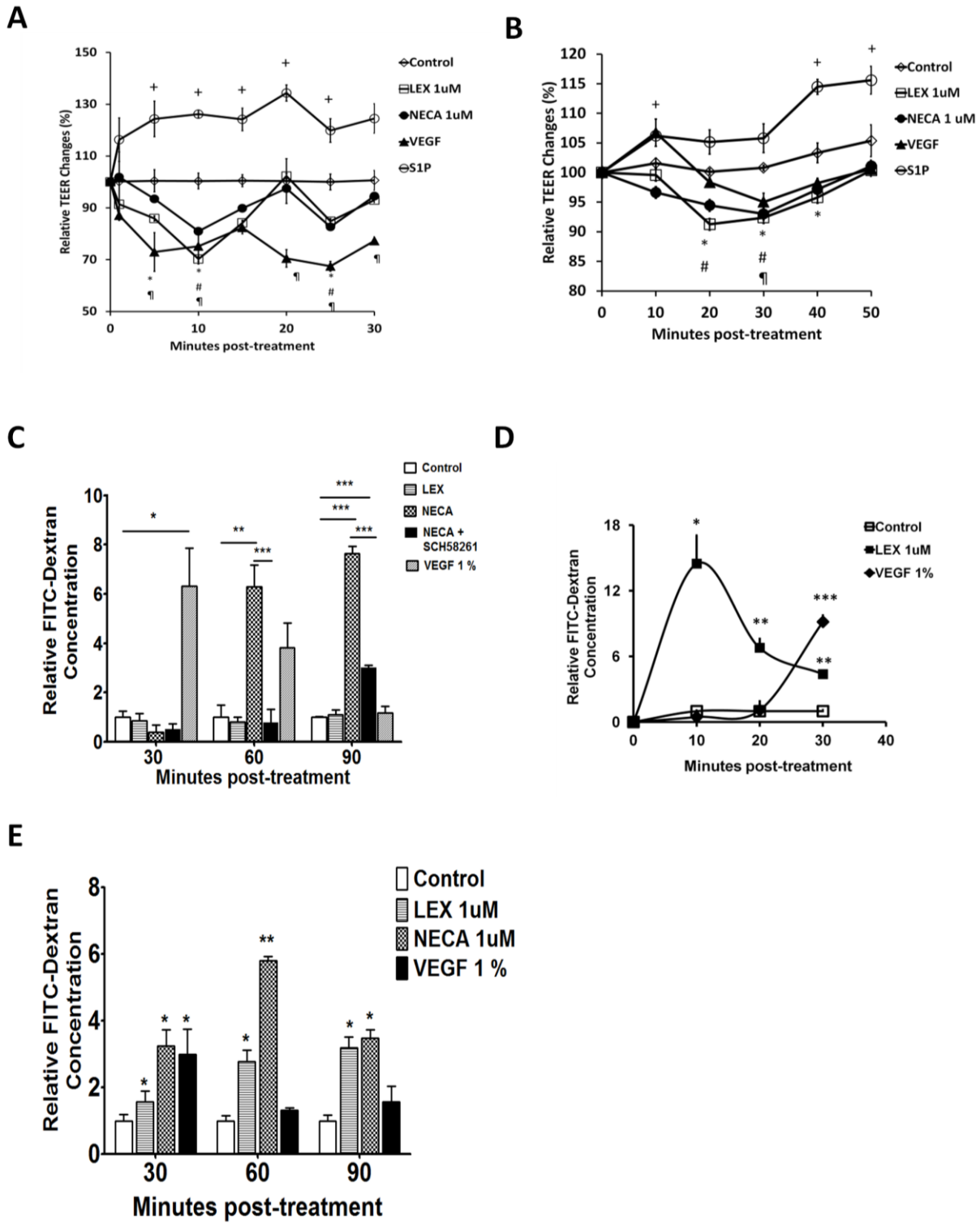
A
Relative TEER Changes (%)
Minutes post-treatment
Control
LEX 1uM
NECA 1uM
VEGF
S1P
B
Relative TEER Changes (%)
Minutes post-treatment
Control
LEX 1uM
NECA 1 uM
VEGF
S1P
C
Relative FITC-Dextran Concentration
Minutes post-treatment
Control
LEX
NECA
NECA + SCH58261
VEGF 1 %
D
Relative FITC-Dextran Concentration
Minutes post-treatment
Control
LEX 1uM
VEGF 1%
E
Relative FITC-Dextran Concentration
Minutes post-treatment
Control
LEX 1uM
NECA 1uM
VEGF 1 %

Figure 2.2. AR agonists increased trans-endothelial electrical resistance and endothelial cell permeability to passage of 10 kDa FITC-Dextran.

(A) Measurement of trans-endothelial electrical resistance (TEER) in primary human brain endothelial cells (HBMVEC) treated with AR agonists, Lexiscan or NECA or VEGF and SIP as positive and negative controls respectively, and vehicle (control). TEER measurement in primary human brain endothelial cell monolayer (HBMVEC) Data represents mean ± s.e.m. (n=3, + (S1P), ¶ (VEGF), * (Lexiscan), # (NECA) indicate $p<0.05$ by two-tailed student t-test)**.** (B) TEER measurement in mouse brain endothelial cell monolayer (bEnd 3) after treatment with AR agonists. Data represents mean ± s.e.m. (n=3, + (S1P), ¶ (VEGF), * (Lexiscan), # (NECA) indicate $p<0.05$ by two-tailed student t-test). (C) FITC-Dextran extravasation through primary human brain endothelial cell monolayer in the presence of Lexiscan, NECA or NECA and SCH58261 at 30, 60, 90 minutes. Data represents mean ± s.e.m. (n=3, * $p<0.05$, ** $p<0.01$, *** $p<0.001$ two-way ANOVA with Bonferroni multiple comparison test). (D) Early time course measurement of FITC extravasation by Lexiscan. Data represents mean ± s.e.m. (n=3, * $p<0.05$, ** $p<0.01$, *** $p<0.001$ by two-way ANOVA with Bonferroni multiple comparison test). (E) 10 kDa FITC-Dextran extravasation in the presence of Lexiscan or NECA in mouse brain endothelial cell monolayer. Data represents mean ± s.e.m. (n=3, * $p<0.05$, ** $p<0.01$, two-way ANOVA with Bonferroni multiple comparison test).

course. We then examined earlier time points as we observed that Lexiscan decreased TEER within 5 minutes (Fig 2.2.A). Indeed, by 10 minutes, Lexiscan induced a robust increase in FITC-Dextran extravasation across hBBB, which declined by 30 minutes (Fig 2.2. D). These collective data indicate that A2A AR activation by Lexiscan causes a rapid and potent increase in hBBB permeability which is followed by a rapid reversal. NECA, by contrast, showed a more gradual reversal in hBBB permeability. These properties were similarly observed in mouse brain endothelial cells (Fig 2.2.E). These data are the first to demonstrate the effects of an FDA-approved A2A AR agonist in primary human brain endothelial cell permeability which has strong translational potential for drug delivery.

A2A AR signaling promotes paracellular trans-endothelial migration of T cells across an in vitro human primary BBB.

Transendothelial-migration (TEM) of leukocytes across the BBB occurs by transcellular or paracellular routes[18-19]. We investigated whether activation of A2A AR has any impact on paracellular versus transcellular TEM of leukocytes across hBBB. Lexiscan (1 uM) increased Jurkat T cell TEM up to 3-fold more than controls by 1 hr and up to 5-fold by 24 hrs (Fig 2.3.A). NECA increased Jurkat T cell TEM by 24 hrs (Fig 2.3.A). To determine whether TEM of these T cells occurred by transcellular and/or paracellular routes, we treated monolayers of primary human brain endothelial cells plated on coverslips with Lexiscan or NECA. Subsequently, Jurkat T cells were plated on endothelial cells monolayer and projections of Jurkat T cells

undergoing paracellular diapedesis were determined by the disruption of junctional VE-Cadherin and the formation of paracellular gaps between adjacent endothelial cells (Fig 2.3.B). Confocal microscopic analysis showed that treatment with Lexiscan or NECA promoted primarily paracellular diapedesis of Jurkat T cells (Fig 2.3.B and C). This was in stark contrast to controls and to previous studies showing that leukocytes undergo TEM across the brain endothelium by both paracellular and transcellular TEM [18-19]. These data indicate that activation of A2A AR preferentially promotes paracellular TEM.

A2A AR activation induces rapid increase in RhoA activity and stress fiber formation in human brain endothelial cells.

Actin-cytoskeletal reorganization is tightly regulated by RhoA[20-23], which is a family of small GTPases activated by G-protein coupled receptor signaling, including ARs[14, 24]. Activation of A2A AR stimulates increase in cyclic adenosine monophosphate (cAMP)[12], which increases RhoA activity[25]. We measured intracellular cAMP activity upon AR activation in primary human brain endothelial cells and observed that Lexiscan induced a rapid increase in cAMP within 1 minute which decreased within 5 minutes and was back to baseline levels by 15 minutes. By contrast, NECA induced a more gradual and modest increase in cAMP that declined by 15 minutes (Fig 2.4.A). Thus, the kinetics of cAMP levels in primary brain endothelial cells demonstrates Lexiscan's is rapid and robust, while

Figure 2. 3.

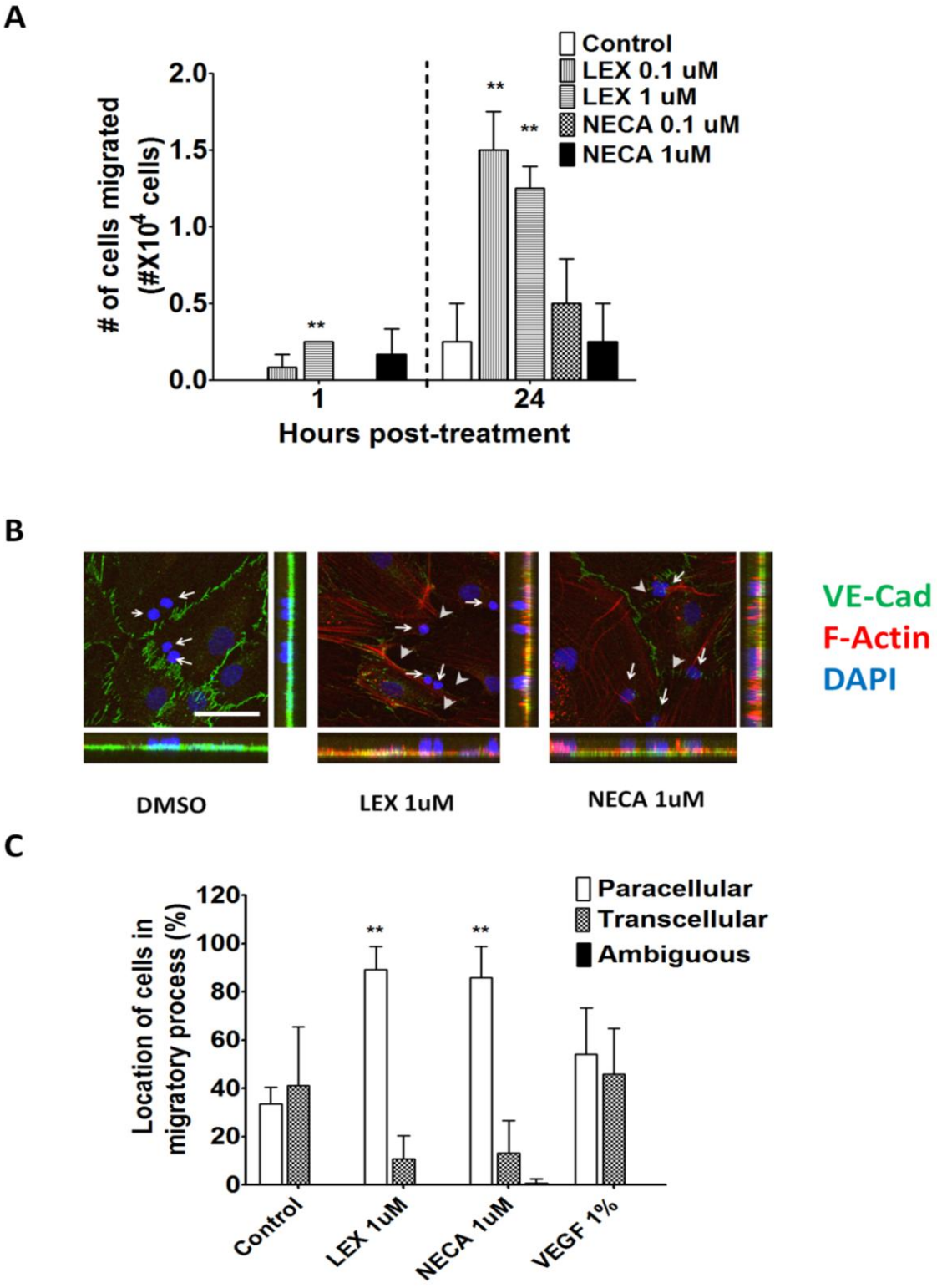
A
Control
LEX 0.1 uM
LEX 1 uM
NECA 0.1 uM
NECA 1uM
# of cells migrated (#X10^4 cells)
2.0
1.5
1.0
0.5
0.0
**
**
**
1
24
Hours post-treatment
B
VE-Cad
F-Actin
DAPI
DMSO
LEX 1uM
NECA 1uM
C
Paracellular
Transcellular
Ambiguous
Location of cells in migratory process (%)
120
100
80
60
40
20
0
**
**
Control
LEX 1uM
NECA 1uM
VEGF 1%

Figure 2.3. AR signaling increases transendothelial migration (TEM) of Jurkat T cells and promotes paracellular TEM across human primary brain endothelial cell barrier.

(A) Transendothelial migration (TEM) of Jurkat T cells across primary human *in vitro* BBB in the presence of varying concentrations (0.1 or 1 uM) of Lexiscan or NECA treatment. TEM of T cell migration was analyzed at 1 hr and 24 hours. Data represents mean ± s.e.m. (** indicates where $p<0.01$, two tailed student t-test). (B) IFA analysis of Jurkat T cells in the process of TEM across a human primary *in vitro* BBB after treatment with AR agonists, Lexiscan or NECA. After treatment with 1uM of Lexiscan or NECA for 2 hours on primary human brain enoothelial cells, cells were washed and $2x10^5$ of Jurkat cells were plated on the endothelial cells for 5 minutes and samples were fixed with 4% paraformaldehyde (PFA). F-actin was stained with AF568 conjugated phalloidin (Red) and VE-Cadherin was stained with anti VE-Cadherin antibody (Green). Nucleus was counter stained with DAPI (Blue). Arrows indicate the nucleus of Jurkat T cells in the migratory process. Arrow heads indicate the disrupted junctional spaces between endothelial cells. Scale bar indicates 50 um. (C) Quantification of T Jurkat cells in the process of paracellular or transcellular TEM across on *in vitro* human primary BBB after treatment with Lexiscan or NECA. Data represents mean ± s.e.m. (** indicates where $p<0.01$, two tailed student t-test). NECA's is gradual. This profile is consistent with TEER (Fig 2.2. A), and BBB permeability induction (Figure 2.2. C and D).

Figure 2.4.

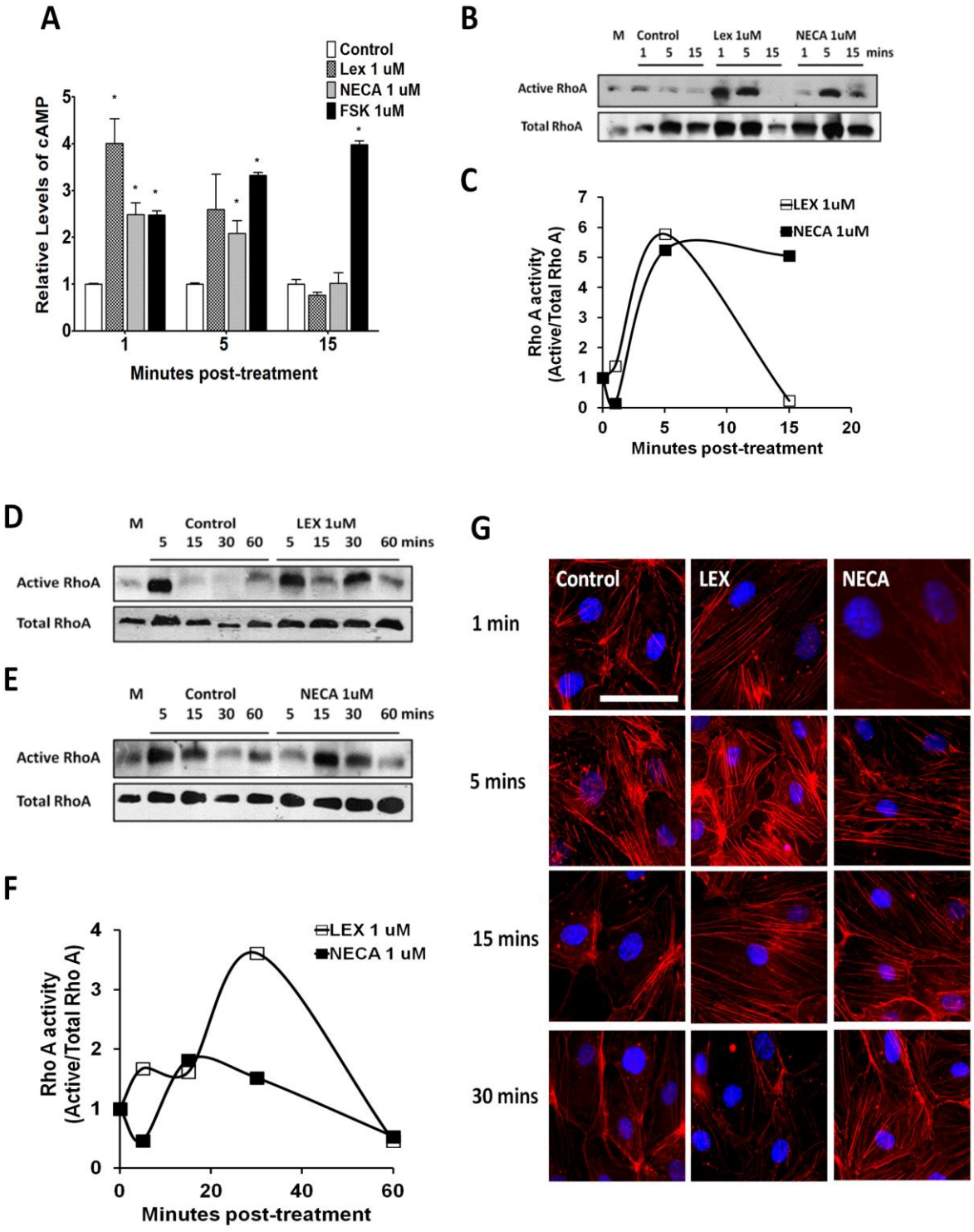
A
Control
Lex 1 uM
NECA 1 uM
FSK 1uM
Relative Levels of cAMP
Minutes post-treatment
B
M Control Lex 1uM NECA 1uM
1 5 15 1 5 15 1 5 15 mins
Active RhoA
Total RhoA
C
LEX 1uM
NECA 1uM
Rho A activity (Active/Total Rho A)
Minutes post-treatment
D
M Control LEX 1uM
5 15 30 60 5 15 30 60 mins
Active RhoA
Total RhoA
E
M Control NECA 1uM
5 15 30 60 5 15 30 60 mins
Active RhoA
Total RhoA
F
LEX 1 uM
NECA 1 uM
Rho A activity (Active/Total Rho A)
Minutes post-treatment
G
Control
LEX
NECA
1 min
5 mins
15 mins
30 mins

Figure 2.4. A2A AR signaling activates RhoA in human brain endothelial cells and induces stress fiber formation.

(A) Changes in the level of cyclic AMP (cAMP) by Lexiscan or NECA were determined in human brain endothelial cells. Intracellular cAMP levels in primary human brain endothelial cells were measured using a cAMP screening kit (Applied biosystems) after treatment with 1 uM of Lexiscan or NECA. 1 uM of Forskolin (FSK) was used as a positive control. (B) RhoA pull down assay performed in HBMVEC, or primary human brain endothelial cells with Lexiscan and NECA stimulation up to 15 minutes. M indicates media only control. (C) Densitometric analysis of western blot data from (B). The band intensity from each treatment group was divided by that of control group from each time point. (D and E) Western blot analysis of active RhoA levels using a pull down assay performed in the human brain endothelial cell line. HCMEC D3 cells lysates were activated with Lexiscan (D), or NECA (E). M indicates media only control. (F) Densitometric analysis of western blot data from (D) and (E). Intensity of band from treated group was divided by that of control group from each time point. (G) IFA analysis of stress fiber formation by Lexiscan and NECA treatment in HBMVEC which was visualized with AF568 conjugated phalloidin (Red). Nucleus was counterstained with DAPI (Blue). Induction of stress fiber formation was determined up to 30 minutes. Scale bar indicates 50 um.

To determine the effect of AR activation on RhoA activity, we performed a RhoA pull down assay using primary human brain endothelial cells and human brain endothelial cell line (HCMEC-D3). In primary human brain endothelial cells, RhoA activity increased rapidly by both Lexiscan and NECA compared to DMSO control (Fig 2.4.B and C). Lexiscan increased RhoA activity within 1 minute, which began to decline after 5 minutes, whereas NECA treatment induced RhoA activity by 5 minutes and it was maintained up to 15 minutes post-NECA treatment (Fig 2.4.B and C). This suggests that the kinetics of cAMP levels in primary brain endothelial cells by Lexiscan and NECA activation follows a similar trend in RhoA activity. Similarly, in HCMEC-D3 cells, Lexiscan induced a rapid increase in RhoA activity within 5 minutes and it peaked at 30 minutes, and declined by 60 minutes in HCMEC-D3 cells (Fig 2.4. D and F). By contrast, NECA induced a modest increase in RhoA activity within 15 minutes and it began to decrease thereafter up to 60 minutes (Fig 2.4.E and F). As the activity of RhoA is directly correlated to stress fiber formation that is coupled with BBB permeability[21], we performed immunofluorescence assay (IFA) to visualize F-actin formation using AF568-conjugated phalloidin (Fig 2.4.G). Lexiscan induced abrupt and rapid stress fiber formation that was maintained up to 15 minutes. In contrast, NECA's formation of stress fibers was maintained up to 30 minutes. Also, more rapid incereases of RhoA activity and F-actin by Lexiscan may explain the rapid increase in the permeability to FITC-Dextran (Figure 4.2.D). These data suggest that activation of A2A AR, either by Lexiscan, or NECA, induced changes in human brain endothelial cells that is consistent with changes in hBBB permeability. Importantly, this permeability in hBBB is reversible. It suggests that the

kinetics of AR activation/de-activation window on BBB endothelial cells can be exploited for drug delivery to the brain.

Signaling through A2A AR down-modulates phosphorylation of focal adhesion in primary human brain endothelial cells.

Focal adhesion is critical in maintaining brain endothelial cells monolayer resistance [26-27]. We next determined the effect of A2A AR activation in phosphorylation of focal adhesion proteins. In primary human brain endothelial cells, the level of phosphorylated Ezrin-Radixin-Moesin (ERM) was transiently decreased by Lexiscan, increased by 15 minutes and decreased again at 30 minutes. In contrast, phosphorylation of focal adhesion kinase (FAK), which is another representative focal adhesion molecule, gradually decreased up to 30 minutes (Fig 2.5.A and B). This indicates that Lexiscan treatment decreased focal adhesion over a short time frame followed by rapid recovery. However, NECA increased phosphorylated ERM, which was maintained for up to 60 minutes after which it decreased by 120 min. Meanwhile, phosphorylated FAK began to decrease at 60 minutes (Fig 2.5.C and D). These results indicate that the phosphorylation of ERM and FAK kinetics correlates with the increased permeability window of Lexiscan and NECA observed in primary human brain endothelial cells (Fig 2.2.C and D). Similar kinetics was observed in HCMEC-D3 cells, which showed that phosphorylated ERM decreased very rapidly after Lexiscan treatment (within 5 minutes), and this decrease was maintained up to 60 minutes (Fig 2.5.E and F). By contrast, NECA increased rapid phosphorylation of

Figure 2.5.

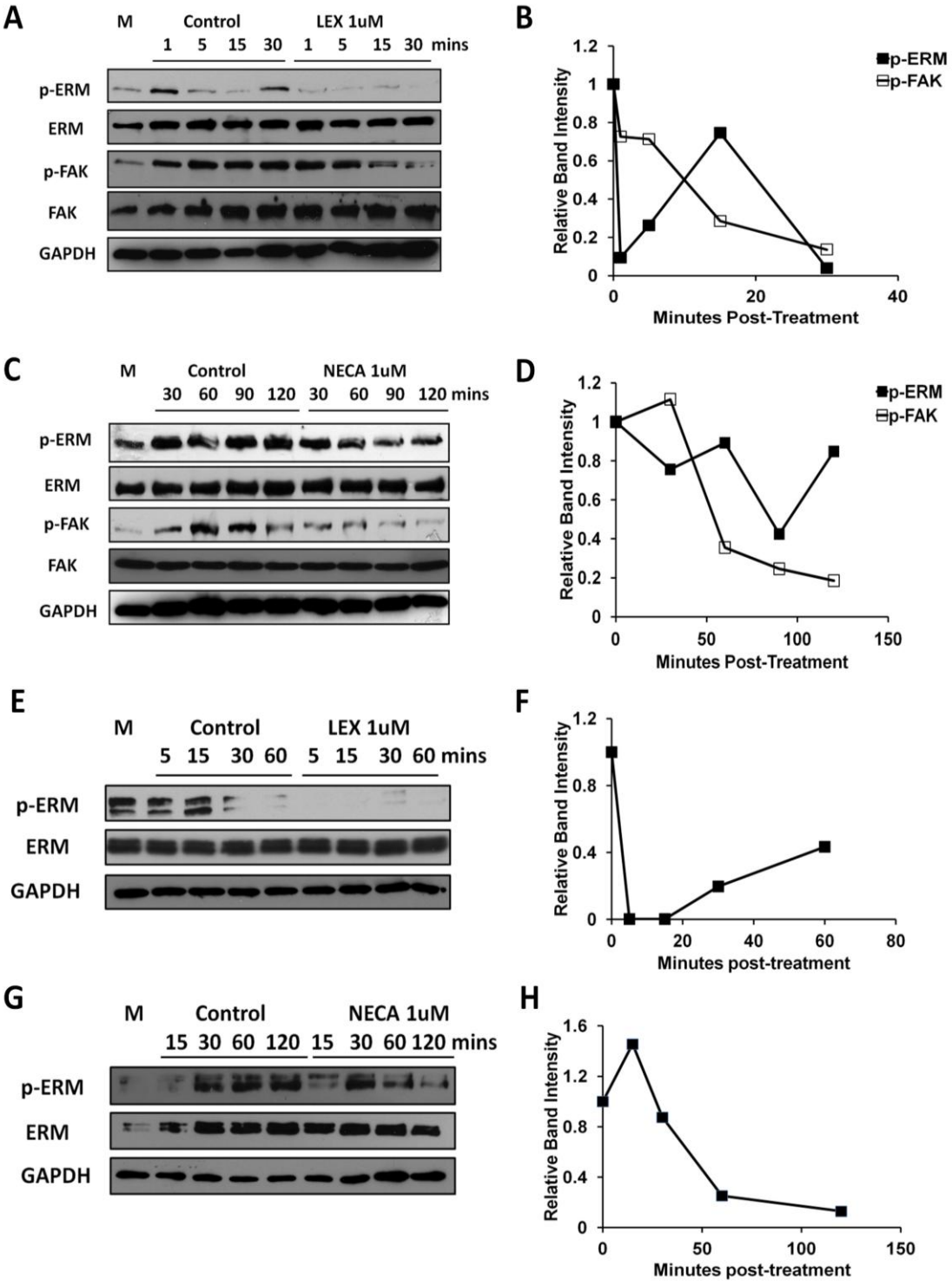
A
M
Control
LEX 1uM
1 5 15 30 1 5 15 30 mins
p-ERM
ERM
p-FAK
FAK
GAPDH
B
p-ERM
p-FAK
Relative Band Intensity
Minutes Post-Treatment
C
M
Control
NECA 1uM
30 60 90 120 30 60 90 120 mins
p-ERM
ERM
p-FAK
FAK
GAPDH
D
p-ERM
p-FAK
Relative Band Intensity
Minutes Post-Treatment
E
M
Control
LEX 1uM
5 15 30 60 5 15 30 60 mins
p-ERM
ERM
GAPDH
F
Relative Band Intensity
Minutes post-treatment
G
M
Control
NECA 1uM
15 30 60 120 15 30 60 120 mins
p-ERM
ERM
GAPDH
H
Relative Band Intensity
Minutes post-treatment

Figure 2.5. Activation of A2A AR decreases the focal adhesion activity of human brain endothelial cell mediated by decrease in phosphorylation of ERM and focal adhesion kinase.

(A) Western blot on phosphorylated ERM (p-ERM) and phosphorylated focal adhesion kinase (p-FAK) were performed in Lexiscan treated primary human brain endothelial cells (HBMVEC) upto 30 minutes. (B) Intensity of the band of phosphorylated form was divided by that of total protein to obtain the ratio. Ratio from treated group was normalized by GAPDH and was divided by the value of control group at each time point (from A) and plotted as graph. (C) Western blot analysis of p-ERM, p-FAK were performed in NECA treated HBMVEC upto 120 minutes. (D) Intensity of the band of phosphorylated form was divided by that of total protein to obtain the ratio. Ratio from treated group was normalized by GAPDH and was divided by the value of control group at each time point (from C) and plotted as graph. (E) Western blot analysis of p-ERM in Lexiscan treated HCMEC-D3 cells up to 60 minutes. (F) Intensity of the band of phosphorylated form was divided by that of total protein to obtain the ratio. Normalized ratio by GAPDH from treated group was divided by that of control group at each time point (from E) and plotted as graph. (G) Western blot analysis of p-ERM in NECA treated HCMEC D3 cells up to 120 minutes. (H) Intensity of the band of phosphorylated form was divided by that of total protein to obtain the ratio. Normalized ratio by GAPDH from treated group was divided by that of control group at each time point (from G) and plotted as graph. In all images M indicates media only control.

ERM that was maintained up to 60 minutes, and began to decrease thereafter (up to 120 minutes) (Fig 2.5.G and H). These data suggest that stimulation of A2A AR caused suppression of micro-adhesion between human brain endothelial cells and their matrix.

Activation of A2A AR disrupts tight and adherens junctional molecules, increases the permeability of chemotherapeutic agents and induces glioblastoma cell death in human brain endothelial cell monolayer.

Claudin-5[28] and vascular endothelial (VE)-Cadherin[29-30], play a major role in formation of vascular network and is necessary for endothelial barrier integrity. We examined the effect of AR signaling on the expression level and/or distribution of VE-Cadherin and Claudin-5 in our human and mouse brain endothelial cell monolayers. In primary human brain endothelial cells, Lexiscan decreased VE-Cadherin expression within 1 minute. It was maintained up to 15 minutes, recovered rapidly by 30 minutes, and lasted up to 90 minutes. The expression level of Claudin-5 gradually decreased up to 30 minutes after Lexiscan treatment (Fig 2.6.A and B). Similar kinetics of VE-Cadherin expression was observed with NECA treatment (Fig 2.6.C and D). In fact, NECA caused a dramatic decline in VE-Cadherin that lasted for 60 minutes and was recovered by 90 minutes. Claudin-5 expression also gradually decreased over 2 hrs with NECA.

In mouse brain endothelial monolayer (bEnd 3 cells), Lexiscan down-regulated VE-cadherin expression in a time dependent manner, from 30 minutes to 1 hr, after

Figure 2.6.

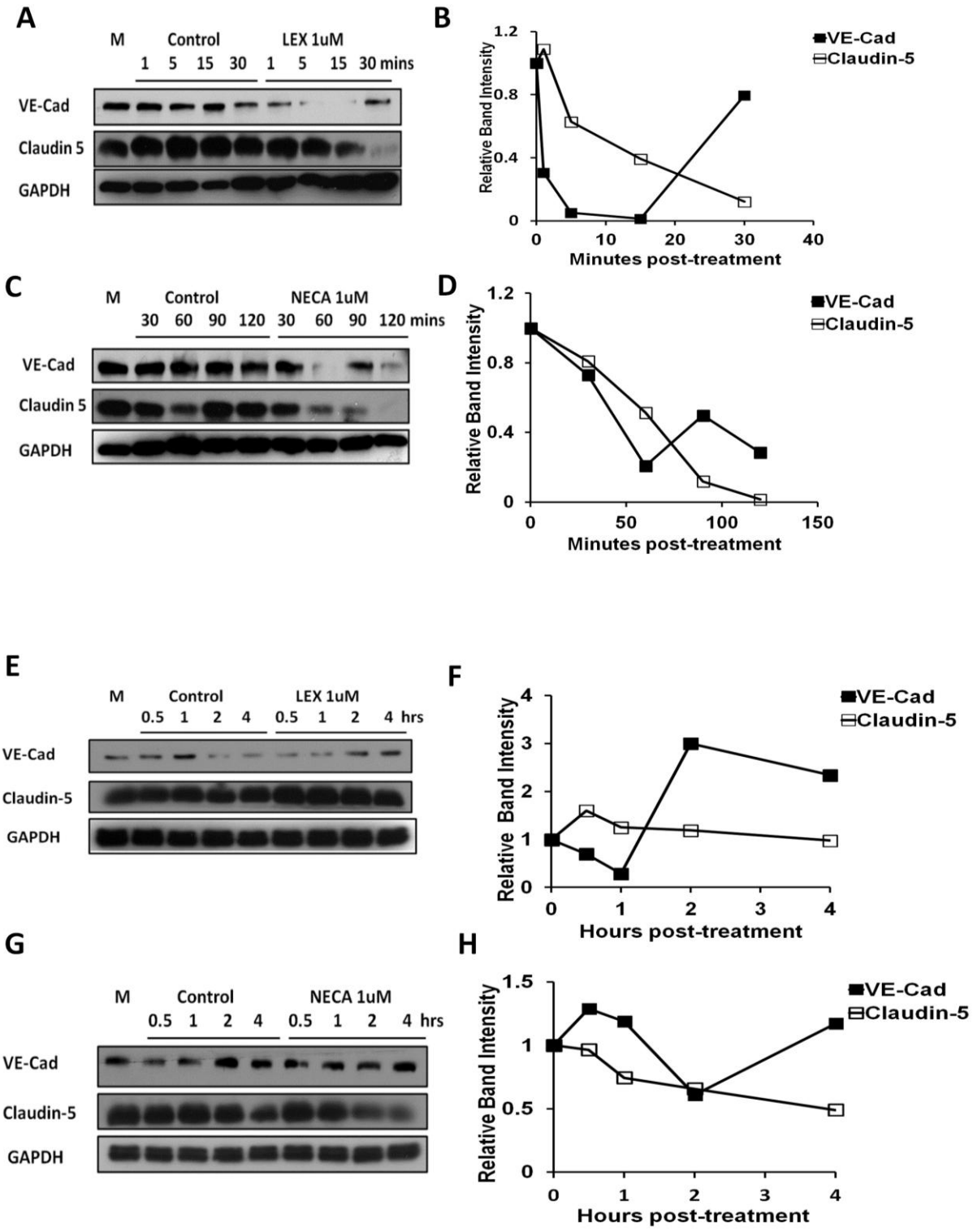
A
M
Control
LEX 1uM
1 5 15 30 1 5 15 30 mins
VE-Cad
Claudin 5
GAPDH
B
Relative Band Intensity
1.2
0.8
0.4
0
0 10 20 30 40
Minutes post-treatment
VE-Cad
Claudin-5
C
M
Control
NECA 1uM
30 60 90 120 30 60 90 120 mins
VE-Cad
Claudin 5
GAPDH
D
Relative Band Intensity
1.2
0.8
0.4
0
0 50 100 150
Minutes post-treatment
VE-Cad
Claudin-5
E
M
Control
LEX 1uM
0.5 1 2 4 0.5 1 2 4 hrs
VE-Cad
Claudin-5
GAPDH
F
Relative Band Intensity
4
3
2
1
0
0 1 2 3 4
Hours post-treatment
VE-Cad
Claudin-5
G
M
Control
NECA 1uM
0.5 1 2 4 0.5 1 2 4 hrs
VE-Cad
Claudin-5
GAPDH
H
Relative Band Intensity
1.5
1
0.5
0
0 1 2 3 4
Hours post-treatment
VE-Cad
Claudin-5

Figure 2.6. Activation of A2A AR decreases expression level of tight and adherens junction molecules in human and mouse brain endothelial cell.

(A-D) Western blot result of VE-Cadherin and Claudin 5 in primary human brain endothelial cells with Lexiscan and NECA activation. (A and B) Western blot analysis of Claudin-5 and VE-Cadherin was performed on the HBMVEC cells treated with Lexiscan upto 30 minutes (A). Normalized intensity of band by GAPDH from treated group was divided by that of control group at each time point and plotted as graph (B). (C and D) Western blot on Claudin-5 and VE-Cadherin was performed on the HBMVEC cells treated with NECA upto 120 minutes (C). Normalized intensity of band by GAPDH from treated group was divided by that of control group at each time point and plotted as graph (D). (E-H) Western blot analysis of Claudin-5 and VE-Cadherin levels in mouse brain endothelial cell line (bEnd3). (E and F) Western blot analysis of Claudin-5 and VE-Cadherin was performed on the bEnd 3 cells treated with Lexiscan upto 4 hours (E). Normalized intensity of band by GAPDH from treated group was divided by that of control group at each time point and plotted as graph (F). (G and H) Western blot on Claudin-5 and VE-Cadherin was performed on the bEnd 3 cells treated with NECA upto 4 hours (G). Normalized intensity of band by GAPDH from treated group was divided by that of control group at each time point and plotted as graph (H). In all western blot images M indicates media only control.

which it increased to baseline levels and was maintained steadily up to 4 hrs (Fig 2.6.E and F). In contrast to VE-cadherin, Lexiscan induced a transient increase in Claudin-5, which returned to baseline and remained at steady state up to 4 hours (Fig 2.6.E and F). NECA treatment decreased VE-Cadherin levels after 2 hrs, which is much later than Lexiscan, with a gradual return to baseline levels by 4 hrs. Claudin-5 expression was gradually decreased after 1 hr with significant decrease by 4 hrs after NECA treatment (Fig 2.6.G and H). This is in striking contrast to Lexiscan which induced a rapid and robust decrease in VE-cadherin levels but had minimal effect on Claudin-5. This indicates that the expression level of adherens junction molecules, is decreased by both Lexiscan and NECA, but Lexiscan's effect is more potent and occurs much earlier than NECA's. Thus in mouse brain endothelial cells, A2A AR specific agonist Lexiscan, exerts its effect specifically through down-regulation of VE-Cadherin.

IFA analysis showed that treatment with Lexiscan or NECA caused junctional disruption of VE-Cadherin (Fig 2.7.A and B).We also confirmed that VE-Cadherin disruption was mediated by A2A AR, as a specific A2A AR antagonist, SCH58261, concomitant with NECA treatment inhibited NECA's effects (Fig 2.7.A and B, 5 and 30 minutes post-treatment, respectively). This indicates that the window of increased permeability to polymerized Dextran observed in primary brain endothelial cells by Lexiscan (up to 30 minutes) and NECA (30-90 minutes) (Fig 2.2.C and D) matches the window of VE-Cadherin and phosphorylated focal adhesion molecules down-regulation (Figure 2.6.F and H).

Figure 2.7.

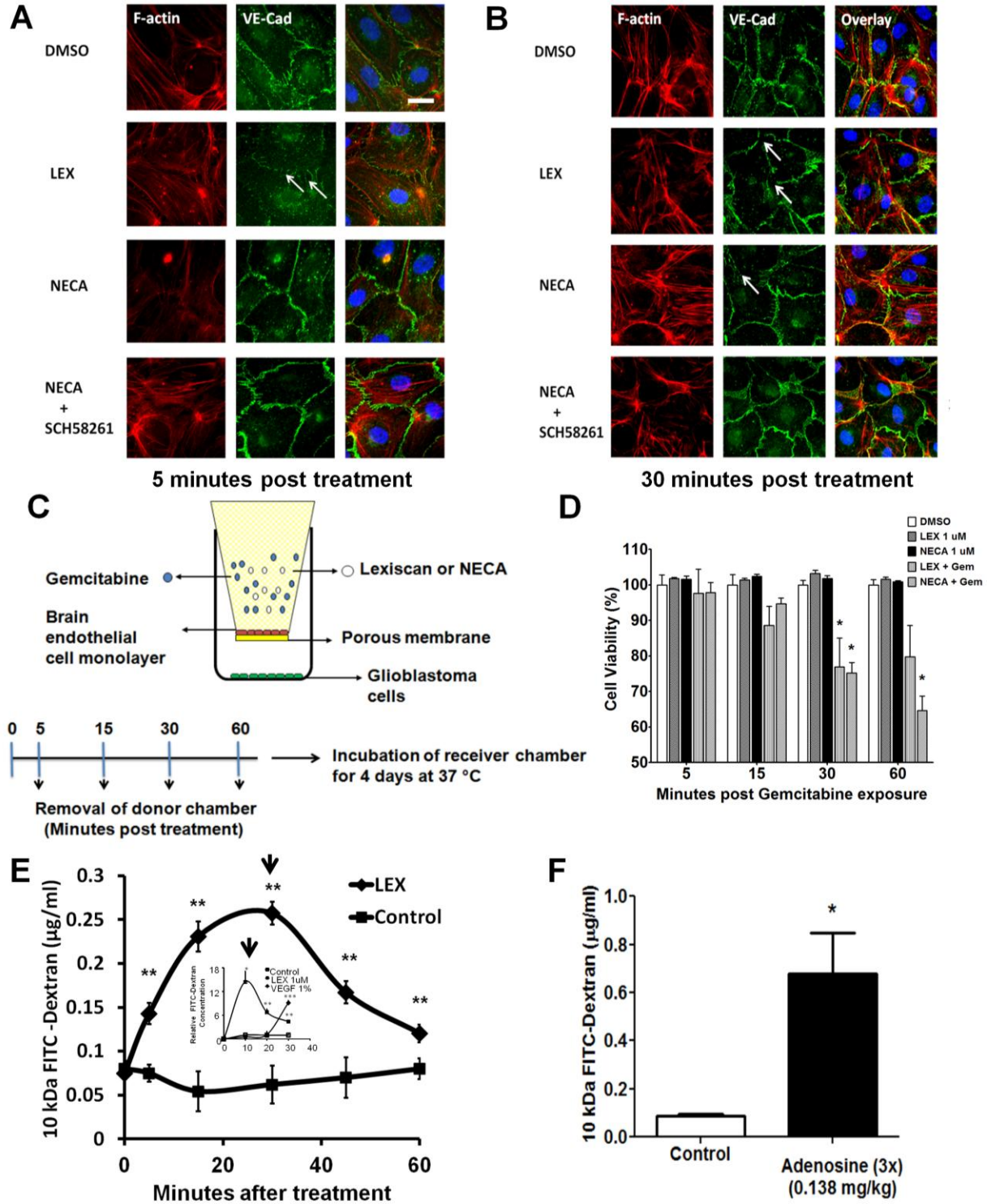
A
F-actin
VE-Cad
DMSO
LEX
NECA
NECA + SCH58261
5 minutes post treatment
B
F-actin
VE-Cad
Overlay
DMSO
LEX
NECA
NECA + SCH58261
30 minutes post treatment
C
Gemcitabine
Lexiscan or NECA
Brain endothelial cell monolayer
Porous membrane
Glioblastoma cells
0 5 15 30 60
Incubation of receiver chamber for 4 days at 37 °C
Removal of donor chamber (Minutes post treatment)
D
DMSO
LEX 1 uM
NECA 1 uM
LEX + Gem
NECA + Gem
Cell Viability (%)
Minutes post Gemcitabine exposure
E
LEX
Control
10 kDa FITC -Dextran (µg/ml)
Minutes after treatment
Control
LEX 1uM
VEGF 1%
Relative FITC-Dextran Concentration
F
10 kDa FITC-Dextran (µg/ml)
Control
Adenosine (3x) (0.138 mg/kg)

Figure 2.7. Activation of A2A AR disrupts adherens junction molecules in primary human brain endothelial cell and increases the permeability to chemotherapeutics, Gemcitabine.

(A and B) IFA of VE-cadherin (Green) and F-actin (Red) in HBMVEC cells 5 and 30 minutes post-treatment with Lexiscan and NECA. Additionally, NECA was treated concomitantly with SCH58261 which is A2A specific antagonist. Arrows indicate the disrupted junction formation. Nucleus was counterstained with DAPI (Blue). Scale bar indicates 25 um. (C and D) AR agonists increase the permeability to chemotherapeutics, Gemcitabine, in primary human brain endothelial monolayer. Changes in permeability to the chemotherapeutic drug, Gemcitabine, after AR activation was determined using primary human brain endothelial cell monolayer. Donor chamber was treated with Gemcitabine (Gem) (10 ug/ml) for 5, 15, 30, 60 minutes with or without 1uM of Lexiscan or NECA and donor chambers were removed. Receiver chambers on which the YFP-transfected human glioblastoma cells (U251) were cultured and further incubated for 96 hrs and cell viability was measured by the relative intensity of YFP signal compared to untreated YFP-U251 (n=3). Lexiscan or NECA only treatment group was also set as control to test its effect on glioma cell viability (n=3). Data represents mean ± s.e.m. (* indicates where $p<0.05$, two tailed student t-test). (E) Selective A2A AR agonist Lexiscan increases the permeability of the BBB to 10 kDa FITC-Dextran in mice. Lexiscan (0.05 mg/kg) was intravenously administered concomitantly with 10 kDa FITC-Dextran and perfused with ice-cold PBS at different time point (n=10). Brain was collected and processed for analysis of FITC-Dextran concentration using fluometry (** indicates where $p<0.01$, two tailed student t-test). Graph from Figure 2D showing the effect of Lexiscan on hBBB permeability to 10 kDa FITC-Dextran was juxtaposed as inset for

comparison. Arrows indicate the time point with maximal FITC-Dextran concentration from two different graphs. (F) Adenosine increases the peremeability of the BBB to 10 kDa FITC-Dextran in mice. Adenosine was intravenously administered three times (0.138 mg/kg, 20 seconds apart) concomitantly with 10 kDa Dextran and perfused with ice cold PBS at 1 minute after treatment (n=2). Brain was collected and processed for analysis of FITC-Dextran concentration using fluometry (* indicates where $p<0.05$, two tailed student t-test).

Glioblastoma multiforme (GBM) is an aggressive type of brain tumors whose treatment is limited by the BBB that blocks the entry of chemotherapeutic agents into the brain[1, 31]. We next determined whether AR activation could increase the permeability of hBBB to the chemotherapeutic drug, Gemcitabine which is effective in killing GBM (*in vitro*) but does not cross the BBB. Both Lexiscan and NECA decreased glioblastoma cell viability from 30 to 60 minutes. This is compared to DMSO that did not induce any changes in glioblastoma cell viability. Further, we tested the effect of Lexiscan or NECA without Gemcitabine on the glioblastoma viability and we did not observe any significant effect. (Fig 2.7.C and D). Based on this result, we speculate that the decrease in glioblastoma cell viability observed by Lexiscan and NECA is attributed to increased hBBB permeability to Gemcitabine at the indicated time points.

To determine whether the kinetics of Lexiscan modulation of the human BBB coincides with in vivo BBB permeability, we treated mice with 10 kDa FITC dextran in the presence or absence of Lexiscan (Figure 2.7.E). We observed that Lexiscan treated mice has significantly more FITC-Dextran in their brains compared to vehicle treated controls. Moreover, the kinetics of dextran entry in to the brain closely correlates with the kinetics of Lexiscan modulation of the in vitro human BBB permeability. We next tested the hypothesis that adenosine (with a half-life of 8-10 sec) is an endogenous modulator of BBB permeability that signals the recruitment of substances to sites of damage or inflammation (Figure 2.7.F). We treated mice with FITC-Dextran with or without adenosine for 1 minute in a triple-injection manner (20 seconds apart). Adenosine treatment increased FITC-Dextran in the brain up to 4 times

more than vehicle treated animals. Because adenosine, like other purines, are danger signaling molecules, these findings suggest that adenosine signaling at the BBB may signal the recruitment of substances (cells and or molecules) into the brain under conditions of inflammation or injury.

2.5. Discussion

Drug delivery to the brain is one of the most challenging factors facing drug development for CNS diseases [1, 4, 6]. Many efficacious drug candidates are developed against neurological diseases but most are dropped from the pipeline because they cannot cross the BBB to effectively treat diseases of the brain. To circumvent this hurdle, a variety of approaches are used to make access to the brain easier. These range from modification of drug properties to invasive delivery methods [4]. Our goal in this study was to determine whether human brain endothelial cells have the capacity to be permeabilized upon AR activation and to reveal the molecular mechanism behind the increased BBB permeability. Also, we hoped to evaluate the potential applicability of Lexiscan, which is an FDA-approved A2A AR agonist to permeabilize human brain endothelial barrier cells and increase drug delivery to the brain for treatment of neurological diseases. We used primary human brain endothelial cells and a human brain endothelial cell line (HCMEC-D3) as *in vitro* models for human BBB. We established that human brain endothelial cells highly and abundantly express CD73, which produces extracellular adenosine and express the A2A AR. Our findings indicate that not only do human brain endothelial cells have the capability to produce and respond to adenosine, but that activation of the A2A AR, Lexiscan or NECA potently permeabilize the *in vitro* human BBB. Importantly, the increase in BBB permeability upon A2A AR activation is rapid and reversible, two key components that are critical for patients' safety.

Activation of A2A AR induces a rapid increase in RhoA activity and actin stress fiber formation [16, 32]. Also, upon AR activation, focal adhesion, which enhances micro attachment between endothelial cells and their extracellular matrix, decreases as the phosphorylation of ERM decreases [26]. Although we did not directly test the relationship between changes in the phosphorylation level of focal adhesion molecules and endothelial monolayer permeability, we speculate that these changes possibly might be important factors affecting endothelial permeability as the kinetics of phosphorylation level matches with kinetics of permeability. Also, we observed rapid decrease of VE-Cadherin and Claudin-5 after Lexiscan treatment, while NECA induced a more gradual decrease in their expression. Thus, increased RhoA activity, and induction of stress fiber formation, is consistent with decreased TEER, increased extravazation of polymerized Dextran and increased T cell TEM across our *in vitro* human brain endothelial barriers in the presence of both Lexiscan and NECA treatment. Most striking was A2A AR signaling promoted exclusively paracellular TEM. This is notable as most studies show that leukocyte migration into the CNS or in vitro BBB models occur by both paracellular and transcellular pathways [18-19]. Thus, in vivo paracellular TEM under physiological conditions may be mediated by AR signaling. As proof of principle that AR stimulation permeabilizes human brain endothelial barrier cells, we determined the effect of BBB permeability to Gemcitabine extravasation on glioblastoma viability. Gemcitabine is one of few chemotherapeutic drugs that kill glioblastomas but it does not cross the BBB. Consistent with the kinetics of BBB permeability induced by AR activation, we observed time-dependent cell death of glioblastoma cells. We attributed this to be due

to the increased permeability window, increasing Gemcitabine concentration in the lower transwell chamber with glioblastoma cells. We further determined that Lexiscan permeabilized the BBB in mice with very similar kinetics observed in the human in vitro BBB model. Finally, we showed that despite the extremely short half life of adenosine which lasts about 10 seconds, also significantly permeabilized the BBB to FITC-Dextran in 1 minute. Taken together, we propose that adenosine modulation of the BBB is an endogenous mechanism developed in response to stress, to recruit substances to sites of inflammation or injury. This suggests that modulation of human BBB by AR signaling may be a viable tool for the delivery of therapeutics to the brain.

These studies are the first to investigate A2A AR signaling in human primary brain endothelial cells. Moreover, they are the first to utilize an FDA-approved AR agonist and demonstrate its function in human primary brain endothelial cell function. They make use of an endogenous mechanism for BBB control and they demonstrate the potential for precise, time dependent modulation of BBB permeability. These results strongly suggest that modulation of A2A AR, is a potential target for delivery of therapeutic drugs to the brain, or the delivery of stem cells in treatment of a wide range of neurological diseases including brain tumors, Alzheimer's or HIV-AIDS.

References

1. Deeken, J.F. and W. Loscher, *The blood-brain barrier and cancer: transporters, treatment, and Trojan horses.* Clin Cancer Res, 2007. **13**(6): p. 1663-74.
2. Abbott, N.J., L. Ronnback, and E. Hansson, *Astrocyte-endothelial interactions at the blood-brain barrier.* Nat Rev Neurosci, 2006. **7**(1): p. 41-53.
3. Giacomini, K.M., et al., *Membrane transporters in drug development.* Nat Rev Drug Discov, 2010. **9**(3): p. 215-36.
4. Pardridge, W.M., *The blood-brain barrier: bottleneck in brain drug development.* NeuroRx, 2005. **2**(1): p. 3-14.
5. Ribatti, D., et al., *Development of the blood-brain barrier: a historical point of view.* Anat Rec B New Anat, 2006. **289**(1): p. 3-8.
6. Hossain, S., T. Akaike, and E.H. Chowdhury, *Current approaches for drug delivery to central nervous system.* Curr Drug Deliv, 2010. **7**(5): p. 389-97.
7. Hasko, G., et al., *Adenosine receptors: therapeutic aspects for inflammatory and immune diseases.* Nat Rev Drug Discov, 2008. **7**(9): p. 759-70.
8. Jacobson, K.A. and Z.G. Gao, *Adenosine receptors as therapeutic targets.* Nat Rev Drug Discov, 2006. **5**(3): p. 247-64.
9. Blackburn, M.R., et al., *Adenosine receptors and inflammation.* Handb Exp Pharmacol, 2009(193): p. 215-69.

10. Fredholm, B.B., et al., *International Union of Basic and Clinical Pharmacology. LXXXI. Nomenclature and classification of adenosine receptors--an update.* Pharmacol Rev, 2011. **63**(1): p. 1-34.

11. Carman, A.J., et al., *Adenosine receptor signaling modulates permeability of the blood-brain barrier.* J Neurosci, 2011. **31**(37): p. 13272-80.

12. Mills, J.H., et al., *Human brain endothelial cells are responsive to adenosine receptor activation.* Purinergic Signal, 2011. **7**(2): p. 265-73.

13. Mills, J.H., et al., *CD73 is required for efficient entry of lymphocytes into the central nervous system during experimental autoimmune encephalomyelitis.* Proc Natl Acad Sci U S A, 2008. **105**(27): p. 9325-30.

14. Sohail, M.A., et al., *Adenosine induces loss of actin stress fibers and inhibits contraction in hepatic stellate cells via Rho inhibition.* Hepatology, 2009. **49**(1): p. 185-94.

15. Pollard, T.D. and J.A. Cooper, *Actin, a central player in cell shape and movement.* Science, 2009. **326**(5957): p. 1208-12.

16. Spindler, V., N. Schlegel, and J. Waschke, *Role of GTPases in control of microvascular permeability.* Cardiovasc Res, 2010. **87**(2): p. 243-53.

17. Li, G., et al., *Permeability of endothelial and astrocyte cocultures: in vitro blood-brain barrier models for drug delivery studies.* Ann Biomed Eng, 2010. **38**(8): p. 2499-511.

18. Carman, C.V. and T.A. Springer, *Trans-cellular migration: cell-cell contacts get intimate.* Curr Opin Cell Biol, 2008. **20**(5): p. 533-40.

19. Wolburg, H., K. Wolburg-Buchholz, and B. Engelhardt, *Diapedesis of mononuclear cells across cerebral venules during experimental autoimmune encephalomyelitis leaves tight junctions intact.* Acta Neuropathol, 2005. **109**(2): p. 181-90.

20. Tominaga, T., et al., *Diaphanous-related formins bridge Rho GTPase and Src tyrosine kinase signaling.* Mol Cell, 2000. **5**(1): p. 13-25.

21. Jaffe, A.B. and A. Hall, *Rho GTPases: biochemistry and biology.* Annu Rev Cell Dev Biol, 2005. **21**: p. 247-69.

22. Adamson, R.H., et al., *Rho and rho kinase modulation of barrier properties: cultured endothelial cells and intact microvessels of rats and mice.* J Physiol, 2002. **539**(Pt 1): p. 295-308.

23. Riento, K. and A.J. Ridley, *Rocks: multifunctional kinases in cell behaviour.* Nat Rev Mol Cell Biol, 2003. **4**(6): p. 446-56.

24. Rex, C.S., et al., *Different Rho GTPase-dependent signaling pathways initiate sequential steps in the consolidation of long-term potentiation.* J Cell Biol, 2009. **186**(1): p. 85-97.

25. Jeyaraj, S.C., et al., *Cyclic AMP-Rap1A signaling activates RhoA to induce alpha(2c)-adrenoceptor translocation to the cell surface of microvascular smooth muscle cells.* Am J Physiol Cell Physiol, 2012. **303**(5): p. C499-511.

26. Bretscher, A., K. Edwards, and R.G. Fehon, *ERM proteins and merlin: integrators at the cell cortex.* Nat Rev Mol Cell Biol, 2002. **3**(8): p. 586-99.

27. Wu, M.H., *Endothelial focal adhesions and barrier function.* J Physiol, 2005. **569**(Pt 2): p. 359-66.

28. Stevenson, B.R. and B.H. Keon, *The tight junction: morphology to molecules.* Annu Rev Cell Dev Biol, 1998. **14**: p. 89-109.

29. Hordijk, P.L., et al., *Vascular-endothelial-cadherin modulates endothelial monolayer permeability.* J Cell Sci, 1999. **112 (Pt 12)**: p. 1915-23.

30. Millan, J., et al., *Adherens junctions connect stress fibres between adjacent endothelial cells.* BMC Biol, 2010. **8**: p. 11.

31. Adamson, C., et al., *Glioblastoma multiforme: a review of where we have been and where we are going.* Expert Opin Investig Drugs, 2009. **18**(8): p. 1061-83.

32. Wojciak-Stothard, B. and A.J. Ridley, *Rho GTPases and the regulation of endothelial permeability.* Vascul Pharmacol, 2002. **39**(4-5): p. 187-99.

Chapter 3

A2A adenosine receptor signaling modulates the trans-cellular permeability of the blood brain barrier by regulating the multi-drug resistant protein, P-glycoprotein expression.

3.1. Abstract

The blood brain barrier (BBB) is critically important to protect the brain from toxic insults from the peripheral circulation and to maintain normal brain physiology. However the BBB poses a tremendous hurdle for drug delivery to the central nervous system (CNS) to treat diseases such as brain cancer and neurodegenerative diseases such as Alzheimer's. The drug transporter, P-glycoprotein (P-gp), is highly expressed on brain endothelial cells and blocks the entry of most drugs delivered to the brain. In this study, we set out to determine whether adenosine signaling mediated by the A2A adenosine receptor (AR) can alter the function of the efflux transporter, P-gp and hence mediate transcellular permeability of the BBB. In human primary brain endothelial cells and a human brain endothelial cell line, which we used as as *in vitro* BBB models, we demonstrated that activation of the A2A AR with an FDA-approved A2AAR agonist, Lexiscan, rapidly and potently decreased P-gp expression and function in a time-dependent and reversible manner. In addition, a broad-spectrum AR agonist NECA, also decreased P-gp expression and function albeit at slower kinetics than Lexiscan. We showed that the downregulation of P-gp expression/function coincides exquisitely with the accumulation of a chemotherapeutic drug, Epirubicin in the brains of wild type mice. Based on these data, we propose that activation of A2A AR on BBB endothelial cells offers a kinetic window for drug delivery to the brain in a relatively safe manner. We propose that AR-mediated signaling at the BBB is an endogenous mechanism designed to transiently open the BBB to deliver substances to the CNS during CNS stress and damage. We believe this study would potentially open

the door to studies on AR modulation of the BBB to deliver drugs into the brain to treat diseases such as brain cancers and Alzheimer's.

3.2. Introduction

The brain is one of the most vascularized organs in the body. This high vascularity enables the efficient and constant supply of oxygen and nutrients from the peripheral circulation to the brain to maintain its proper function [1-2]. The brain vasculature is lined by a single layer of specialized endothelial cells that provide a physical barrier against entry of unwanted substances from the circulation. In addition, tight and adherens junction molecules seal the spaces between adjacent endothelial cells generating even greater resistance. This physical separation by endothelial cells and junction molecules forms the blood brain barrier (BBB). The BBB is insulated with extracellular matrix proteins, pericytes and astrocytic end-feet processes, creating stability, insulation and extremely high resistance and together they are referred to as the neurovascular unit (NVU) [2-3]. In addition to providing a physical barrier, brain endothelial cells are equipped with efflux and influx transporters and receptors. These influx and efflux proteins are also expressed on astrocytic endfeet processes and thus selectively regulate the entry of substances into the brain [3]. The high resistance of the BBB does not allow the entry of molecules larger than 450 Da to cross the BBB. This is critical limit entry of harmful substances including infectious agents and toxins, and to maintain the complex brain physiology and strict ionic environment [2, 4].

However, while the protection provided by the BBB is essential to the health of the host, it hampers the delivery of drugs into the brain to treat neurological disorders such as Alzheimer's Disease (AD) or primary brain cancers [5-6]. Many available drugs with the potential to treat these diseases are not effectively delivered to

the brain due to the physical hindrance and efflux transporters imposed by the BBB. There have been numerous attempts to overcome the hindrance of drug delivery by the BBB which include physical disruption of the BBB, drug modification, and intrathecal injection of drugs into the brain [7-10]. However, these approaches have suffered from shortcomings including toxicity, decreased drug efficacy, and invasiveness that can result in brain damage.

Cells and soluble factors cross the BBB through the paracellular or transcellular pathways [11-12]. Passage across the paracellular pathway disrupts cell-to-cell junction to gain access to the brain. On the other hand, the transcellular pathway is mediated through transporters highly expressed on the luminal side of brain endothelial cells that allows for selective entry of molecules into the brain while maintaining normal brain physiology [12-13]. However, multidrug resistant (MDR) transporters, especially drug efflux transporters, are highly expressed in brain endothelial cells and hinder the effective delivery of drugs into the CNS [5, 9, 14]. One of the most widely known drug transporter expressed in brain endothelial cells is P-glycoprotein (P-gp) [15-16]. P-gp was first observed and described in drug-resistant cancer cells that highly express it. In breast cancer cells, P-gp prevents effective chemotherapeutic treatment by blocking chemotherapeutic drug uptake [17-19]. Later studies showed that P-gp is also highly expressed on capillaries of liver, sex organs, and the brain and is involved in expulsion of xenobiotics from the CNS [20-23]. P-gp is composed of two ATP binding cassettes (ABC) and two trans-membrane domains. The drug binding pocket of P-gp is non-specific and this allows for a broad spectrum of drugs as substrates [24-26]. Many drugs developed for treatment of brain disorders

are largely classified as P-gp substrates thus, significant efforts are placed on developing methods to bypass the hindrance posed by P-gp [27-29]. Recent studies from our lab showed AR signaling regulates the permeability of the BBB [30-31].

Adenosine is a purine nucleoside that functions as an important local signaling molecule, and is involved in various physiological functions including neurotransmission, cardiac pace, and immune regulation [32-34]. Extracellular adenosine is generated by conversion of adenosine triphosphate (ATP) into adenosine di- and mono phosphates (ADP and AMP) by nucleoside triphosphate diphosphohydrolase-1 (CD39), and AMP is further converted into adenosine by the action of 5'-Ecto-nucleotidase (CD73). Extracellular adenosine mediates its action through its four receptors, A1, A2a, A2b, and A3. ARs are 7-transmembrane G-protein coupled receptors that are widely distributed on various cell types in the body and their activation induce changes in the level of second messenger signaling including Ca^{2+} or cyclic AMP (cAMP) [34-36]. In our previous study, we showed that mice lacking CD73 and are unable to synthesize extracellular adenosine have tighter BBBs and are protected from experimental allergic encephalitis (EAE), the animal model for multiple sclerosis [37-38]. More recently, we showed that activation of A2A AR with a broad spectrum AR agonist or an FDA-approved specific A2A AR agonist, Lexiscan, increased accumulation of drugs into the brain in a time- and dose-dependent, manner [31]. BBB opening under AR signaling was reversible. We showed that the duration of BBB permeability was dependent on the half life of the AR agonist. In our recent work, we showed that activation of AR signaling exerted its effects on the paracellular pathway by altering VE-Cadherin and Claudin-5 expression to promote BBB

permeability in human primary brain endothelial cells. We demonstrated that activation of AR signaling with Lexiscan or NECA mediated BBB permeability by RhoGTPase modulation [30].

In this study, we wish to determine whether activation of AR signaling exerts its effects on the transcellular pathway by way of P-gp modulation. We hypothesized that AR-mediated signaling may increase trans-cellular permeability of the BBB by down-regulating P-gp. To test our hypothesis, we used the FDA-approved A2A AR agonist Lexiscan or the broad spectrum AR agonist NECA to determine the impact of A2A AR activation on P-gp expression and function. We observed that activation of the A2A AR by Lexiscan, or NECA downregulates the expression level of P-gp in primary mouse and human brain endothelial cells. P-gp expression was downregulated by A2A AR signaling, and this downregulation coincided with increased accumulation of Rhodamine 123 (Rho123), a classical P-gp substrate. Further, we observed that A2A AR activation by Lexiscan increased accumulation of the P-gp substrate, Epirubicin, in the mouse brain in a rapid and reversible manner. NECA also increased the accumulation of Epirubicin which was observed at later time points. These data strongly suggest that A2A AR signaling potently increases the trans-cellular permeability of BBB endothelial cells. We anticipate that these studies in the future could exert a high impact in the field of drug delivery to the brain to treat neurodegenerative diseases.

3.3. Materials and Methods

Cells and materials

Human Brain Endothelial Cell (HCMEC-D3) was kindly provided by Dr. Weksler in Weill Medical Center (New York, NY). Primary human brain endothelial cells were purchased from cell sciences. Lexiscan (A2a specific agonist) was purchased from Toronto research chemicals. Rhodamine 123 was purchased from Sigma-Aldrich. Epirubicin, PSC 833, Verapramil, NECA was purchased from Tocris. Lexiscan was purchased from Toronto Chemicals. Anti-CD31 antibody was purchased from R&D bioscience. P-glycoprotein and C219 antibody was purchased from genetex. Ubiquitin and GAPDH antibodies were purchased from cell signaling technology. Mouse anti-Caveolin 1 antibody was kindly provided by Dr. Gary Whittaker from College of veterinary medicine in Cornell University (Ithaca, NY).

Mouse Primary Brain Endothelial Cell Culture

Mouse was sacrificed under the IACUC protocol of College of Veterinary Medicine in Cornell University. Meninges of brain were removed and ground using plunger and centrifuged at X 3,000 g for 5 mins. Obtained pellet was dissolved in 18 % dextran and centrifuged at X 10000 g for 10 mins and digested with DMEM containing collagenase, DNAse, Dispase at 37'C for 75 mins. Sample was centrifuged for 5 mins at X 3200 g and the pellet was washed with warm PBS. Pellet was resuspended in DMEM/F12 with puromycin, heparin, 20 % PDS, L-glutamine and plated onto the proper plate.

Subcellular localization analysis of P-glycoprotein in brain endothelial cells

To analyze the subcellular localization of P-glycoprotein in the HCMEC-D3 and primary brain endothelial cells, we plated cells on the coverslip and fixed with PFA for 20 mins. Cells were washed with 0.5 % BSA two times and incubated with 5% goat serum for 45 mins. Cell was incubated with 1:200 anti P-glycoprotein (BD-bioscience) for overnight. Coverslip was washed two times and incubated with anti-mouse secondary antibody conjugated with AF 647 for 1 hr. Cell surface and was stained with AF 568 Wheat Germ Agglutinin (WGA, invitrogen, 1:200) or anti-CD31(R&D bioscience, 1:200). For co-staining for caveolae, cells were stained with mouse anti-caveolin 1 (BD bioscience, 1:200)

Immunoprecipitation assay

4G Sepharose beads were purchased from Invitrogen and incubated with human P-glycoprotein antibody (BD-bioscience) for overnight at 4'C using rocking shaker. Beads were washed with using lysis buffer containing protease inhibitor for two times and lysates from primary brain endothelial cells were incubated for overnight at 4'C using rocking shaker. Samples were spun down at 4,000 G for 2 minutes and washed with lysis buffer containing protease inhibitor for 3 times. Samples were eluted with 0.1 M glycine (pH 2.8) and the eluent was mixed with sample buffer which was loaded on the 10 % SDS-PAGE gel run for 2 hrs at 100 V and subsequently transferred to nitrocellulose paper for western blot analysis.

Western Blot

HCMEC-D3 and HBMVEC cells were plated in 12 well plates and were grown until it reached 100 % confluency. The media was replaced with fresh media containing 1 uM of lexiscan or NECA with proper vehicle control (DMSO) for upto 72 hrs. Cell was lysed by lysis buffer containing protease inhibitor cocktail and stored for later use (-70'C). For brain samples, half of the brain was homogenized and lysed with lysis buffer and centrifuged at 12,000 rpm for 20 minutes and 1:10 diluted samples were used for analysis. Sample was loaded on 7 % SDS PAGE at 100 V for 1 hr and transferred to the nitrocellulose paper. It was blocked with 1 % BSA and incubated with anti-P-glycoprotein antibody (Genetex, 1:2000) for overnight. Subsequently it was washed with TBST and incubated with anti-Rabbit secondary antibody (1:2000) for 1 hr. It was washed with TBST and developed with ECL substrate and exposed to X-ray film. Anti- GAPDH antibody was used as loading control. The intensity of band was analyzed with densitometric analysis and plotted as graph for analysis of time course effect of AR signaling on P-glycoprotein expression.

Rho123 uptake assay

Human brain endothelial cells and primary brain endothelial cells were plated onto 48 well plate until it reached 100% confluency and the media was replaced with fresh media containing different concentration of lexiscan or NECA containing Rho123 (2.5uM) with DMSO control upto 4 hrs (n=4). Reaction was terminated by adding 250 ul of ice-cold PBS. Plate was washed with 250 ul of ice-cold PBS for 3 times and lysed with lysis buffer. Each sample was analyzed using Fluometer (Biotek)

with excitation at 488 nm and emission at 523 nm. For microscopic analysis of Rhodmaine 123 uptake, cells were cultured on coverslip and sae concentration of Rho123 was treated with or without Lexiscan or NECA wit DSMO control. Reaction was terminated by adding ice-cold PBS and washed with ice-cold PBS for 3 times. Cells were fixed with PFA and co-stained with anti-human P-glycoprotein. Cells were visualized with Zeiss fluorescent microscope and captured with axiovision software.

Rho123 extravasation assay

Primary human brain endothelial was plated on the 3 um of porous membrane (Corning) until it reached to 100 % confluency. Media was replaced with HBSS and acclimated for 4 hours before initiation of experiments. Rho123 (2.5uM) with or without Lexiscan or NECA (0.25 uM) was applied on the upper chamber of porous membrane upto 48 hrs (n=4). Media at the bottom chamber were collected at different time points and each sample was analyzed using Fluometer (Biotek) with excitation at 488 nm and emission at 523 nm.

Epirubicin brain accumulation assay

For Lexiscan study, 10 mg/kg of Epirubicin was injected with or without Lexiscan (0.05 mg/kg) at different time point and mice were sacrificed. For NECA study, NECA (0.08 mg/kg) was treated along with control at different time point and same concentration of Epirubicin was injected for 30 minutes and mice were sacrificed. At indicated time point, mice were perfused with ice-cold PBS and brain was collected for further analysis. Brain was grinded and spun down in Tris-HCl

(pH=8.0) at 12,000 rpm for 30 minutes and supernatant was transferred to a new tube and precipitated with same volume of MeOH. Samples were spun down at 12,000 rpm for 30 minutes and the concentration for Epirubicin was analyzed with fluometry with emission at 488 nm and excitation at 575 nm.

Immunofluorescence assay of frozen section

Mouse treated with Lexiscan (1uM) at different time point was infused with ice-cold PBS and sacrificed. Half of the brain was cut and put in the cassette and filled with OCT solution. Samples were snap frozen with liquid nitrogen and cut with cryostat (10 um) and fixed with acetone for 5 minutes and incubated with C219 for P-glycoprotein stain and Glut1 (endothelial marker 1:100), at 4'C for overnight. Sections were washed with PBS and additionally stained with secondary antibody conjugated with fluorchrome. Full images of the brain sections were visualized and recorded using Aperio Scan Scope (Leica Biosystems, Germany).

Statistical analysis

All statistical analysis was carried out using GraphPad 5.0 software. Statistical significances were assessed using unpaired two tailed Student's t-test. P values less than 0.05 were considered to be statistically significant.

3.4. Results

P-gp is highly expressed in primary human brain endothelial cells and a human brain endothelial cell line.

Studies have shown that P-gp is highly expressed on the luminal side of BBB endothelial cells, and on the plasma membrane due to its functional property as a transporter. First, to confirm expression of P-gp in human brain endothelial cells, we performed immunofluorescence staining (IFA) of endothelial cells with an antibody specific for P-gp. We observed, HCMEC D3 cells, which is a human brain endothelial cell line, expressed abundant P-gp in the cytoplasm and to a lesser extent on the cell surface (Fig 3.1.A). Similarly, in human primary brain endothelial cells, HBMVEC, we observed high P-gp expression (Fig 3.1.A). We next determined whether P-gp co-localized with caveolae which are plasma membrane proteins associated with transcytosis. In human primary brain endothelial cells we observed strong co-locaization with caveolin-1, which is the marker for caveolae (Fig 3.1.B). Moreover, immuno-precipitation of P-gp showed that it interacts with caveolin-1 (Fig 3.1.C). This suggests that P-gp may frequently circulate in these endothelial cells by caveolae-protein transport system.

Since we observed mostly cytoplasmic localization of P-gp (in contrast to cell surface localization observed in multi-drug resistant cancer cells), we next determined P-gp functionality using a Rhodamine 123 (Rho123) uptake assay. Rho123 is a substrate of P-gp and is widely used to measure the functionality of P-gp and has a reciprocal relationship to P-gp. Brain endothelial cells were treated with a competitive

Figure 3.1.

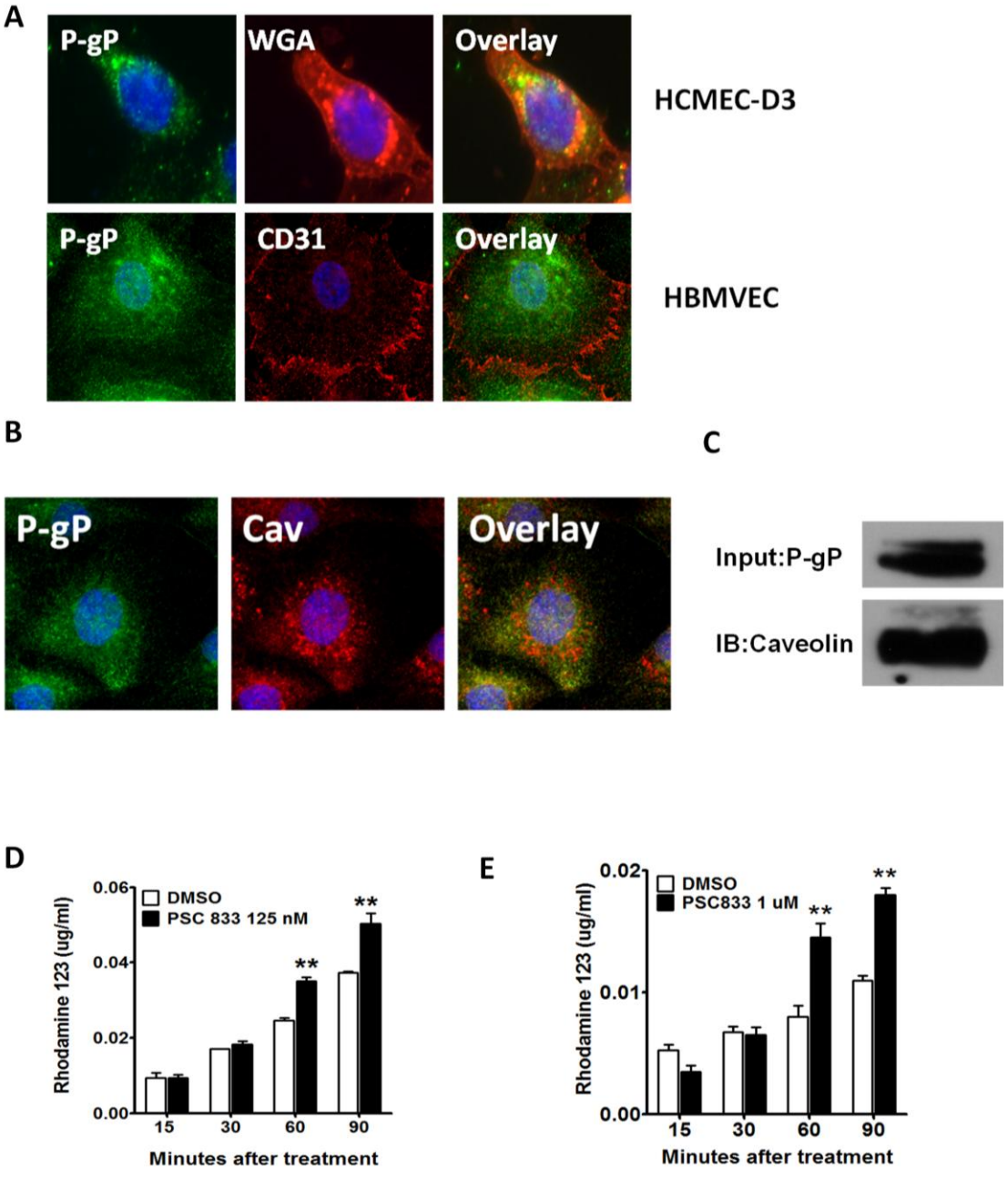
A
P-gP
WGA
Overlay
HCMEC-D3
P-gP
CD31
Overlay
HBMVEC
B
P-gP
Cav
Overlay
C
Input:P-gP
IB:Caveolin
D
DMSO
PSC 833 125 nM
Rhodamine 123 (ug/ml)
0.06
0.04
0.02
0.00
15
30
60
90
Minutes after treatment
**
**
E
DMSO
PSC833 1 uM
Rhodamine 123 (ug/ml)
0.02
0.01
0.00
15
30
60
90
Minutes after treatment
**
**

Figure 3.1. P-gp is highly expressed in primary human brain endothelial cells lines and a human brain endothelial cell line. (A) P-glycoprotein (Green) is expressed in both human brain endothelial cell line (HCMEC-D3) and human primary brain endothelial cell (HBMVEC). Cells were counter stained with wheat germ agglutamin (WGA) for HCMEC-D3 and CD31 for HBMVEC (Red) for cell membrane staining and DAPI for nucleus staining (Blue) (B) P-glycoprotein (Green) is co-localized with caveolin-1 (Red) which is the marker for caveolae in primary human brain endothelia cells. (C) Immunoprecipitation assay on Caveolin on the lysate of primary brain endothelial cells. Lysate was pulled down using anti-P-gp antibody and immunoblotted using anti-Caveolin antibody. (D and E) Inhibition of P-glycoprotein with PSC 833 induces increased Rho123 uptake in human brain endothelial cell line HCMEC-D3 (D) and primary human brain endothelial cells (E). * indicates where $P<0.05$ (n=3, two tailed student t-test).

inhibitor of P-gp, PSC 833 and Rho123 uptake was measured. We observed that Rho123 accumulation was increased in a time dependent manner in both human primary brain endothelial cells and the human brain endothelial cell line (Fig 3.1.D and E). P-gp down regulation was observed beginning at 60 minutes and was maintained up to 90 minutes indicating that P-gp function was effectively downregulated in HCMEC-D3 by the functional inhibitor (Fig 3.1.D). P-gp down regulation was observed in primary human brain endothelial cells beginning at 15 minutes and was maintained up to 90 minutes (Fig 3.1.E). These results indicated that these cells are valid *in vitro* models to test the modulation and function of P-gp by AR signaling.

Activation of A2A AR downregulates P-gp expression and function in brain endothelial cells.

Previously, we have shown that AR-mediated signaling increases the permeability of the BBB to entry of large molecules *in vivo* and *in vitro* [30, 39]. In this study, to test the hypothesis that AR signaling regulates P-gp function, we used *in vitro* BBB models to determine if AR signaling indeed can inhibit the expression and function of P-gp. First, we tested the effect of AR signaling on P-gp expression level in primary mouse brain endothelial cells that were grown to form monolayers and then treated with or without 1 uM of the A2A AR agonist Lexiscan, or NECA, a broad spectrum AR agonist, at different time point up to 72 hrs. Western blot analysis of P-gp showed rapid down regulation of P-gp beginning at 30 minutes, which were maintained up to 1 hour (Supplementary Fig 3.1.A). This was reversed at 4 hours and

began to decrease thereafter up to 48 hours then reversed at 72 hrs (Supplementary Fig 3.1.A). In NECA treated primary (mouse) brain endothelial cells, P-gp expression decreased very rapidly and it remained downregulated for up to 4 hours, and by 8 hours it returned to baseline levels (Supplementary Fig 3.1.B).

We next performed similar experiments in the human brain endothelial cell line and in human primary brain endothelial cells. Monolayers of HCMEC-D3 cells were treated with NECA or Lexiscan and P-gp expression was analyzed by western blot analysis. In HCMEC-D3 cells, Lexiscan treatment induced rapid decrease in P-gp expression beginning from 30 minutes and was maintained up to 1 hr. Interestingly, at 24 to 48 hrs, P-gp expression decreased even more prominently (Fig 3.2.A). NECA also decreased P-gp expression up to 4 hrs, and P-gp returned to basal levels at 8 hrs and declined again from 48 hrs to 72 hrs (Fig 3.2.B). As proof that P-gp downregulation by Lexiscan and NECA correlates with increased substrate accumulation, we evaluated accumulation Rho123 in brain endothelial cells. Lexiscan increased Rho123 accumulation in HCMEC D3 cell line from 15 minutes and was maintained up to 90 minutes (Fig 3.2.C). NECA treatment showed similar trend in Rho123 accumulation although it was not statistically significant (Fig 3.2.D). This suggests that decrease in P-gp expression level by AR activation is consistent with decreased P-gp functionality. As cell lines do not always faithfully reproduce all the characteristics as primary cells, we next examined the effect of Lexiscan and NECA treatment on P-gp expression in primary human brain endothelial cells.

Figure 3.2.

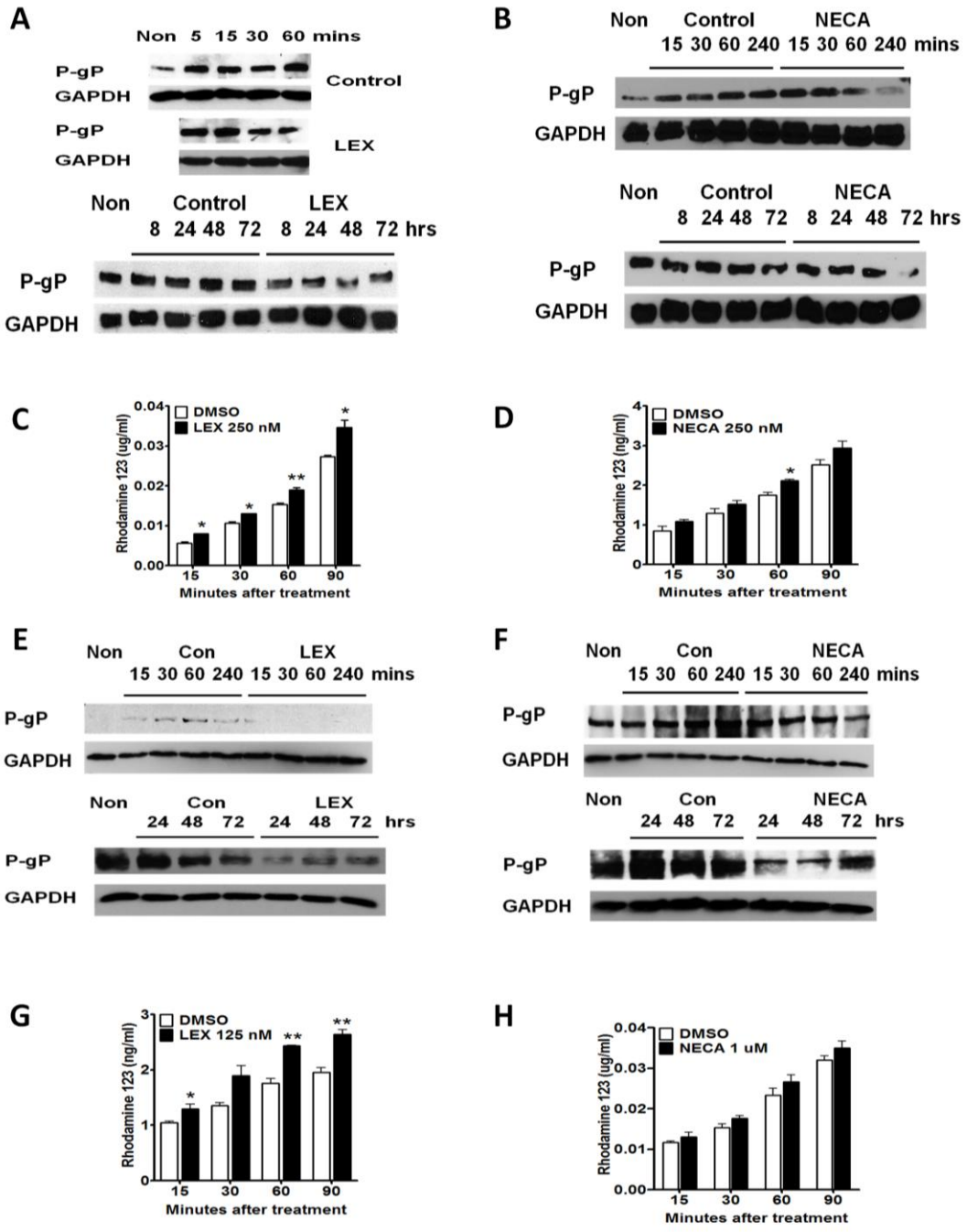
A
Non 5 15 30 60 mins
P-gP
GAPDH
Control
P-gP
GAPDH
LEX
Non Control LEX
8 24 48 72 8 24 48 72 hrs
P-gP
GAPDH
B
Non Control NECA
15 30 60 240 15 30 60 240 mins
P-gP
GAPDH
Non Control NECA
8 24 48 72 8 24 48 72 hrs
P-gP
GAPDH
C
DMSO
LEX 250 nM
Rhodamine 123 (ug/ml)
Minutes after treatment
D
DMSO
NECA 250 nM
Rhodamine 123 (ng/ml)
Minutes after treatment
E
Non Con LEX
15 30 60 240 15 30 60 240 mins
P-gP
GAPDH
Non Con LEX
24 48 72 24 48 72 hrs
P-gP
GAPDH
F
Non Con NECA
15 30 60 240 15 30 60 240 mins
P-gP
GAPDH
Non Con NECA
24 48 72 24 48 72 hrs
P-gP
GAPDH
G
DMSO
LEX 125 nM
Rhodamine 123 (ng/ml)
Minutes after treatment
H
DMSO
NECA 1 uM
Rhodamine 123 (ug/ml)
Minutes after treatment

Figure 3.2. A2A AR activation decreases expression and functionality of P-glycoprotein in human brain endothelial cell line and human primary brain endothelial cell. (A and B) Western blot analysis of P-glycoprotein on HCMEC-D3 cells treated with Lexiscan (1 uM) (A) or NECA (1 uM) (B) upto 72 hrs were performed. GAPDH was used as loading control. (C and D) Rho123 uptake assay on HCMEC-D3 cells treated with Lexiscan (1 uM) (C) or NECA (1 uM) (D) was performed. Concentration of Rho123 was analyzed with fluometry with excitation at 488 nm and emission at 523 nm. *, ** indicate where $P<0.05$ and $P<0.01$, respectively (n=4, two tailed student t-test). (E and F) Western blot analysis of P-glycoprotein on primary brain endothelial cells treated with Lexiscan (1 uM) (E) or NECA (1 uM) (F) upto 72 hrs were performed. GAPDH was used as loading control. (G and H) Rho123 uptake assay on primary brain endothelial cells treated with Lexiscan (1 uM) (G) or NECA (1 uM) (H) was performed. Concentration of Rho123 was analyzed with fluometry with excitation at 488 nm and emission at 523 nm. . *, ** indicate where $P<0.05$ and $P<0.01$, respectively (n=4, two tailed student t-test).

Both Lexiscan and NECA treatment exerted similar effect on P-gp expression level in human primary brain endothelial cells as was observed in human brain endothelial cell line, HCMEC- D3 (Fig 3.2. E and F). Similar to HCMEC-D3 cells, Lexiscan induced rapid downmodulation of P-gp expression which began to decrease at 30 minutes and was recovered by 4 hours. This down- modulatory trend was once again induced up to 48 hrs and recovered by 72 hrs (Fig 3.2.E). In NECA treatment group, the expression level of P-gp begins to decrease from 1 hour and was maintained up to 72 hrs (Fig 3.2.F). This was recapitulated in the Rho123 uptake assay which showed Lexiscan rapidly suppressed P-gp function beginning from 15 minutes and was maintained up to 4 hrs. NECA showed a trend in P-gp suppression but it did not reach statistical significance (Fig 3.2.G and H). We next determined P-gp functionality in a transmigration assay using primary human brain endothelial cells. Lexiscan induced rapid increase in permeability to Rho123 beginning from 5 to 60 minutes, it returned to the steady state by 2 hrs, it increased again by 4 hrs and was maintained up to 12 hrs. NECA's effect occurred at 12 hours and maintained up to 24 hrs (Fig 3.3.A and B). To further dissect the effect of AR signaling on the functionality of P-gp and Rho123 accumulation in primary human brain endothelial cells, endothelial cells were treated with Rho123 with or without Lexiscan and Rho123 accumulation was visualized by IFA at different time points. Lexiscan increased the accumulation of Rho123 beginning from 15 minutes to 1 hr. NECA treatment increased Rho123 accumulation at later time points, beginning from 4 hrs and was maintained up to 24 hours (Fig 3.3.C-F). This indicates that NECA treatment also increased Rho123 accumulation in primary human brain endothelial cells as shown by IFA. Overall, these results indicate

Figure 3.3.

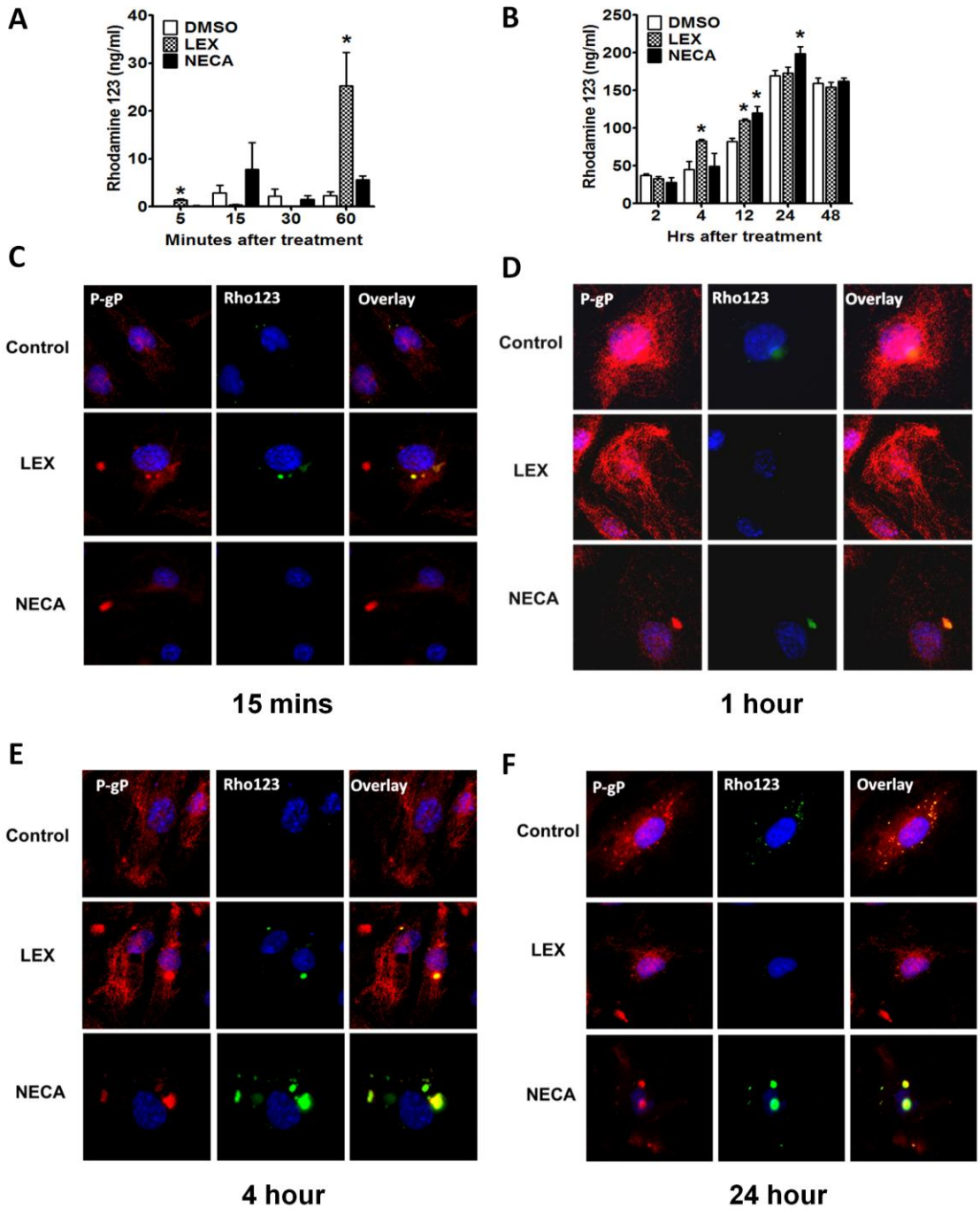
A
Rhodamine 123 (ng/ml)
DMSO
LEX
NECA
Minutes after treatment
B
Rhodamine 123 (ng/ml)
Hrs after treatment
C
P-gP
Rho123
Overlay
Control
LEX
NECA
15 mins
D
1 hour
E
4 hour
F
24 hour

Figure 3.3. Activation of A2A AR by Lexiscan induces rapid transmigration of Rho123 through *in vitro* human BBB and its accumulation in primary brain endothelial cell. (A and B) Rho123 migration assay with *in vitro* blood brain barrier model using primary human brain endothelial cells cultured on porous membrane. Cells on porous membrane were treated with Lexiscan (0.25 uM) or NECA (0.25 uM) concomitantly with 2.5 uM of Rho123 and concentration of Rho123 at the bottom chambers was analyzed with fluometry with excitation at 488 nm and emission at 523 nm. Short time point upto 60 minutes (A) and long time point upto 48 hrs (B) are plotted separately. * indicates where $P<0.05$ (n=4, two tailed student t-test). (C-F) Primary human brain endothelial cells were cultured on the coverslip and treated with 2.5 uM of Rho123 with or without 1 uM of Lexiscan or NECA at different time point (15 minutes, 1, 4, 24 hours). Cells were fixed with 4% PFA and co-stained with P-glycoprotein and visualized with fluorescent microscope.

that activation of A2A AR by Lexiscan, potently and rapidly increase the transcellular permeability in human brain endothelial cells in a reversible manner. While NECA exhibited similar effects, its permeability kinetics occurred later and was less potent than Lexiscan's. These results indicates that AR activation, specifically, A2A AR activation has a potent effect on P-gp expression and function and that this effect is multi-modal suggesting that multiple mechanisms may be involved in P-gp downregulation/function under AR signaling.

A2A AR activation induces rapid downmodulation of P-gp, by activation of MMP9, ubiquitinilyation and translocation to insoluble fraction compartment.

To better understand the mechanism behind the rapid down regulation of P-gp observed after Lexiscan treatment, we used CSK buffer which extracts insoluble cytoskeletal materials to determine whether P-gp is contained in the insoluble fraction as this might explain its rapid down-modulation upon Lexiscan treatment. Comparison of P-gp expression level in cytoskeletal fraction to P-gp in whole lysate showed increased P-gp in the cytoskeletal fraction compared to control (Fig 3.4.). P-gp levels increased from 5 to 15 minutes, it returned to baseline by 30 minutes and was maintained up to 60 minutes (Fig 3.4.A). By contrast, in whole lysate, P-gp levels declined compared to DMSO control beginning at 5 minutes and was maintained up to 60 minutes (Fig 3.4.B). This suggests that P-gp in the soluble fraction may have been translocated to the cyotskeletal fraction by the A2A AR signaling at early time point and may explain the rapid decrease in P-gp level upon Lexiscan treatment.

Figure 3.4.

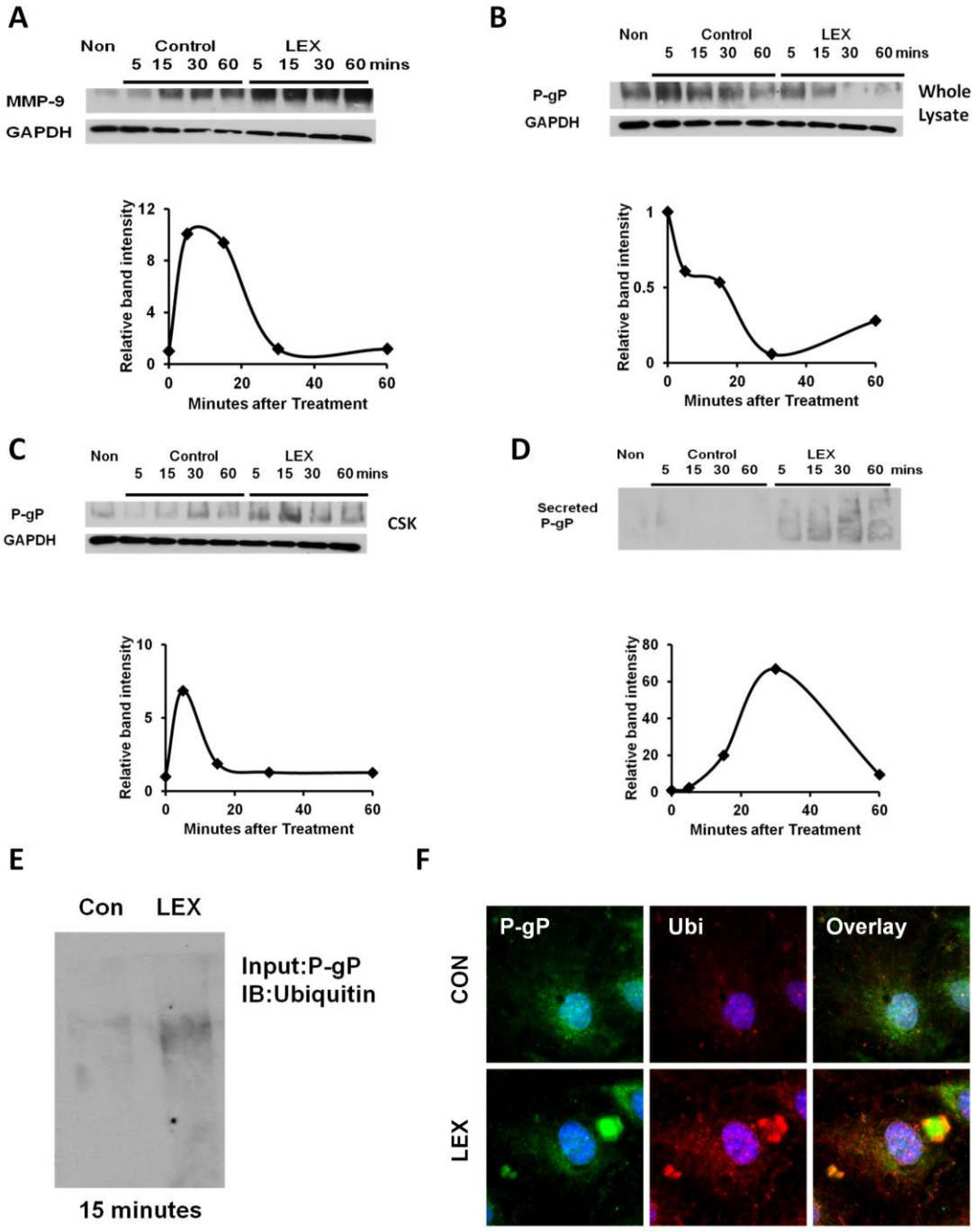
A
Non
Control
LEX
5 15 30 60 5 15 30 60 mins
MMP-9
GAPDH
Relative band intensity
Minutes after Treatment
B
Non
Control
LEX
5 15 30 60 5 15 30 60 mins
P-gP
GAPDH
Whole Lysate
Relative band intensity
Minutes after Treatment
C
Non
Control
LEX
5 15 30 60 5 15 30 60 mins
P-gP
GAPDH
CSK
Relative band intensity
Minutes after Treatment
D
Non
Control
LEX
5 15 30 60 5 15 30 60 mins
Secreted P-gP
Relative band intensity
Minutes after Treatment
E
Con
LEX
Input:P-gP
IB:Ubiquitin
15 minutes
F
P-gP
Ubi
Overlay
CON
LEX

Figure 3.4. A2A AR activation induces rapid downmodulation of P-gp, by activation of MMP9, ubiquitinilyation and translocation to insoluble fraction compartment. (A and B) Western blot analysis of P-gp in human primary brain endothelial cells upon activation with Lexiscan at different time point which was lysed using RIPA buffer (A) and CSK buffer (B). GAPDH was used as loading control. Intensity of band was normalized using GAPDH and plotted as graph. (C) Western blot analysis of matrix metalloproteinase 9 (MMP9) in human primary brain endothelial cells upon activation with Lexiscan at different time point. GAPDH was used as loading control. Intensity of band was normalized using GAPDH and plotted as graph. (D) Western blot analysis of secreted P-gp in human primary brain endothelial cells upon activation with Lexiscan at different time point. Intensity of band was plotted as graph. (E) Immunoprecipitation analysis of Ubiquitinylation of P-gp in human primary brain endothelial cells upon activation with Lexiscan for 15 minutes. P-gp was pulled down with an anti P-gp antibody and immunoblotted with anti ubiquitin antibody. (F) IFA of ubiquitinyltion of P-gp in human primary brain endothelial cells upon activation with Lexiscan for 15 minutes. Cells were fixed and permeablized and stained with anti P-gp (Green) and anti-ubiquitin (Red) antibody. Nucleus was counterstained with DAPI (Blue).

We next explored the possibility that matrix metalloproteinase 9 (MMP 9) which can be induced by various ARs, and degrades extracellular matrix molecules

may become activated and cleave P-gP, resulting in its rapid decrease as early as 5 minutes after Lexiscan treatment. We observed increased expression of MMP 9 beginning from 5 minutes that matched the same kinetics of P-gp decrease (Fig 3.4.C). We also observed increase in secreted P-gp that was released into the media with similar kinetics to MMP9 expression (Fig 3.4.D). This suggests that MMP9 is at least in part responsible for the early and rapid decrease in P-gp levels upon Lexiscan treatment (Fig 3.4.C and D).

We next determined whether A2A AR activation by Lexiscan can activate ubiqutinylation of P-gp and thereby results in its rapid decrease. Primary human brain endothelial cells were treated with Lexiscan for 15 minutes, and immunoprecipitation for P-gp was performed and the eluent was immunoblotted against an antibody for Ubiquitin. The results showed that treatment of primary human brain endothelial cells with Lexiscan for 15 minutes induced increased ubiquitinylation of P-gp compared to vehicle control (Fig 3.4.E). This was further captured by strong colocalization of P-gp with ubiquitin after 15 minutes of treatment of primary human brain endothelial cells with Lexiscan, further indicating that Lexiscan can induce rapid ubiquitinilyation of P-gp and helps to explain its rapid down-modulation by Lexiscan stimulation (Fig 3.4.F).

Ablation of CD73 or ARs increased P-gp expression, and decreased P-gp substrate accumulation in the brain.

To determine whether our *in vitro* data can be captured *in vivo*, we sought to determine whether signaling via the A2A AR regulates P-gp expression and functionality in brain of mice. First, we examined primary brain endothelial cells from brains of mice with genetic deletion of A1, A2A AR or CD73 to determine whether P-gp expression is altered in their absence compared to WT mice. We observed increased expression of P-gp in primary brain endothelial cells from mice lacking A1 or A2A AR or CD73 compared to WT controls (Fig 3.5.A). Moreover, we observed significant decrease in the accumulation of P-gp substrate Rho123 in brain primary brain endothelial cells (Fig 3.5.A and B). We next determined if increased P-gp is observed in the endothelial cells within the brains of these KO animals. We found that A2A AR and CD73 KO animals showed stronger P-gp signal than A1 AR KO mice which showed similar P-gp expression to WT. This indicates that extracellular adenosine acting through its A2A receptor is the major signaling component involved in P-gp expression/function (Fig 3.5.C and D).

AR activation down-modulates P-gp expression and function in brain endothelial cells *in vivo*.

Since we observed endogenous expression of P-gp is decreased in brain capillaries of CD73 KO and A2A AR KO mice, we next determined whether activation of A2A AR with Lexiscan or NECA can induce downregulation of P-gp expression and function in brain endothelial cells in these mice compared to WT.

Figure 3.5.

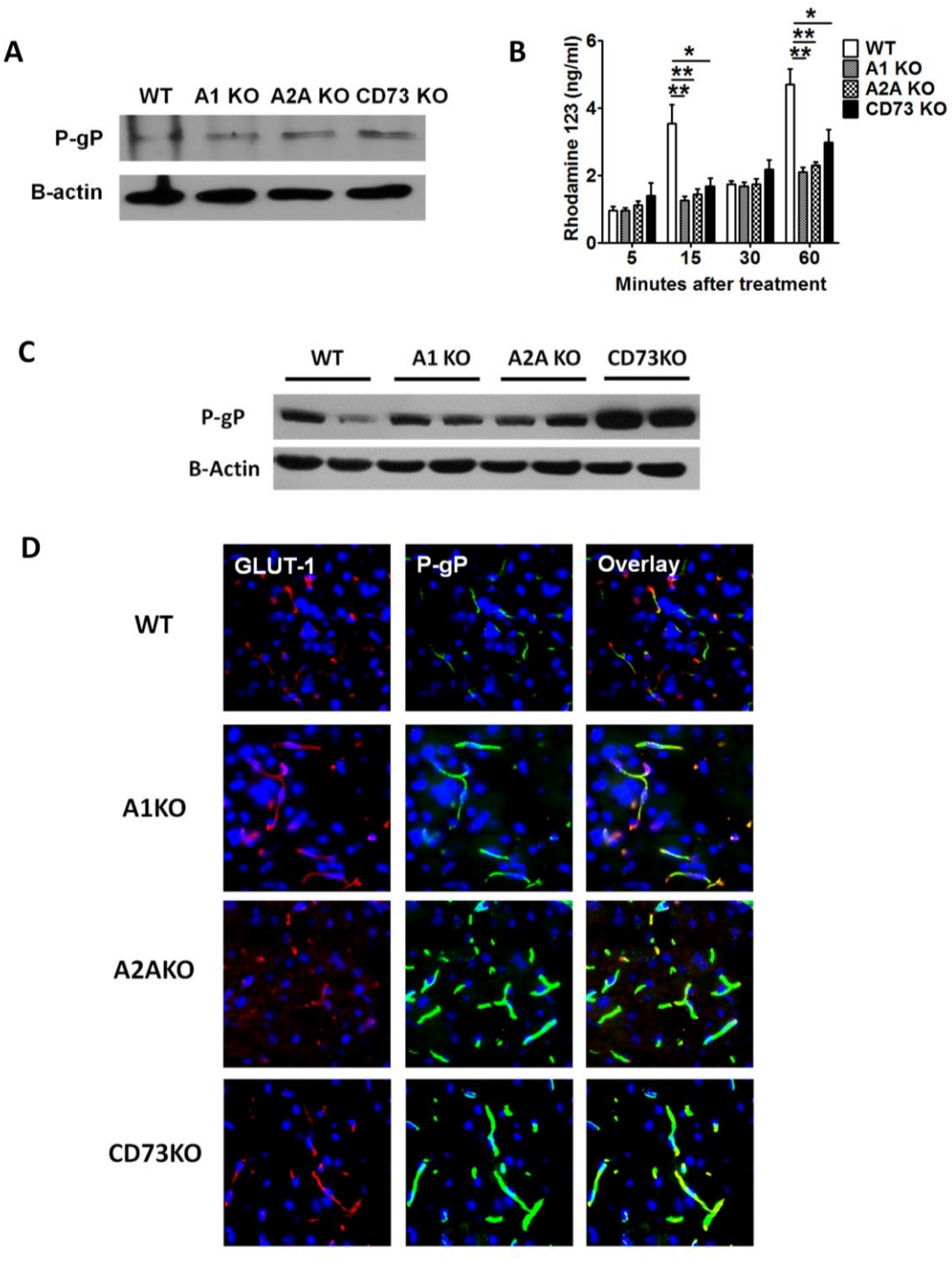
A
WT
A1 KO
A2A KO
CD73 KO
P-gP
B-actin
B
Rhodamine 123 (ng/ml)
Minutes after treatment
5
15
30
60
WT
A1 KO
A2A KO
CD73 KO
C
WT
A1 KO
A2A KO
CD73KO
P-gP
B-Actin
D
GLUT-1
P-gP
Overlay
WT
A1KO
A2AKO
CD73KO

Figure 3.5. Ablation of ARs and 5' ecto-nucleotidase induces the increase in the P-glycoprotein expression and functionality in brain vascular endothelial cells. (A) Western blot analysis of P-gp from primary brain endothelial cells of brains of WT, A1, A2A, CD73 KO mice. Beta actin was used as loading control. (B) Rho123 uptake assay using primary brain endothelial cells from brains of WT, A1, A2A, CD73 KO mice. Cells were cultured until it reached full confluency and treated with 2.5 uM of Rho123 at 5, 15, 30, 60 minutes and analyzed by fluometry with excitation at 488 nm and emission at 523 nm. *, ** indicate where $P<0.05$ and $P<0.01$, respectively (n=4, two tailed student t-test). (C) Western blot analysis on the P-gp expression level from the brain of WT, A1 KO, A2A KO, CD73 KO. Beta actin was used as loading control. (D) IFA on the brain of WT, A1 KO, A2A KO, CD73 KO. Brain frozen section was stained with GLUT1 (Red), P-gP (Green) and counterstained with DAPI (Blue). Nucleus was counterstained with DAPI (Blue)

Figure 3.6.

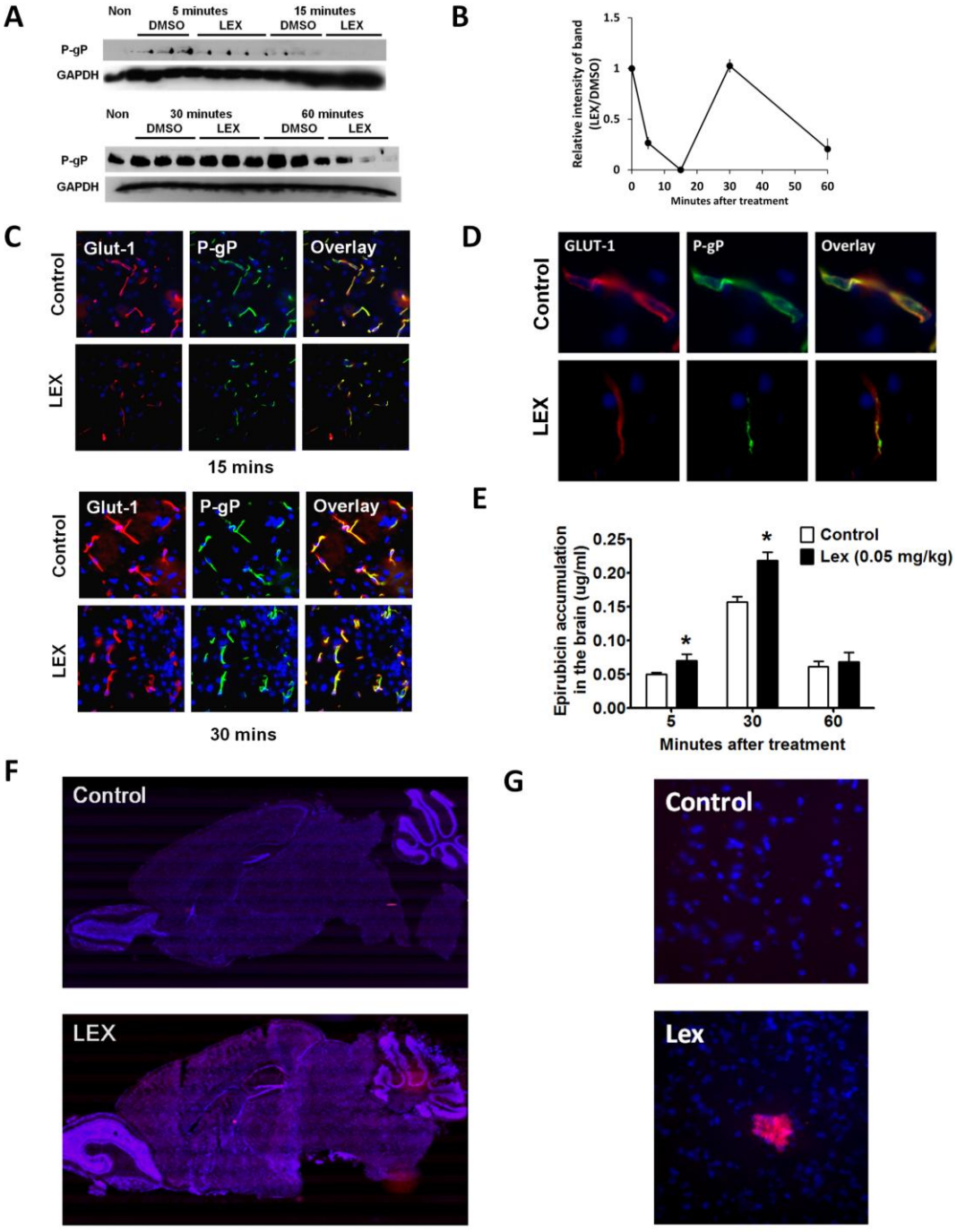
A
Non
5 minutes
15 minutes
DMSO
LEX
DMSO
LEX
P-gP
GAPDH
Non
30 minutes
60 minutes
DMSO
LEX
DMSO
LEX
P-gP
GAPDH
B
Relative intensity of band (LEX/DMSO)
1.5
1
0.5
0
0
10
20
30
40
50
60
Minutes after treatment
C
Glut-1
P-gP
Overlay
Control
LEX
15 mins
Glut-1
P-gP
Overlay
Control
LEX
30 mins
D
GLUT-1
P-gP
Overlay
Control
LEX
E
Epirubicin accumulation in the brain (ug/ml)
0.25
0.20
0.15
0.10
0.05
0.00
*
*
Control
Lex (0.05 mg/kg)
5
30
60
Minutes after treatment
F
Control
LEX
G
Control
Lex

Figure 3.6. A2A receptor activation by Lexiscan induces rapid and reversible down regulation of P-glycoprotein expression and functionality in the brain vascular endothelial cells *in vivo*. (A) Western blot analysis on the P-glycoprotein expression level in the Lexiscan treated mouse brain. GAPDH was used as loading control. (B) Densitometric analysis of the P-glycoprotein expression level normalized by GAPDH. Intensity of bands from Lexiscan treated brains were divided by that of DMSO treated brains. (C and D) Immnofluorescence assay on Lexiscan treated mouse brain (15 and 30 minutes). Brain frozen section were stained with GLUT1 (Red), P-gP (Green) and counterstained with DAPI (Blue). (E) Epirubicin brain accumulation assay in the Lexiscan treated mice. 10 mg/kg of Epirubicin was injected retro-orbitally with or without 0.05 mg/kg of Lexiscan. Mice were perfused with ice-cold PBS and sacrificed at different time points and the accumulation of Epirubicin in the brain was measured using fluormetry with excitation at 488 nm and emission at 590 nm. * indicates where $P<0.05$ (n=4, two tailed student t-test). (F and G) Fluroescent microscopic analysis of Epirubicin accumulation in the brain with Lexiscan treatment. 10 mg/kg of Epirubicin was injected retro-orbitally with or without 0.05 mg/kg of Lexiscan for 15 minutes. Mice were perfused with ice-cold PBS and sacrificed and brain was sectioned for microscopic analysis for full brain image (F) and focal zoomed image (G). Epirubicin is in red and nucleus was counter stained with DAPI (blue).

Lexiscan treatment decreased P-gp expression from 5 minutes to 15 minutes and was recovered at 30 minutes as shown by western blot and IFA (Fig 3.6.A-D). Next, to test whether these changes in P-gp expression level in these KO animals directly affect the functionality of P-gp and its substrate accumulation in the brain, we used epirubicin which has auto-fluoresces, allowing us to quantify its accumulation in the brain by fluormetry.

Consistent with P-gp down modulation, Epirubicin accumulation in the brain begins to increase at 5 minutes and it was maintained up to 30 minutes and returned to baseline by 60 minutes (Fig 3.6.E). This kinetic profile of P-gp downregulation matched exactly with the kinetics of Epirubicin accumulation into the brain (Fig 6A and B). Also, fluorescent images of brain sections showed that Lexiscan treatment increased the accumulation of Epirubicin compared to control (Fig 3.6.F and G). This indicates that A2A AR activation rapidly decrease P-gp expression and function, resulting in the accumulation of P-gp substrate in the brain.

Similarly, NECA induced a gradual decrease in P-gp expression level beginning from 2 hours and was maintained up to 18 hrs (Fig 3.7.A and B). The kinetics of Epirubicin accumulation in the brain showed transient decrease at 2 hours, peaked at 4 hours, and returned to baseline at 12 hours compared to controls (Fig 3.7.C). Interestingly, the kinetics of Epirubicin accumulation in the brain induced by Lexiscan and NECA is very similar to the time window of P-gp down-regulation *in vitro* (Fig 3.2). Based on these findings, we conclude that signaling via the A2A AR on BBB cells activate the transcellular pathway mediated by P-gp. We believe that we

have provided a compelling case for adenosine signaling via the A2A receptor that in the future may lead us closer to drug delivery to the CNS.

Figure 3.7.

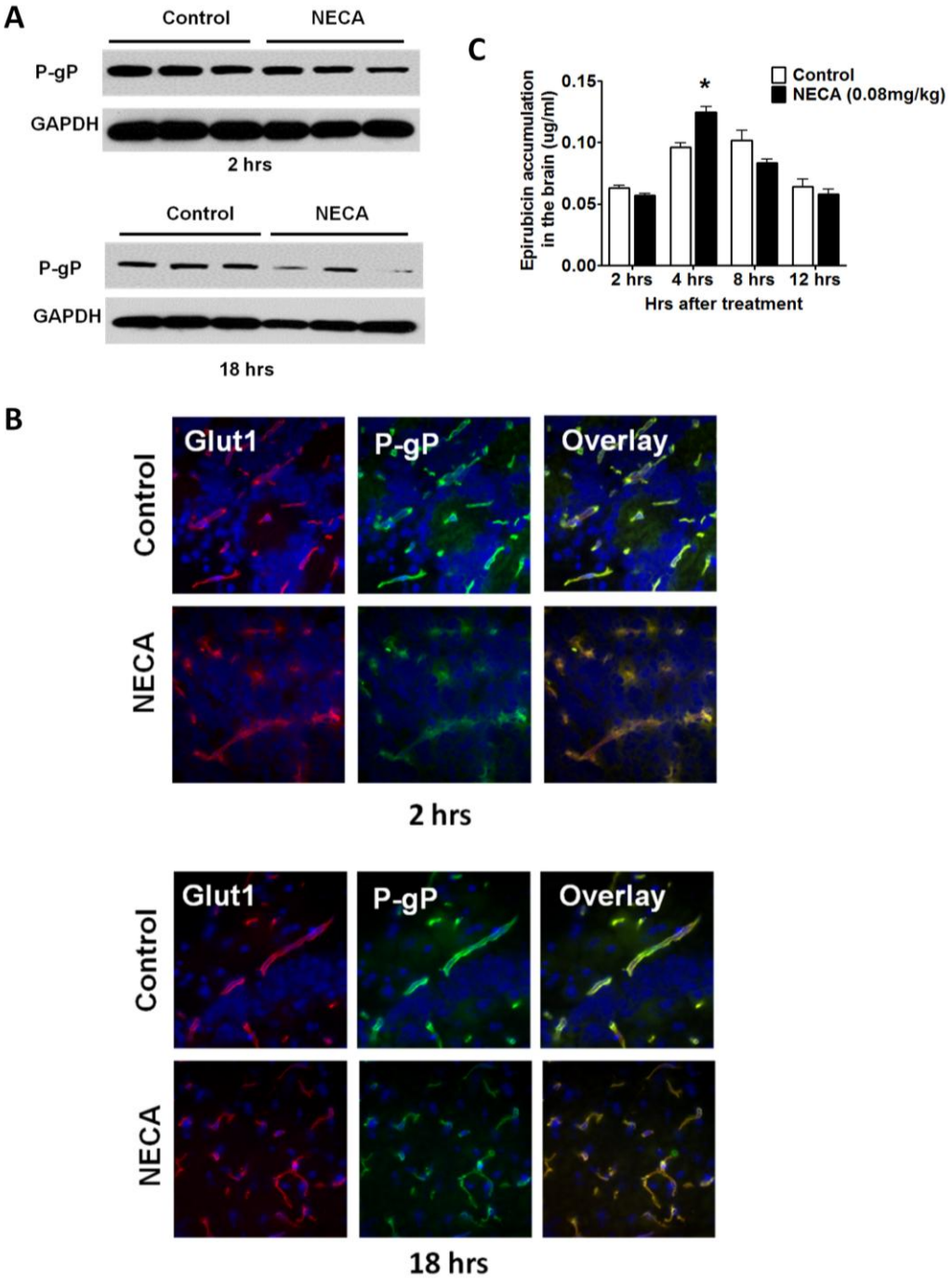
A
Control
NECA
P-gP
GAPDH
2 hrs
Control
NECA
P-gP
GAPDH
18 hrs
C
Control
NECA (0.08mg/kg)
Epirubicin accumulation in the brain (ug/ml)
0.15
0.10
0.05
0.00
*
2 hrs
4 hrs
8 hrs
12 hrs
Hrs after treatment
B
Glut1
P-gP
Overlay
Control
NECA
2 hrs
Glut1
P-gP
Overlay
Control
NECA
18 hrs

Figure 3.7. Broad spectrum AR agonist NECA induces gradual and delayed down regulation of P-glycoprotein expression and functionality in the brain vascular endothelial cells. (A and B) Western blot analysis (A) and IFA (B) on the P-glycoprotein in NECA treated mouse brain at 2 and 18 hours after treatment. For western blot analysis, GAPDH was used as loading control. Brain frozen section were stained with GLUT1 (Red), P-gP (Green) and counterstained with DAPI (Blue). (C) Epirubicin brain accumulation assay in the NECA treated mice. 10 mg/kg of Epirubicin was injected retro-orbitally and treated for 15 minutes after indicated treatment time of mice with or without 0.08 mg/kg of NECA. Mice were perfused with ice-cold PBS and sacrificed at different time points and the accumulation of Epirubicin in the brain was measured using fluormetry with excitation at 488 nm and emission at 590 nm. * indicates where $P<0.05$ (n=4, two tailed student t-test).

3.5. Discussion

The BBB is necessary to protect the brain and maintain its homeostasis. However, its restrictive nature hampers the ability to get therapeutics into the brain. As the world population lives longer, the trend in neurodegenerative diseases increase, especially Alzheimer's. Billions of dollars are spent on drug development to bypass the BBB or to modify drugs such that they would have easier access in traversing the BBB which blocks the delivery of the vast majority of drugs to the brain. After millions-to billions are spent on developing these drugs many of them are dropped from the pipeline as they do not show efficacy or are too large to pass the BBB.

Cells and soluble molecules enter the brain through para-cellular or trans-cellular pathways that are mediated by cell-to-cell junction or transporters, respectively. A variety of transporters and receptors are highly expressed on brain endothelial cells that selectively restrict or allow the entry of substances, some of which are necessary for normal brain function, such as glucose and amino acids, while others are expelled. Our previous studies showed that activation of the A2AAR increases BBB permeability to entry of large molecules that is mediated by increased paracellular permeability, induced RhoA activity and rearrangement of the actin-cytoskeleton in brain endothelial cells. However, since molecules enter the CNS by both transcellular and/or paracellular routes and the transcellular pathway is regulated by efflux transporters, such as P-gp, we wished to determine whether AR signaling also exerted regulatory effects on the trans-cellular pathway of the BBB mediated by P-gp. Not surprisingly, many drugs are expelled by efflux transporters even before entering the brain and therefore are dropped from the drug development pipeline in the

course of their development. This poses tremendous economic loss and obstacles for public health, in particular, for treatment of CNS diseases. Hence, it is imperative and urgent that we better understand how these processes operate.

In this study, we used a human brain endothelial cell line and primary human and mouse brain endothelial cells as *in vitro* models to investigate the impact of AR signaling on P-gp function, and then we determined whether our in vitro data can be racapitualted in vivo in mice. Our *in vitro* data showed that activation of AR significantly and potently altered P-gp expression/function. P-gp expression was rapidly down modulated in both primary human and mouse brain endothelial cells and in a human brain endothelial cell line by activation of A2A AR with Lexiscan treatment. In NECA treatment, down modulation of P-gp occurred later than that of Lexiscan. We believe the difference in both Lexiscan and NECA's effects is a result of the difference in their half lives: Lexiscan's half life is approximately 2.5 minutes whereas NECA's is 5 hours. The down modulation of P-gp by AR activation strikingly correlates with P-gp function that was confirmed by Rho123 accumulation and extravazation assays in primary human brain endothelial cells.

As we observed a potent and rapid down modulation of P-gp that occured over multiple time points after lexiscan treatment of primary human brain endothelial cells, we hypothesized that AR activation may regulate P-gp expression and function by multiple mechanisms. We next investigated the molecular mechanism behind the rapid down modulation of P-gp. In an insoluble fractionation assay, we observed that a significant amount of P-gp is moved into the insoluble fraction in the upon Lexiscan treatment of primary human brain endothelial cells. Moreover, we observed soluble P-

gp in brain endothelial culture supernatants suggesting P-gp is cleaved and released into the extracellular environment. Consistent with this notion, we found concomitant increase in MMP-9 levels which suggests that MMP9 may also be involved in downregulation of P-gp upon AR activation. It is also reported that P-gp is regulated by ubiqutinylation. In support of this, we observed rapid ubiquitinylation of P-gp by Lexiscan both by IFA and immunoproecipitation analysis. Together, these findings suggest that A2A AR activation of human and mouse brain endothelial cells regulate P-gp expression/function by multiple mechanisms.

Consistent with our *in vitro* findings, we observed AR activation exerted similar effects on P-gp expression and function *in vivo*. In mouse brain endothelial cells, Lexiscan's effects on P-gp was rapid, occurring within 5 minutes, whereas the effect of NECA was observed 2 hrs later. These findings are consistent with findings in our in vitro analyses in human brain endothelial cell models. As proof of principle that AR activation causes P-gp downregulation resulting in increased accumulation of P-gp substrates, we examined the effects of lexiscan treatment on the accumulation of the chemotherapeutic drug Epirubicin, which is a P-gp substrate. We observed that AR activation increased the accumulation of Epirubicin in the brain which coincides with the kinetics of P-gp down-modulation. Consistent with our observation in vitro in human brain endothelial cells, Lexiscan's effect on accumulation of Epirubicin was rapid whereas NECA's was gradual. We believe this difference in permeability kinetics between the two agonists stems from differences in their half-lives (Lexiscan, 2.5 minutes and NECA, 5 hrs).

P-gp has long posed a tremendous hindrance to drug delivery to the brain and across biological barrier in general. This molecule functions by expelling drugs and xenobiotics from cells and it alters drug Pharmacokinetics. Its broad substrate spectrum allows it to expel drugs from almost all different classes. Moreover, P-gp expression or upregulation in various cancers and cell types poses a poor prognosis for cancers. Therefore, our data showing that signaling via the A2A AR alters P-gp function has very broad appeal beyond the CNS. It suggests that AR modulation may be a *bona fide* mechanism of altering P-gp function to effectively treat all major cancers in general. We propose that these studies stands to open the door to studies well beyond just modulation of the BBB.

Until recently, the brain was considered a formidable fortress that doesn't allow the entry of molecules or cells into the CNS. However, with technological advancement and emerging studies revealed that the brain is not totally cutoff from the rest of the body, rather, it is selectively separated in order to maintain proper brain physiology. Adenosine is a damage/danger-signaling molecule that responds to cell stress or tissue damage by inducng a cascade of events involving recruitment of cells and substances across biological needed to repair damage tissues. Therefore, adenosine is an endogenous (built in system) modulator that regulates the BBB permeability to recruit molecules into the CNS (to repair it) during CNS damage or stress. We posit that this system operated by AR signaling operates as a door and adenosine is the key that signals its opening. We propose that this built in mechanism relies on the extremely short half life of adenosine (about 10 secs) to reverse the BBB permeability.

Taken together, we believe that in future, AR modulation of the BBB may offer a safe means of delivering drugs into the CNS. Based on these studies, AR signaling in modulation of BBB permeability offers a time line of drug delivery to the brain. This can be transient or gradual depending on A2A AR agonist used. ARs, and the enzymes that generate it are expressed directly on BBB cells. AR pharmagological agents are abundant and some are already FDA-approved and removes some potential hurdles for use. In summary, our data showing that AR mediates P-gp function in BBB permeability is exciting, highly translational and stands to have a high impact on public health. In future, A2A AR modulation of BBB via regulation of P-gp may provide a real alternative to treating brain tumors like gliomas for which there is no cure and where the life span of glioma patients is 18 months.

References

1. Abbott, N.J., *Astrocyte-endothelial interactions and blood-brain barrier permeability.* J Anat, 2002. **200**(6): p. 629-38.
2. Abbott, N.J., L. Ronnback, and E. Hansson, *Astrocyte-endothelial interactions at the blood-brain barrier.* Nat Rev Neurosci, 2006. **7**(1): p. 41-53.
3. Deeken, J.F. and W. Loscher, *The blood-brain barrier and cancer: transporters, treatment, and Trojan horses.* Clin Cancer Res, 2007. **13**(6): p. 1663-74.
4. Gabathuler, R., *Approaches to transport therapeutic drugs across the blood-brain barrier to treat brain diseases.* Neurobiol Dis, 2010. **37**(1): p. 48-57.
5. Abbott, N.J., *Blood-brain barrier structure and function and the challenges for CNS drug delivery.* Journal of inherited metabolic disease, 2013. **36**(3): p. 437-49.
6. Ballabh, P., A. Braun, and M. Nedergaard, *The blood-brain barrier: an overview: structure, regulation, and clinical implications.* Neurobiology of disease, 2004. **16**(1): p. 1-13.
7. Neuwelt, E.A., et al., *Osmotic blood-brain barrier disruption. Computerized tomographic monitoring of chemotherapeutic agent delivery.* J Clin Invest, 1979. **64**(2): p. 684-8.
8. Elliott, P.J., et al., *Intravenous RMP-7 selectively increases uptake of carboplatin into rat brain tumors.* Cancer Res, 1996. **56**(17): p. 3998-4005.

9. Pardridge, W.M., *Drug transport across the blood-brain barrier.* Journal of cerebral blood flow and metabolism : official journal of the International Society of Cerebral Blood Flow and Metabolism, 2012. **32**(11): p. 1959-72.

10. Cook, A.M., et al., *Intracerebroventricular administration of drugs.* Pharmacotherapy, 2009. **29**(7): p. 832-45.

11. Daneman, R. and A. Prat, *The Blood-Brain Barrier.* Cold Spring Harb Perspect Biol, 2015. **7**(1).

12. Abbott, N.J., *Astrocyte-endothelial interactions and blood-brain barrier permeability.* Journal of anatomy, 2002. **200**(6): p. 629-38.

13. Pascual, J.M., et al., *GLUT1 deficiency and other glucose transporter diseases.* European journal of endocrinology / European Federation of Endocrine Societies, 2004. **150**(5): p. 627-33.

14. Pardridge, W.M., *The blood-brain barrier: bottleneck in brain drug development.* NeuroRx : the journal of the American Society for Experimental NeuroTherapeutics, 2005. **2**(1): p. 3-14.

15. Begley, D.J., *ABC transporters and the blood-brain barrier.* Current pharmaceutical design, 2004. **10**(12): p. 1295-312.

16. Beaulieu, E., et al., *P-glycoprotein is strongly expressed in the luminal membranes of the endothelium of blood vessels in the brain.* Biochem J, 1997. **326 (Pt 2)**: p. 539-44.

17. Chung, H.C., et al., *P-glycoprotein: the intermediate end point of drug response to induction chemotherapy in locally advanced breast cancer.* Breast Cancer Res Treat, 1997. **42**(1): p. 65-72.

18. Filipits, M., et al., *Immunocytochemical detection of the multidrug resistance-associated protein and P-glycoprotein in acute myeloid leukemia: impact of antibodies, sample source and disease status.* Leukemia, 1997. **11**(7): p. 1073-7.

19. Oda, Y., et al., *Expression of MDR1/p-glycoprotein and multidrug resistance-associated protein in childhood solid tumours.* Virchows Arch, 1997. **430**(2): p. 99-105.

20. Hebert, M.F., *Contributions of hepatic and intestinal metabolism and P-glycoprotein to cyclosporine and tacrolimus oral drug delivery.* Adv Drug Deliv Rev, 1997. **27**(2-3): p. 201-214.

21. Kusuhara, H., et al., *P-Glycoprotein mediates the efflux of quinidine across the blood-brain barrier.* J Pharmacol Exp Ther, 1997. **283**(2): p. 574-80.

22. Schinkel, A.H., *P-Glycoprotein, a gatekeeper in the blood-brain barrier.* Adv Drug Deliv Rev, 1999. **36**(2-3): p. 179-194.

23. Yang, C.P., et al., *Progesterone interacts with P-glycoprotein in multidrug-resistant cells and in the endometrium of gravid uterus.* J Biol Chem, 1989. **264**(2): p. 782-8.

24. Gottesman, M.M. and V. Ling, *The molecular basis of multidrug resistance in cancer: the early years of P-glycoprotein research.* FEBS Lett, 2006. **580**(4): p. 998-1009.

25. Gottesman, M.M., S.V. Ambudkar, and D. Xia, *Structure of a multidrug transporter.* Nat Biotechnol, 2009. **27**(6): p. 546-7.

26. Aller, S.G., et al., *Structure of P-glycoprotein reveals a molecular basis for poly-specific drug binding.* Science, 2009. **323**(5922): p. 1718-22.

27. Jette, L., M. Potier, and R. Beliveau, *P-glycoprotein is a dimer in the kidney and brain capillary membranes: effect of cyclosporin A and SDZ-PSC 833.* Biochemistry, 1997. **36**(45): p. 13929-37.

28. Horton, J.K., et al., *Characterization of a novel bisacridone and comparison with PSC 833 as a potent and poorly reversible modulator of P-glycoprotein.* Mol Pharmacol, 1997. **52**(6): p. 948-57.

29. van Asperen, J., et al., *Enhanced oral bioavailability of paclitaxel in mice treated with the P-glycoprotein blocker SDZ PSC 833.* Br J Cancer, 1997. **76**(9): p. 1181-3.

30. Kim, D.G. and M.S. Bynoe, *A2A Adenosine Receptor Regulates the Human Blood-Brain Barrier Permeability.* Molecular neurobiology, 2014.

31. Carman, A.J., et al., *Adenosine receptor signaling modulates permeability of the blood-brain barrier.* J Neurosci, 2011. **31**(37): p. 13272-80.

32. Hasko, G., et al., *Adenosine receptor signaling in the brain immune system.* Trends in pharmacological sciences, 2005. **26**(10): p. 511-6.

33. Hasko, G., et al., *Adenosine receptors: therapeutic aspects for inflammatory and immune diseases.* Nature reviews. Drug discovery, 2008. **7**(9): p. 759-70.

34. Jacobson, K.A. and Z.G. Gao, *Adenosine receptors as therapeutic targets.* Nature reviews. Drug discovery, 2006. **5**(3): p. 247-64.

35. Fredholm, B.B., et al., *International Union of Basic and Clinical Pharmacology. LXXXI. Nomenclature and classification of adenosine receptors--an update.* Pharmacol Rev, 2011. **63**(1): p. 1-34.

36. Fredholm, B.B., et al., *Structure and function of adenosine receptors and their genes.* Naunyn-Schmiedeberg's archives of pharmacology, 2000. **362**(4-5): p. 364-74.

37. Mills, J.H., et al., *CD73 is required for efficient entry of lymphocytes into the central nervous system during experimental autoimmune encephalomyelitis.* Proc Natl Acad Sci U S A, 2008. **105**(27): p. 9325-30.

38. Mills, J.H., et al., *A2A adenosine receptor signaling in lymphocytes and the central nervous system regulates inflammation during experimental autoimmune encephalomyelitis.* Journal of immunology, 2012. **188**(11): p. 5713-22.

39. Carman, A.J., et al., *Adenosine receptor signaling modulates permeability of the blood-brain barrier.* The Journal of neuroscience : the official journal of the Society for Neuroscience, 2011. **31**(37): p. 13272-80.

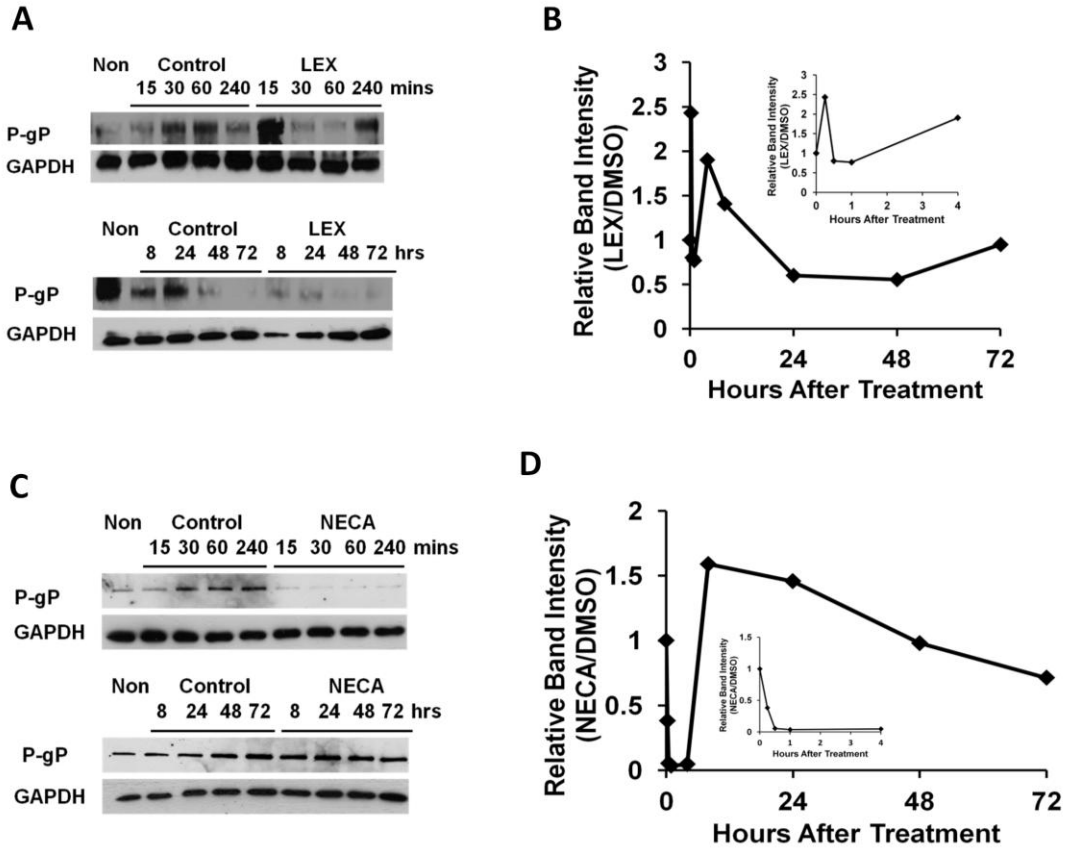

Supplementary Figure 3.1.

Supplementary Figure 3.1. A2A AR activation decreases expression of P-glycoprotein in primary mouse brain endothelial cell. (A) Western blot analysis of P-glycoprotein on primary brain endothelial cells treated with Lexiscan (1 uM) upto 72 hrs were performed. GAPDH was used as loading control. (B) Intensity of P-glycoprotein from western blot (A) was measured and divided by that of GAPDH from each time point and plotted as graph. Short time point (up to 4 hrs) were plotted separately and put as inlet. (C) Western blot analysis of P-glycoprotein on primary brain endothelial cells treated with NECA (1 uM) upto 72 hrs were performed. GAPDH was used as loading control. (D) Intensity of P-glycoprotein from western blot (C) was measured and divided by that of GAPDH from each time point and plotted as graph. Short time point (u pto 4 hrs) were plotted separately and put as inlet.

Chapter 4

Discussion and Conclusion

Since the finding of the existence of blood brain barrier (BBB) by Paul Ehrlich over a hundred years ago [1], the brain has been considered a privileged organ that prevents the entry of molecules and cells [2-6]. This mysterious and unique barrier system protects the brain from aberrant immune responses and assault by toxic substances and pathogens from the periphery [7-10]. Also, this selective transport system allows for the maintenance of nutritional status and an ionic environment, both of which are critically important for normal brain neuronal electrophysiology [11-13]. However, the BBB also acts as a bottleneck for drug delivery into the CNS [14-15]. As life expectancy increases, the number of patients with neurodegenerative diseases is expected to increase to 13.8 million people. The social cost for treatment and care of these patients is estimated to cost around 1.3 trillion dollars [16]. In such circumstances, the need for the development of drugs for CNS diseases, especially neurodegenerative diseases, is increasing tremendously [14, 17]. However, many CNS drugs are dropped out of the pipeline because they do not show the desired effects of crossing the blood brain barrier [15, 17-18]. This has created a new avenue of research on regulating the permeability of the blood brain barrier and increasing drug delivery to the brain to enhance the treatment efficacy for brain diseases [18]. Many studies have attempted to develop a method for increasing the permeability of the BBB, including increasing the osmotic pressure in the peripheral circulatory system, modifying drugs, producing hybrid antibodies, applying focal ultrasonics and drug transporter blockers, and injecting directly into the cranium [17, 19-21]. However, these methods have been found to be 1) invasive, 2) hard to predict in terms of a window of action, 3) irreversible, and 4) ineffective [17, 22]. Shortcomings of the

aforementioned methods have brought up the need to develop a potent, safe, and reversible method for increasing blood brain barrier permeability [17-18, 22].

In a study by Mills *et al.* (2008), CD73 KO mice, lacking endogenous extracellular adenosine, showed reduced severity against experimental autoimmune encephalitis (EAE) compared to wild type mice [23]. The reduced severity of disease was correlated with brains from these knockout animals, showing less infiltration of pathogenic CD4 T cells, which are a major inducer of EAE. Also, the pathogenicity of the immune cells was stronger than that of wild type mice, suggesting reduced permeability of the blood brain barrier in these mice [23]. Additionally, blockade of A2A AR using SCH58216, which is an A2A AR specific blocker, induced less severe EAE compared to the vehicle control, suggesting the critical role of A2A AR in tightening the barrier that prevents transmigration of immune cells through the blood brain barrier [23]. This study led us to explore the effects of adenosine receptor signaling/endogenous adenosine in regulating the permeability of the blood brain barrier [22]. We found that blood brain barrier permeability is increased by the broad spectrum adenosine receptor agonist NECA, which gradually increases permeability to large molecules beginning from 1 hour and peaking at 5 hours [22]. The FDA approved A2A AR agonist Lexiscan also increased permeability rapidly, beginning at 5 minutes and peaking at 30 minutes, and declining thereafter [22]. The effect is safe, reversible, and potent, showing promise for clinical application [22]. This study opened a new avenue for demonstrating the important and critical role of extra-cellular adenosine in the regulation of blood brain barrier permeability.

The activation of adenosine receptors can be an efficient method for enhancing drug delivery. We hypothesized that an influx of large molecules would be mediated by an increase in paracellular permeability. However, questions still remained: 1) If adenosine receptor signaling can indeed increase the permeability of the blood brain barrier, what are the mechanisms behind this increased paracellular permeability? and 2) Can adenosine receptor signaling increase transcellular permeability by downregulating drug transporters, which are highly expressed on the brain endothelial cells? To address these fundamental questions, we first used human primary brain endothelial cells to test our hypothesis [24]. Similar to the results observed from the *in vivo* study by Carman et al., human brain endothelial cells showed increased permeability from A2A AR activation by Lexiscan and the broad spectrum agonist NECA [24]. The kinetics of permeability for NECA increased beginning at 60 minutes and were maintained for up to 90 minutes, whereas those of Lexiscan began at 5 minutes and were gone by 30 minutes. These results show that the kinetics of permeability were similar to what was observed in vivo in the study by Carman *et al*. Also, such a short time window showing an increase in the permeability of the BBB and its reversibility by the Lexiscan treatment is critically important and beneficial for safety issues, as it can reduce the entry of unwanted molecules into the brain that can be potentially harmful for its physiology [12, 18, 22, 24].

To further study the mechanisms behind increased permeability in human brain endothelial cells by AR mediated signaling, we focused on the Rho-GTPase signaling pathway. Rho-GTPase is well known for its regulatory effect on determining cell morphology and is dependent on actin-cytoskeletal reorganization [25-27].

Activation of Rho-GTPase induces stress fiber formation, creating centripetal traction and causing increased junctional spaces [28-29]. Indeed, Lexiscan induced a very rapid increase in the RhoA activity of the human primary brain endothelial cells that diminished after 5 minutes, whereas NECA gradually increased the activity for up to 15 minutes [24]. This observation is opposite from the research of other groups, which has shown that AR activation is actually reversed when mediated by the inhibition of Rho-GTPase [30]. This might occur due to the different roles of AR signaling on Rho-GTPase activation in different cell types, suggesting that the phenomenon is brain endothelial cell specific. Adenosine receptor signaling increased the cyclic AMP level by activating Gs protein, as we have observed, and such increased cyclic AMP level may have induced the increased activity of RhoA [31-33]. Lexiscan increased the cAMP level very rapidly, whereas that of NECA was delayed, which can explain the early window of permeability [24]. Rapid increase of RhoA activity was correlated with an increase in stress fiber formation, which disrupted the adherens and tight junction molecules VE Cadherin and Cluadin-5 as well as focal adhesion molecules such as ERM and FAK, which are critically important for maintaining the integrity of the brain vascular endothelial layers [34-38]. Therefore, the disruption or decreased expression level of these proteins may partially explain the increased permeability of the human brain endothelial layer.

The transcelullar pathway comprises the majority of selective transport of molecules to the brain, and we wanted to determine the effect of AR signaling on the regulation of transcellular permeability by regulating the drug transporter P-

glycoprotein [13, 39-45]. P-glycoprotein is highly expressed on brain endothelial cells, blocking the entry of the xenobiotics to the brain [41, 46-47].

First, we used our in vitro human and mouse primary brain endothelial cells to address our questions. Lexiscan, which is the A2A receptor agonist, indeed decreased very rapidly and potently the P-glycoprotein expression level and the functionality of the *in vitro* model. NECA, which is the broad spectrum AR agonist, also decreased the expression level and functionality of this drug transporter, but it was in a gradual and delayed manner. Such a downregulatory effect of P-glycoprotein by AR signaling was also observed in a later *in vivo* study. In the Lexiscan-treated mice, the kinetics of epirubicin (the P-glycoprotein substrate) accumulation was increased very rapidly at early time points (5 and 30 minutes), and returned to basal levels at 60 minutes. In contrast, in NECA treated mice, the epirubicin accumulation was increased at a 4 hour time point and returned to its basal level at 8 and 12 hours. The kinetics of the epirubicin uptake assay are very similar to those of the FITC-Dextran accumulation assay, which was performed by Carman *et al.* and might be attributed to the different half-lives of Lexiscan (2.5 minutes) and NECA (5 hrs). Recent studies from other groups have demonstrated that disruption of endocytic circulatory pathways can decrease the functionality of P-glycoprotein [48]. Also, pregnane X receptor localized at the nucleus can recognize the signal and regulate the P-glycoprotein expression level [49]. Further studies are required to reveal the mechanism behind AR induced regulation of P-glycoprotein expression. Our studies strongly suggest that adenosine receptor signaling can increase not only the

paracellular pathway but also the transcellular pathway as a mode of action to increase the delivery to the brain.

Our current study is heavily focused on the role of adenosine receptor signaling in regulating the permeability of brain endothelial cells, which compose the front line of the blood brain barrier. However, future study requires understanding its role in the regulation of other components of the blood brain barrier, including pericytes and astrocytes. Since these components help to increase the resistance of the blood brain barrier, studying whether extracellular adenosine plays a significant role in regulating the permeability or integrity of these components would provide important information for the enhanced delivery of therapeutics to the brain. Also, the transcellular pathway is mediated by a variety of transporters, not just by P-glycoprotein, indicating a further avenue for study. Indeed, some transporters use transcytosis to mediate export to the parenchyma of organs; hence, increased transporter activity may be beneficial in increasing delivery of molecules to the brain. Further studies would be required to determine whether AR signaling can increase the activity of these transporters and used to enhance the delivery of molecules to the brain. Furthermore, it would be worthwhile to study the mechanisms behind the delivery of molecules across the endothelial barriers. It is our key finding that the downmodulation of P-glycoprotein by adenosine receptor signaling can increase the permeability of P-glycoprotein substrates, though how the substrates that have entered the endothelial cells can escape its borders is not clearly understood. In future studies, it would be interesting to explore whether such migration is mediated through active or passive pathways.

For possible future application of AR signaling in the clinical field, it would be necessary to determine the time window for maximizing drug delivery to the brain. Since the half-lives of target drugs vary tremendously, determining the proper time point of AR agonist injections for augmenting certain drugs would be a prerequisite for effective drug delivery. Studying the possible drug-to-drug interaction is also important for further increasing the applicability of AR activation.

Regulating blood brain barrier permeability is not just confined to increasing drug delivery to the brain. Our findings demonstrating the increased paracellular permeability of Jurkat T cells through human brain endothelial cells by AR signaling also suggest increased permeability of cells to the brain[24]. Future regenerative therapeutic plans will require the delivery of neuronal stem cells to the brain, which might be injected from the periphery. Our findings can be used to test whether AR signaling can indeed increase the transmigration of these stem cells to treat neurological diseases.

For several decades, the mysterious existence of the blood brain barrier was considered a formidable fortress that did not allow the entry of cells and molecules. However, several seminal studies, including ours, show that we can indeed regulate the permeability of the BBB. We strongly believe that further in-depth study will allow us to increase the permeability in a safer and potent manner, potentially saving millions of people suffering from neurological diseases.

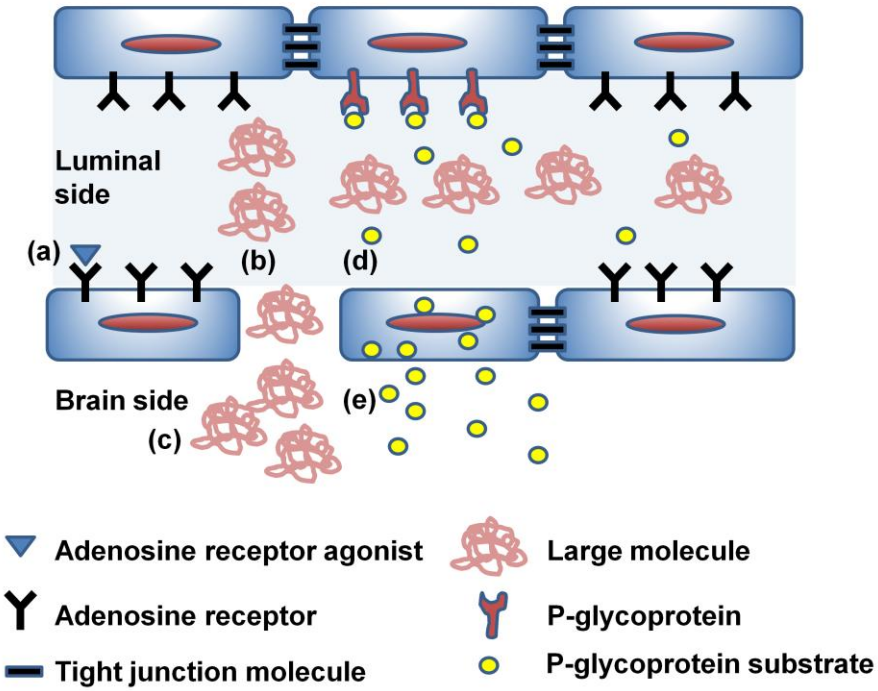

Figure 4.1. Summary of the effect of adenosine receptor signaling on the paracellular and transcellular permeability of the blood brain barrier. Upon activation, the adenosine receptor (a) induces conformational changes of endothelial cells and disrupts tight junction molecules (b). This leads to increased paracellular permeability of the blood brain barrier, enhancing the influx of large molecules (c). Also, it induces the downmodulation of P-glycoprotein, which is the major drug transporter expressed on the brain endothelial cells (d) and increases the influx of drugs that are P-glycoprotein substrates (e).

References

1. Ehrlich, P., *Das Sauerstoff-Bedurfnis des Organismus: eine farbenanalytische Studie.* Berlin: Hirschward, 1885.
2. Goldmann, E., *Vitalfarbung am Zentralnervensystem: beitrag zur Physiopathologie des plexus chorioideus der Hirnhaute.* Abh Preuss Akad Wiss Physik-Math, 1913. **1**: p. 1-60.
3. Reese, T. and M. Karnovsky, *Fine structural localization of a blood-brain barrier to exogenouse peroxidase.* J Cell Biol, 1967. **34**: p. 207-217.
4. Lewandowsky, M., *Zur Lehre der Zerebrospinalflussigkeit.* Z Klin Med 1900. **40**: p. 480-484.
5. Goldmann, E., *Die aussere und innere sekretion des gesunden und kranken Organismus im Licht der vitalen Farburg.* Beitr Klin Chir, 1909. **64**: p. 192-265.
6. Ribatti, D., et al., *Development of the blood-brain barrier: A historical point of view.* The Anatomical Record Part B: The New Anatomist, 2006. **289B**(1): p. 3-8.
7. Abbott, N.J., *Astrocyte-endothelial interactions and blood-brain barrier permeability.* Journal of anatomy, 2002. **200**(6): p. 629-38.
8. Ballabh, P., A. Braun, and M. Nedergaard, *The blood-brain barrier: an overview: structure, regulation, and clinical implications.* Neurobiology of disease, 2004. **16**(1): p. 1-13.
9. Rubin, L.L. and J.M. Staddon, *The cell biology of the blood-brain barrier.* Annu Rev Neurosci, 1999. **22**: p. 11-28.

10. Bergers, G. and S. Song, *The role of pericytes in blood-vessel formation and maintenance.* Neuro-oncology, 2005. **7**(4): p. 452-64.

11. Adamson, C., et al., *Glioblastoma multiforme: a review of where we have been and where we are going.* Expert Opin Investig Drugs, 2009. **18**(8): p. 1061-83.

12. Daneman, R. and A. Prat, *The Blood-Brain Barrier.* Cold Spring Harb Perspect Biol, 2015. **7**(1).

13. Devraj, K., et al., *GLUT-1 glucose transporters in the blood-brain barrier: differential phosphorylation.* Journal of neuroscience research, 2011. **89**(12): p. 1913-25.

14. Deeken, J.F. and W. Loscher, *The blood-brain barrier and cancer: transporters, treatment, and Trojan horses.* Clin Cancer Res, 2007. **13**(6): p. 1663-74.

15. Pardridge, W.M., *The blood-brain barrier: bottleneck in brain drug development.* NeuroRx, 2005. **2**(1): p. 3-14.

16. *2014 Alzheimer's disease facts and figures.* Alzheimer's & Dementia: The Journal of the Alzheimer's Association. **10**(2): p. e47-e92.

17. Hossain, S., T. Akaike, and E.H. Chowdhury, *Current approaches for drug delivery to central nervous system.* Curr Drug Deliv, 2010. **7**(5): p. 389-97.

18. Rajadhyaksha, M., et al., *Current Advances in Delivery of Biotherapeutics across the Blood-Brain Barrier.* Curr Drug Discov Technol, 2011. **8**(2): p. 87-101.

19. Bradley, W.G., Jr., *MR-guided focused ultrasound: a potentially disruptive technology.* J Am Coll Radiol, 2009. **6**(7): p. 510-3.

20. Neuwelt, E.A., et al., *Osmotic blood-brain barrier disruption. Computerized tomographic monitoring of chemotherapeutic agent delivery.* J Clin Invest, 1979. **64**(2): p. 684-8.

21. Yu, Y.J., et al., *Therapeutic bispecific antibodies cross the blood-brain barrier in nonhuman primates.* Science translational medicine, 2014. **6**(261): p. 261ra154.

22. Carman, A.J., et al., *Adenosine receptor signaling modulates permeability of the blood-brain barrier.* J Neurosci, 2011. **31**(37): p. 13272-80.

23. Mills, J.H., et al., *CD73 is required for efficient entry of lymphocytes into the central nervous system during experimental autoimmune encephalomyelitis.* Proc Natl Acad Sci U S A, 2008. **105**(27): p. 9325-30.

24. Kim, D.G. and M.S. Bynoe, *A2A Adenosine Receptor Regulates the Human Blood-Brain Barrier Permeability.* Molecular neurobiology, 2014.

25. Wojciak-Stothard, B., et al., *Rho and Rac but not Cdc42 regulate endothelial cell permeability.* Journal of cell science, 2001. **114**(Pt 7): p. 1343-55.

26. Hall, A., *Rho GTPases and the actin cytoskeleton.* Science, 1998. **279**(5350): p. 509-14.

27. Jaffe, A.B. and A. Hall, *Rho GTPases: biochemistry and biology.* Annu Rev Cell Dev Biol, 2005. **21**: p. 247-69.

28. Spindler, V., N. Schlegel, and J. Waschke, *Role of GTPases in control of microvascular permeability.* Cardiovasc Res, 2010. **87**(2): p. 243-53.

29. Pollard, T.D. and J.A. Cooper, *Actin, a central player in cell shape and movement.* Science, 2009. **326**(5957): p. 1208-12.

30. Sohail, M.A., et al., *Adenosine induces loss of actin stress fibers and inhibits contraction in hepatic stellate cells via Rho inhibition.* Hepatology, 2009. **49**(1): p. 185-94.

31. Jeyaraj, S.C., et al., *Cyclic AMP-Rap1A signaling activates RhoA to induce alpha(2c)-adrenoceptor translocation to the cell surface of microvascular smooth muscle cells.* Am J Physiol Cell Physiol, 2012. **303**(5): p. C499-511.

32. Sheth, S., et al., *Adenosine receptors: expression, function and regulation.* International journal of molecular sciences, 2014. **15**(2): p. 2024-52.

33. Sebastiao, A.M. and J.A. Ribeiro, *Adenosine receptors and the central nervous system.* Handb Exp Pharmacol, 2009(193): p. 471-534.

34. Wu, M.H., *Endothelial focal adhesions and barrier function.* J Physiol, 2005. **569**(Pt 2): p. 359-66.

35. Stevenson, B.R. and B.H. Keon, *The tight junction: morphology to molecules.* Annu Rev Cell Dev Biol, 1998. **14**: p. 89-109.

36. Aijaz, S., M.S. Balda, and K. Matter, *Tight junctions: molecular architecture and function.* Int Rev Cytol, 2006. **248**: p. 261-98.

37. Hirao, M., et al., *Regulation mechanism of ERM (ezrin/radixin/moesin) protein/plasma membrane association: possible involvement of phosphatidylinositol turnover and Rho-dependent signaling pathway.* J Cell Biol, 1996. **135**(1): p. 37-51.

38. Hordijk, P.L., et al., *Vascular-endothelial-cadherin modulates endothelial monolayer permeability.* J Cell Sci, 1999. **112 (Pt 12)**: p. 1915-23.

39. Kohno, K., et al., *The direct activation of human multidrug resistance gene (MDR1) by anticancer agents.* Biochem Biophys Res Commun, 1989. **165**(3): p. 1415-21.

40. Arceci, R.J., *Clinical significance of P-glycoprotein in multidrug resistance malignancies.* Blood, 1993. **81**(9): p. 2215-22.

41. Schinkel, A.H., et al., *P-glycoprotein in the blood-brain barrier of mice influences the brain penetration and pharmacological activity of many drugs.* J Clin Invest, 1996. **97**(11): p. 2517-24.

42. Beaulieu, E., et al., *P-glycoprotein is strongly expressed in the luminal membranes of the endothelium of blood vessels in the brain.* Biochem J, 1997. **326 (Pt 2)**: p. 539-44.

43. Chen, C.C., et al., *Detection of in vivo P-glycoprotein inhibition by PSC 833 using Tc-99m sestamibi.* Clin Cancer Res, 1997. **3**(4): p. 545-52.

44. Gottesman, M.M., S.V. Ambudkar, and D. Xia, *Structure of a multidrug transporter.* Nat Biotechnol, 2009. **27**(6): p. 546-7.

45. Giacomini, K.M., et al., *Membrane transporters in drug development.* Nat Rev Drug Discov, 2010. **9**(3): p. 215-36.

46. Begley, D.J., et al., *Functional expression of P-glycoprotein in an immortalised cell line of rat brain endothelial cells, RBE4.* J Neurochem, 1996. **67**(3): p. 988-95.

47. Pardridge, W.M., et al., *Brain microvascular and astrocyte localization of P-glycoprotein.* J Neurochem, 1997. **68**(3): p. 1278-85.

48. Fu, D. and I.M. Arias, *Intracellular trafficking of P-glycoprotein.* Int J Biochem Cell Biol, 2012. **44**(3): p. 461-4.

49. Chan, G.N., et al., *Regulation of P-glycoprotein by orphan nuclear receptors in human brain microvessel endothelial cells.* J Neurochem, 2011. **118**(2): p. 163-75.

Appendices

Additional projects done during Ph.D. degree

Appendix 1.

Itk signals promote neuroinflammation by regulating $CD4^+$ T cell activation and trafficking

*Originally published in Journal of Neuroscience.

Kannan and Kim *et al* Journal of Neurosci 2015

A1.1. Abstract

Here we demonstrate that Itk signaling in $CD4^+$ T cells promotes experimental autoimmune encephalomyelitis (EAE), the animal model of multiple sclerosis (MS). We show that $Itk^{-/-}$ mice exhibit reduced disease severity, and transfer of $Itk^{-/-}$ $CD4^+$ T cells into T cell deficient recipients lower disease severity. We observed a significant reduction of $Itk^{-/-}$ $CD4^+$ T cells in the central nervous system (CNS) of $Itk^{-/-}$ mice or recipients of $Itk^{-/-}$ $CD4^+$ T cells during EAE, which is consistent with attenuated disease. $Itk^{-/-}$ $CD4^+$ T cells exhibit defective response to myelin antigen stimulation due to displacement of F-actin from the $CD4^+$ co-receptor. This results in inadequate transmigration of $Itk^{-/-}$ $CD4^+$ T cells into the CNS and across brain endothelial barriers *in vitro*. Finally, $Itk^{-/-}$ $CD4^+$ T cells show significant reduction in production of Th1 and Th17 cytokines, and exhibit skewed Teff:Treg cell ratios. These results indicate signaling by Itk promotes autoimmunity and CNS inflammation, suggesting that it may be a viable target for treatment of MS.

A1.2. Introduction

Tec family non-receptor tyrosine kinases are critical for the regulation of intracellular signaling in lymphocytes for proper immune responses. The Tec kinase Itk regulates signaling via the T cell receptor (TCR) and has been shown to be involved in the activation of intracellular calcium signaling pathways, MAPK pathways, and TCR-induced polarization of actin cytoskeleton, supporting an integral role for Itk in T cell activation and function [1-2]. Mice deficient in Itk exhibit significant alteration in T helper (Th) cell development and function, including Th2 and Th17, as well as T regulatory cell development [3-5]. Itk also regulates the development of *i*NKT cells and their ability to produce cytokines. This has made Itk a promising target for the development of drugs that target Th cytokine mediated diseases [6-7].

Multiple sclerosis (MS) is a multifaceted neuroinflammatory disease impacted by environmental factors such as infection, vitamin D deficiency and gonadal hormones [8-10]. Although the etiology of MS is unknown, it is evident that aberrations in the immune response compartment can either trigger its onset or exacerbate its pathogenicity [11]. Thus, imbalance in factors that induce and/or prolong inflammation versus those that resolve and/or suppress inflammation impacts disease outcome. MS is characterized by infiltration of inflammatory immune cells into the CNS [12]. $CD4^+$ and $CD8^+$ T cells play critical roles in the disease pathogenesis [13]. $CD4^+$ T cells in MS lesions have been determined to be largely of the Th1 and Th17 lineages [14]. The murine model of MS, EAE, is induced in

susceptible mouse strains following immunization with myelin components, such as myelin oligodendrocyte glycoprotein (MOG), or by passive transfer of myelin antigen-specific T cells [15]. Like MS, the neuroinflammatory response in EAE is mediated mainly by effector Th1 and Th17 cells that migrate to the CNS where they attack myelin sheath resulting in demyelination and subsequent paralysis [16]. These pathogenic effector Th cells can be controlled by T regulatory cells (Tregs) that suppress inflammatory responses [17].

We investigated the role of Itk in the development of EAE and found that $Itk^{-/-}$ mice are significantly protected from EAE and have diminished frequency of immune cells in their CNS. Similarly, in a transfer model of EAE, recipients lacking $CD4^+$ T cells and are reconstituted with $Itk^{-/-}$ $CD4^+$ T cells develop attenuated EAE compared to recipients reconstituted with WT $CD4^+$ T cells. We also found that $Itk^{-/-}$ $CD4^+$ T cells are defective in their ability to migrate across an *in vitro* BBB. $Itk^{-/-}$ $CD4^+$ T cells exhibit defects in actin cytoskeleton reorganization in response to myelin antigen stimulation, resulting in diminished ability to proliferate, and also show defective Th1 and Th17 cytokine production. Based on these findings, we conclude that Itk promotes $CD4^+$ T cell migration into the CNS and contribute to neuroinflammation. We propose that inhibitors of Itk signaling have strong potential as therapeutics against MS.

A1.3. Materials and Methods

Mice. Wild-type (WT) mice were obtained from Jackson laboratories, and $Itk^{-/-}$ mice were as previously described. All mice were on the C57Bl/6 background and were used when they were 6- to 8-weeks of age. Mice of both sexes were used and were maintained in specific pathogen free environment. All experiments were approved by the Office of Research Protection's Institutional Animal Care and Use Committee at Cornell University.

T cell purification. Naïve $CD4^+$ T cells were isolated from spleens and lymph nodes using the Miltenyi Naïve $CD4^+$ T cell isolation kit according to manufacturer's instructions.

Flow cytometry and intracellular cytokine staining. To stain for intracellular cytokines and transcription factors, cells were stimulated with PMA/Ionomycin (P/I, Sigma, 50 ng/1 μg/ml) and Brefeldin A (Sigma) for 5 hours. To examine antigen specific recall responses, single cell suspensions of splenocytes or lymph node cells were cultured with indicated concentration of MOG peptide for 72 hours and restimulated either with 10 g/ml of peptide from Myelin Oligodendrocyte Glycoprotein (MOG_{35-55}) or with PMA/Ionomycin (P/I, Sigma, 50 ng/1 μg/ml) in the presence of Brefeldin A (Sigma) for 5 hours. Cells were then fixed/permeabilized using the Foxp3 fixation/ permeabilization kit and stained with the indicated antibodies against surface/ intracellular proteins. Data was acquired and analyzed

using LSRII (BD Biosciences) and FlowJo (TreeStar) respectively. Cells were identified by gating on forward scatter vs. side scatter, gating on the lymphocyte population, followed by gating on $TcR\beta^{+}CD4^{+}$ T cells, and analysis if intracellular cytokine or Foxp3 expression.

Enzyme-linked immunosorbent assay (ELISA). The protein concentrations of cytokines IFNγ and IL17A in cell culture supernatants were quantified using commercially available kits for two-site ELISA (eBioscience) according to manufacturer's instructions.

CFSE labeling and H^3-thymidine Incorporation assay. Splenocytes from immunized WT and $Itk^{-/-}$ mice were incubated at 37^0C for 10 mins in PBS containing 5 mM CFSE (Molecular Probes). Subsequently, the cells were washed twice with complete RPMI 1640 and cultured in the presence of the MOG peptide for 72 hours. For analysis of H^3-thymidine incorporation, cells were seeded at $2x10^6$ cells/ml and left unstimulated or stimulated with MOG peptide for 72 hours with $[H]^3$-thymidine (1 μCi) added for the last 18 hours. Following which cells were washed, pelleted and the radioactivity was quantified and expressed as fold change.

EAE induction, scoring and *in vivo* $CD25^{+}$ cell depletion. EAE was induced as previously described [18]. Briefly, a 1:1 emulsion of MOG peptide (3 mg/ml in PBS) (Anaspec) and complete Freund's adjuvant (CFA, Sigma) was injected subcutaneously (50 μl) into each flank (100 μg). Pertussis toxin (PTX, 200 ng in 200 μl PBS)

(Biological Laboratories Inc.) was given intravenously at the time of immunization and again two days later. Mice were scored daily for EAE based on disease symptom severity; 0=no disease, 0.5 = weak tail (cannot curl tail completely), 1.0 = limp tail (complete inability to move tail), 2=limp tail and partial hind limb paralysis, 3=total hind limb paralysis, 4=both hind limb and fore limb paralysis, 5=death. Mice with a score of 4 were euthanized. For *in vivo* depletion of $CD25^+$ cells, we administered either vehicle (PBS) control or 200 μg of α-CD25 (PC61 mAb) antibody every four days.

Actin cytoskeleton analysis. $CD4^+$ T cells were isolated from MOG peptide-CFA immunized WT or $Itk^{-/-}$ mice and stimulated with the MOG peptide, or α-CD3 antibodies for 24 or 72 hours. Cells were then fixed with 4% paraformaldehyde for 15 mins and permeabilized with 0.2 % Triton X-100. F-actin was stained with Alexa Fluor 568-conjugated Phalloidin (1:200, Invitrogen) and CD4 was detected using APC-conjugated α-CD4 primary antibody (1:100, BD bioscience) for 30 mins. Image was visualized by Leica SP5 confocal microscope and the localization of F-actin and CD4 was analyzed by Leica suite image analysis program.

$CD4^+$ T cell transmigration assay.

For transmigration assays, mouse brain endothelial cell line (bEnd 3, ATCC) was cultured on 8 μm porous membrane insert (BD bioscience) as an *in vitro* model of blood brain barrier [19]. $2.5x10^5$ $CD4^+$ T cells isolated from MOG and CFA immunized WT and $Itk^{-/-}$ mice were placed in the cell containing insert, with media at

the bottom well. The media at the bottom well was collected at 1, 24 hrs after treatment and number of cells that crossed the barrier was counted. For Latrunculin B (LatB) induced transmigration recovery assay, cells were pretreated with DMSO or LatB (1 μM) for 1 hour, washed with media and loaded on the *in vitro* blood brain barrier insert. Cells were collected at 1 and 24 hours after treatment and the number of cells that crossed the barrier was counted.

Th1 and Th17 $CD4^+$ T cell transmigration assay using Itk inhibitor.

For transmigration assay of Th1 and Th17 in the presence of Itk inhibitor, $CD4^+$ T cells were isolated from MOG-T cell receptor (TCR) transgenic mice (2D2-TCR-Tg) and were stimulated with MOG. Cells were further differentiated to Th1 and Th17 $CD4^+$ T cells as was previously described [16]. 5 x 10^5 of Th1 or Th17 $CD4^+$ cells were pretreated with DMSO or Itk inhibitor (1 μM) for 2 hours and loaded onto mouse brain endothelial cells cultured on porous membrane insert containing DMSO or Itk inhibitor (1 μM) with media at the bottom well. Cells at the bottom well were collected at 1 and 24 hrs after treatment and enumerated.

Statistical Analysis.

Results are expressed as means ± SEMs and statistical significance between groups determined either by unpaired Student's *t* test or two-way ANOVA analysis using GraphPad Prism version 5.00 for Windows (GraphPad, San Diego, CA). Values with a probability of $p \leq 0.05$ are considered statistically significant.

A1.4. Results

Itk promotes development of EAE

We investigated the role of Itk in the MOG-induced model of EAE. We observed that disease in $Itk^{-/-}$ mice was significantly attenuated compared to their WT counterparts (Fig. A1. 1A). Moreover, onset of symptoms of EAE in $Itk^{-/-}$ mice was delayed by 10-20 days, and incidence of EAE was significantly less compared to WT mice (Fig. A1. 1A and Table A1. 1). Clinical signs of EAE become evident after inflammatory immune cells invade the CNS and cause destruction of myelin tissue. Consistent with the absence of clinical signs of disease and delayed onset, $Itk^{-/-}$ mice had very few cells in their brain and spinal cord on day 17 post-EAE induction compared to WT mice as determined by immunohistochemistry (Fig. A1. 1B and C) and FACS analysis (Fig. A1. 1D). Analysis of the small proportion of $Itk^{-/-}$ mice that had developed disease by day 31 revealed that they had $CD4^+$ T cells in the brain and spinal cord in similar numbers to WT mice (Fig. A1. 1D). The appearance of $CD4^+$ T cells in the CNS of $Itk^{-/-}$ mice at day 31 post-EAE induction is consistent with the first appearance of clinical signs of disease, which occurs between days 20-30 in those mice. Taken together, these findings suggest that Itk signaling plays an important role in the promotion of autoimmunity and neuroinflammation.

We next determined whether protection conferred by Itk deficiency was solely due to the fact that $Itk^{-/-}$ mice have fewer $CD4^+$ T cells in the periphery [20]. We transferred equal numbers of WT or $Itk^{-/-}$ $CD4^+$ T cells into mice that lack endogenous

Figure A1. 1.

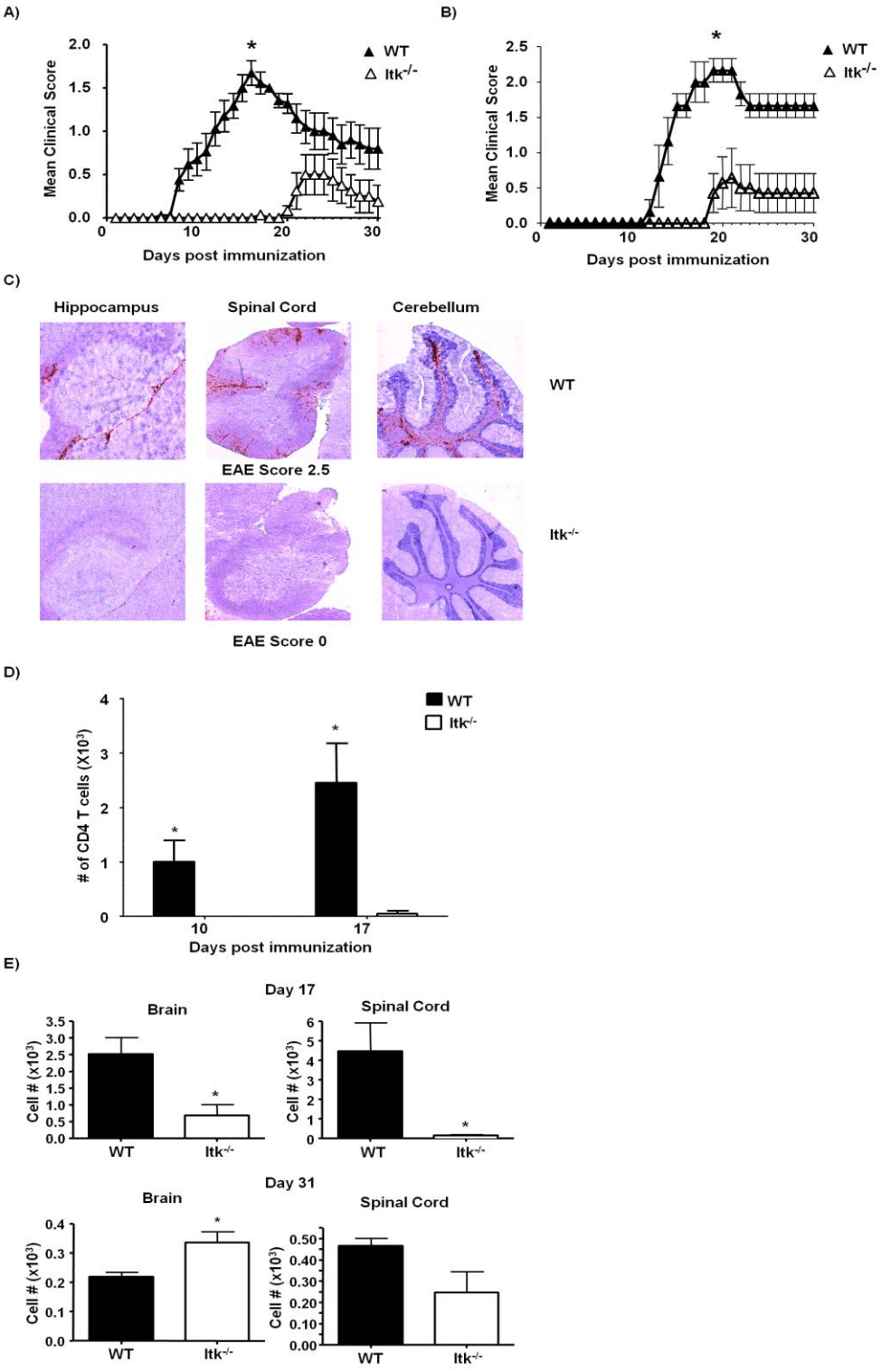
A)
Mean Clinical Score
Days post immunization
WT
Itk-/-
B)
Mean Clinical Score
Days post immunization
WT
Itk-/-
C)
Hippocampus
Spinal Cord
Cerebellum
WT
EAE Score 2.5
Itk-/-
EAE Score 0
D)
# of CD4 T cells (X10³)
Days post immunization
WT
Itk-/-
E)
Day 17
Brain
Spinal Cord
Cell # (x10³)
WT
Itk-/-
Day 31
Brain
Spinal Cord
Cell # (x10³)
WT
Itk-/-

Figure A1. 1. Itk promotes autoimmunity and lymphocyte migration into the CNS. A) WT (n=17) and $Itk^{-/-}$ (n=14) mice were immunized to develop EAE and scored daily for clinical signs of EAE based on a 5 point scale assessing ascending paralysis. Values are means ± SEMs, *p< .05 by 2-way ANOVA. **B**) CNS sections (hippocampus, cerebellum, and spinal cord) from d17 post-EAE induction wild type (top panels) and $Itk^{-/-}$ (bottom panels) mice were stained with α-CD45 to detect immune cell infiltration in the CNS following disease induction (red) vs. a nuclear background (blue/gray). **C**) CNS sections from d10, 17, and 31 post-EAE induction wild type and $Itk^{-/-}$ were stained with α-CD4 and quantified using light microscope from different regions of brain and spinal cord and quantified (n=3, each time point). Values are means ± SEMs, *p< .05 by unpaired student t test. **D**) Cells were isolated from the brain and spinal cord of WT and $Itk^{-/-}$ mice at d17 and day 30 post EAE induction and quantified for the number of $CD4^+$ T cells by FACS analysis. Values are means ± SEMs, *p < .05 by unpaired student t test.

Table A1.1. **Itk signaling promotes EAE.**

Genotype	Incidence[A]	Mean Day of Onset[B]	Mean Max Score[C]
WT	10/10 (100%)	10.06±0.5908	1.906±0.1043
$Itk^{-/-}$	6/13 (46%)	19.17±1.046	0.3125±0.1281

[A]Indicates the number of mice that achieved a score of 0.5 (weak tail) in the experimental group.
[B]Indicates the average day of onset (an EAE score of 0.5, ± SEM).
[C]Indicates the average of the maximum EAE score for each individual mouse (± SEM.).

T cells (TCR$\alpha^{-/-}$ mice) followed by induction of EAE. TCR$\alpha^{-/-}$ recipients of WT $CD4^+$ T cells had a higher EAE incidence and developed significantly more severe disease as compared to recipients of $Itk^{-/-}$ $CD4^+$ T cells (Fig. A1. 2A and Table A1. 2). Consistent with this, TCR$\alpha^{-/-}$ recipients of $Itk^{-/-}$ $CD4^+$ T cells also had fewer immune cell infiltrates in the CNS (Fig. A1. 2B). These results indicate that Itk signaling promotes the development of autoimmune pathologies during EAE and this is due to a $CD4^+$ T cell intrinsic requirement for Itk.

Reduced Th1 and Th17 effector cells in the CNS of $Itk^{-/-}$ mice

Signaling through Itk is critical for the production of IL-17A by Th17 cells [4], and murine and human $CD4^+$ T cells that lack Itk rapidly up regulate IFNγ [5]. Both IFNγ and IL-17A play important roles in EAE and MS pathogenesis [21]. To determine whether Itk regulates the production of these cytokines in EAE, we isolated $CD4^+$ T cells from brain and spinal cord of WT and $Itk^{-/-}$ mice on day 17 and 31 post-EAE induction to assess their cytokine profile by intracellular cytokine staining. We found fewer effector cells infiltrating the CNS of $Itk^{-/-}$ mice, with lower numbers of $IFN\gamma^+$ cells in the brain and spinal cord at day 17, and lower numbers of $IFN\gamma^+$ and $IL17A^+$ T cells at day 31 post-induction of EAE (Fig. A1. 3A and B). These results suggest that Itk signaling is important for the generation and elaboration of effector responses of auto-reactive $CD4^+$ T cells, and suggests that diminution in effector Th1 and Th17 cells may in part be responsible for the attenuated disease in $Itk^{-/-}$ mice.

Figure A1. 2.

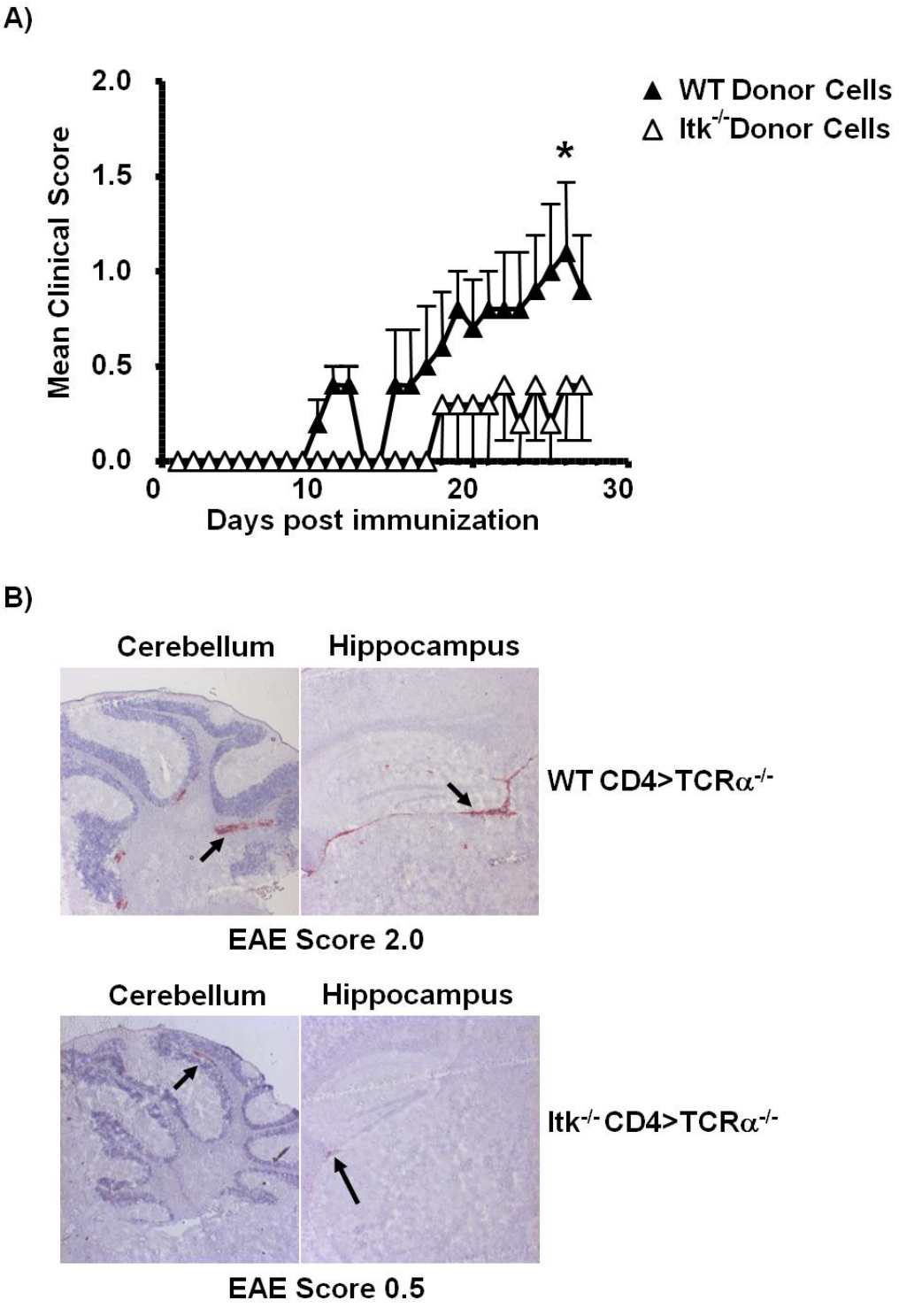
A)
2.0
1.5
1.0
0.5
0.0
Mean Clinical Score
0
10
20
30
Days post immunization
*
▲ WT Donor Cells
△ Itk-/- Donor Cells
B)
Cerebellum
Hippocampus
WT CD4>TCRα-/-
EAE Score 2.0
Cerebellum
Hippocampus
Itk-/- CD4>TCRα-/-
EAE Score 0.5

Figure A1. 2. WT but not Itk$^{-/-}$ CD4^{+} T cells confer disease to TCR$\alpha^{-/-}$ recipients. **A)** 3-4x10^{6} WT or Itk$^{-/-}$ CD4^{+} T cells were transferred into TCR$\alpha^{-/-}$ recipients that were subsequently immunized to develop EAE and scored daily for clinical signs of EAE. Values are means ± SEMs, *p<.05 by 2-way ANOVA, n=5. **B**) CNS sections from the indicated mice at d31 post-EAE induction were stained with α-CD4 (red) and the hippocampal area (left panels) and cerebellar parenchyma (right panels) of the CNS were assessed for the presence of CD4^{+} T cell infiltrates from representative mice that received WT or Itk$^{-/-}$ donor cells. Arrows indicate areas with pronounced CD4^{+} staining.

Table A1.2. Itk signaling plays a cell intrinsic role in $CD4^+$T cells in promoting EAE.

Donor Cells	Incidence[A]	Mean Day of Onset[B]	Mean Max Score[C]
WT	5/5 (100%)	12.20±1.715	1.200±0.3000
$Itk^{-/-}$	2/5 (40%)	20.00±2.000	0.4000±0.2915

[A]Indicates the number of mice that achieved a score of 0.5 (weak tail) in the experimental group.
[B] Indicates the average day of onset (an EAE score of 0.5, ± SEM).
[C] Indicates the average of the maximum EAE score for each individual mouse (± SEM.).

Figure A1. 3.

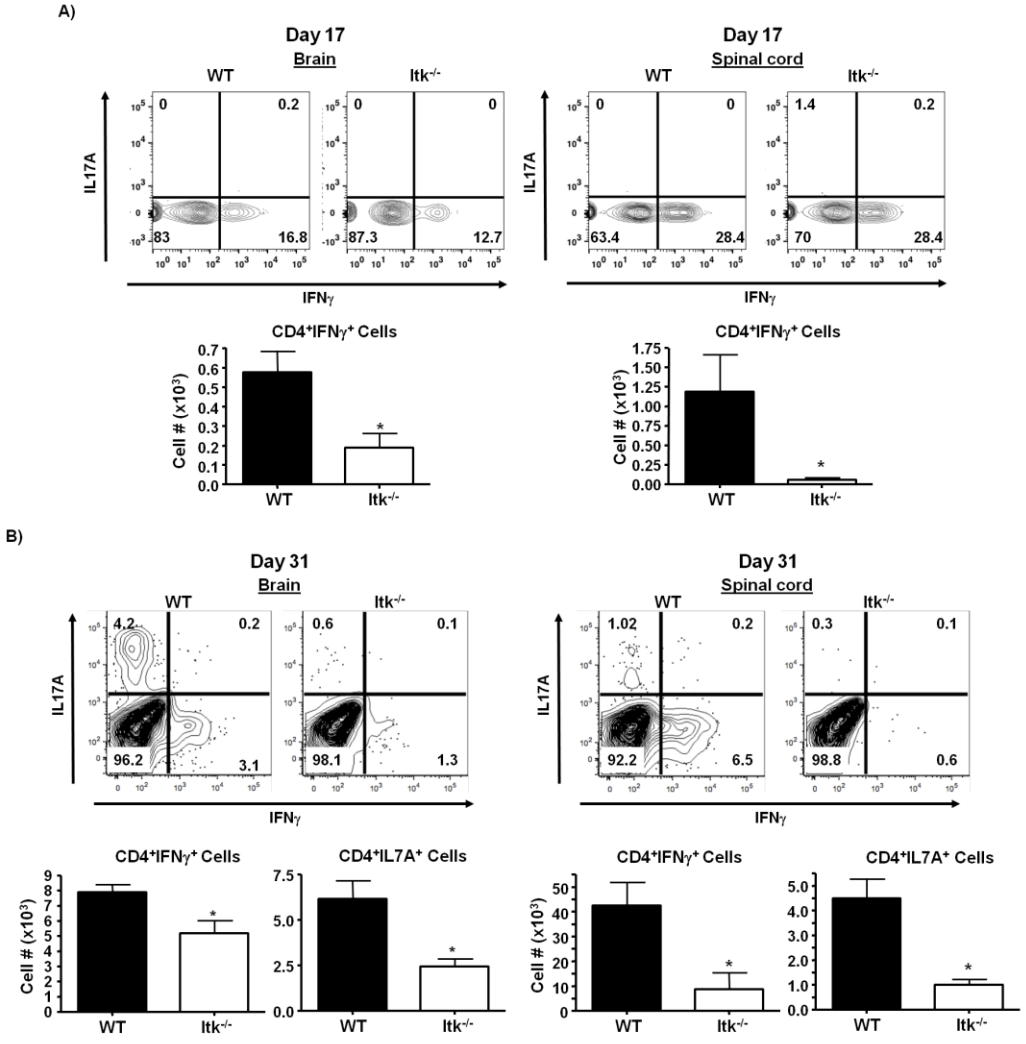
A)
Day 17
Brain
WT
Itk-/-
IL17A
IFNγ
0
0.2
0
0
83
16.8
87.3
12.7
CD4+IFNγ+ Cells
Cell # (x10³)
WT
Itk-/-
Day 17
Spinal cord
1.4
0.2
63.4
28.4
70
28.4
B)
Day 31
Brain
4.2
0.2
0.6
0.1
96.2
3.1
98.1
1.3
CD4+IL7A+ Cells
Day 31
Spinal cord
1.02
0.2
0.3
0.1
92.2
6.5
98.8
0.6

Figure A1. 3. Th1 and Th17 effector cells are decreased in the CNS of Itk$^{-/-}$ mice. Cells isolated from the brain and spinal cord of indicated d17 (**A**) and d31 (**B**) immunized mice were stimulated with PMA/Ionomycin the presence of Brefeldin A for 5 hrs and CD4^{+} T-cells analyzed for the expression of IFNγ and IL17A by FACS (top panels) and quantified for number of cytokine producing cells (bottom panels). Values are means ± SEMs, *$p < .05$ by unpaired student t test.

Itk signaling is critical for regulating the differentiation and function of $CD4^+$ T cells during EAE

Prompted by the paucity of pathogenic $CD4^+$ T cells (Th1 and Th17) in the CNS of $Itk^{-/-}$ mice, we next determined whether there was a defect in Th1 and/or Th17 $CD4^+$ T cell generation in the peripheral lymphoid organs of $Itk^{-/-}$ mice. We found that consistent with the attenuated disease and lack of infiltrating pathogenic Th1 or Th17 cells in the CNS, there were significantly higher numbers of effector Th1 cells when WT splenocytes were stimulated with MOG peptide compared to those from immunized $Itk^{-/-}$ mice 10 days post-EAE induction. However, there was little evidence of effector Th17 cells generated *ex vivo* at this time point (Fig. A1.4A-D). This is especially interesting considering the fact that $Itk^{-/-}$ naïve $CD4^+$ T cells are primed for IFNγ production, with higher basal levels of IFNγ [5, 22]. Furthermore, by day 17 post EAE-induction, WT $CD4^+$ T cells had undergone a switch from Th1 to Th17, producing more IL-17A and less IFNγ in response to MOG peptide restimulation *in vitro*. However, we found little evidence for such a switch in $Itk^{-/-}$ $CD4^+$ T cells. Similarly, fewer $Itk^{-/-}$ $CD4^+$ T cells expressed IL-17A *ex vivo* on day 31 post-EAE induction (Fig. A1.4B and C). Similar results were obtained when cells were restimulated with PMA and Ionomycin (Fig. A1.4D). *In vitro*, WT splenocytes from MOG peptide immunized mice also exhibited higher proliferation, incorporating more H^3 thymidine compared to $Itk^{-/-}$ splenocytes in response to MOG peptide. Additionally, WT $CD4^+$ T cells underwent more divisions (as measured by dilution of CFSE) than $Itk^{-/-}CD4^+$ T cells in response to MOG peptide (Fig A1.4E). Collectively these data suggest that WT $CD4^+$ T cells have better recall responses upon stimulation with

Figure A1. 4.

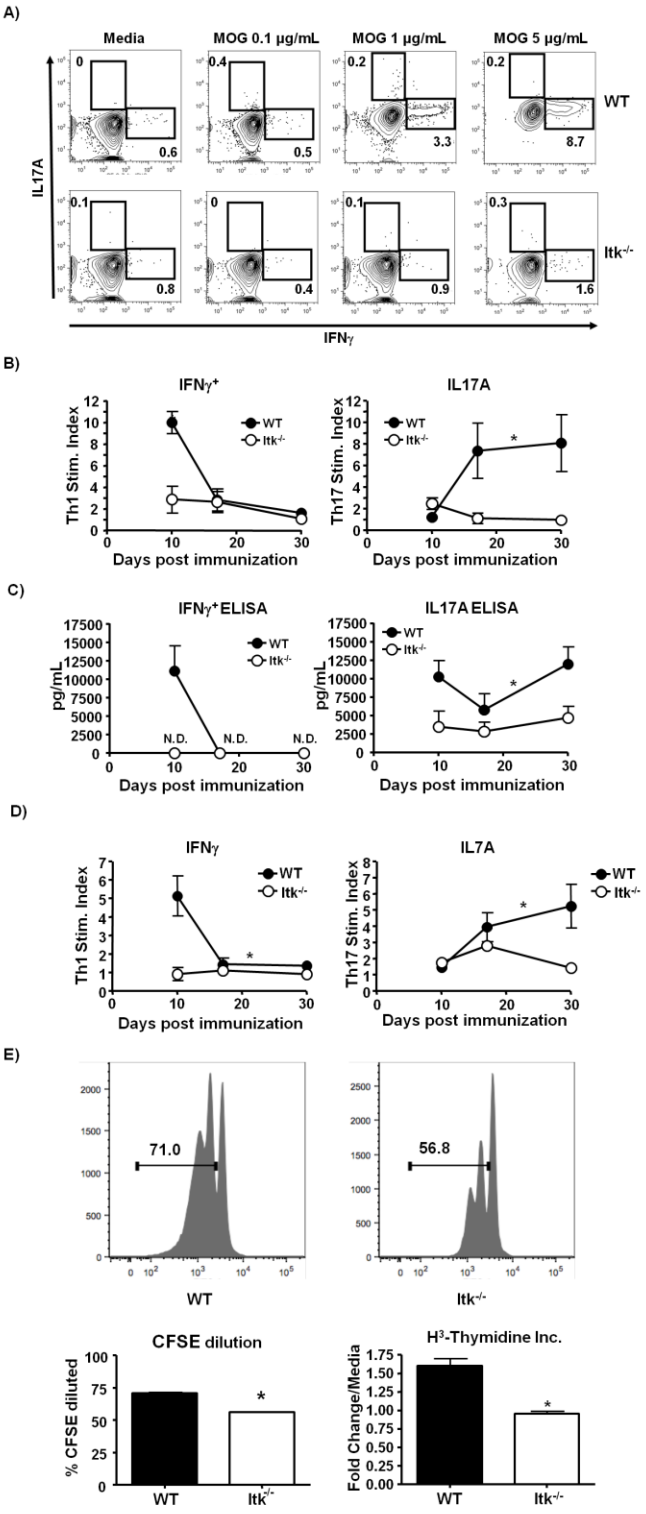
A)
Media
MOG 0.1 µg/mL
MOG 1 µg/mL
MOG 5 µg/mL
WT
Itk-/-
IL17A
IFNγ
B)
IFNγ+
IL17A
Th1 Stim. Index
Th17 Stim. Index
Days post immunization
C)
IFNγ+ELISA
IL17A ELISA
pg/mL
N.D.
D)
IFNγ
IL7A
E)
71.0
56.8
CFSE dilution
% CFSE diluted
H3-Thymidine Inc.
Fold Change/Media

Figure A1. 4. Itk signaling is critical for regulating the differentiation and effector function of CD4$^+$ T cells during EAE. A and B) Splenocytes isolated from d10, d17 and d31 immunized WT and Itk$^{-/-}$ mice were stimulated with 5 μg/ml MOG peptide for 72 hrs. The cells were then restimulated with 10 μg/ml MOG peptide in the presence of Brefeldin A for 5 hrs and CD4$^+$ T-cells analyzed for the expression of IFNγ and IL17A by FACS. Representative flow plots are shown in **A** and quantified for IFNγ (left panel) or IL17A (right panel) stimulation index (fold change in percentage of IFNγ or IL17A producing cells in response to MOG peptide compared to media controls) in **B**. **C**) Cell culture supernatants of cells treated as in (A) were analyzed for the levels of IFNγ and IL17A protein by ELISA. **D)** Splenocytes from **A** were stimulated with PMA/Ionomycin (P/I, Sigma, 50 ng/ 1 μg/ml) in the presence of Brefeldin A for 5 hours and quantified for IFNγ (left panel) or IL17A (right panel) stimulation index (fold change in percentage of IFNγ or IL17A producing cells in response to MOG peptide compared to media controls). **E**) Splenocytes obtained from d17 immunized WT and Itk$^{-/-}$ mice were stimulated with 5μg/ml of MOG peptide for 72 hrs with H^3-thymidine added during the last 18 hrs of culture, and data represented as fold increase in thymidine incorporation over media control (left). Splenocytes obtained from d17 immunized WT and Itk$^{-/-}$ mice were loaded with CFSE and stimulated with 5 μg/ml of MOG peptide for 72 hrs and analyzed for proliferation of CD4$^+$ T-cells by FACS (right), Values are means ± SEMs, *$p < .05$ by unpaired student t test.

MOG peptide, and that Itk signaling regulates the generation of MOG- specific effector Th1 and Th17 cells.

Itk$^{-/-}$ CD4^{+} T cells exhibit altered migration velocity and are ineffective in crossing the blood brain barrier *in vitro*

In EAE and MS, pathogenic immune cells, in particular CD4^{+} T cells, must traverse the brain endothelium and enter the CNS parenchyma and participate in immune responses resulting in tissue damage [23-25]. Given that Itk$^{-/-}$ CD4^{+} T cells exhibit defects in CNS infiltration, which is important for inflammation and resultant CNS pathology, we next determined whether Itk signaling in CD4^{+} T cells is important for their traversal across the blood-brain barrier. We performed migration studies using an *in vitro* BBB model, to evaluate the migratory capacity of WT and Itk$^{-/-}$ CD4^{+} T cells. Itk$^{-/-}$CD4^{+} T cells showed defective migration across the *in vitro* brain endothelial barrier compared to WT CD4 T cells (Fig A1. 5A). This was not due to reduced mobility of Itk$^{-/-}$ CD4^{+} T cells, since these cells traveled at a rate of speed ~3 times faster than WT CD4^{+} T cells on a planar surface (Fig A1. 5B). Thus reduced ability to migrate across the BBB could partially explain the lack of CD4^{+} T cells in the CNS of Itk$^{-/-}$ mice and suggest that Itk signaling may also play an important role in T cell migration across CNS barriers.

Inhibition of Itk signaling decreases MOG-specific Th1 and Th17 cell migration across the BBB.

Figure A1. 5.

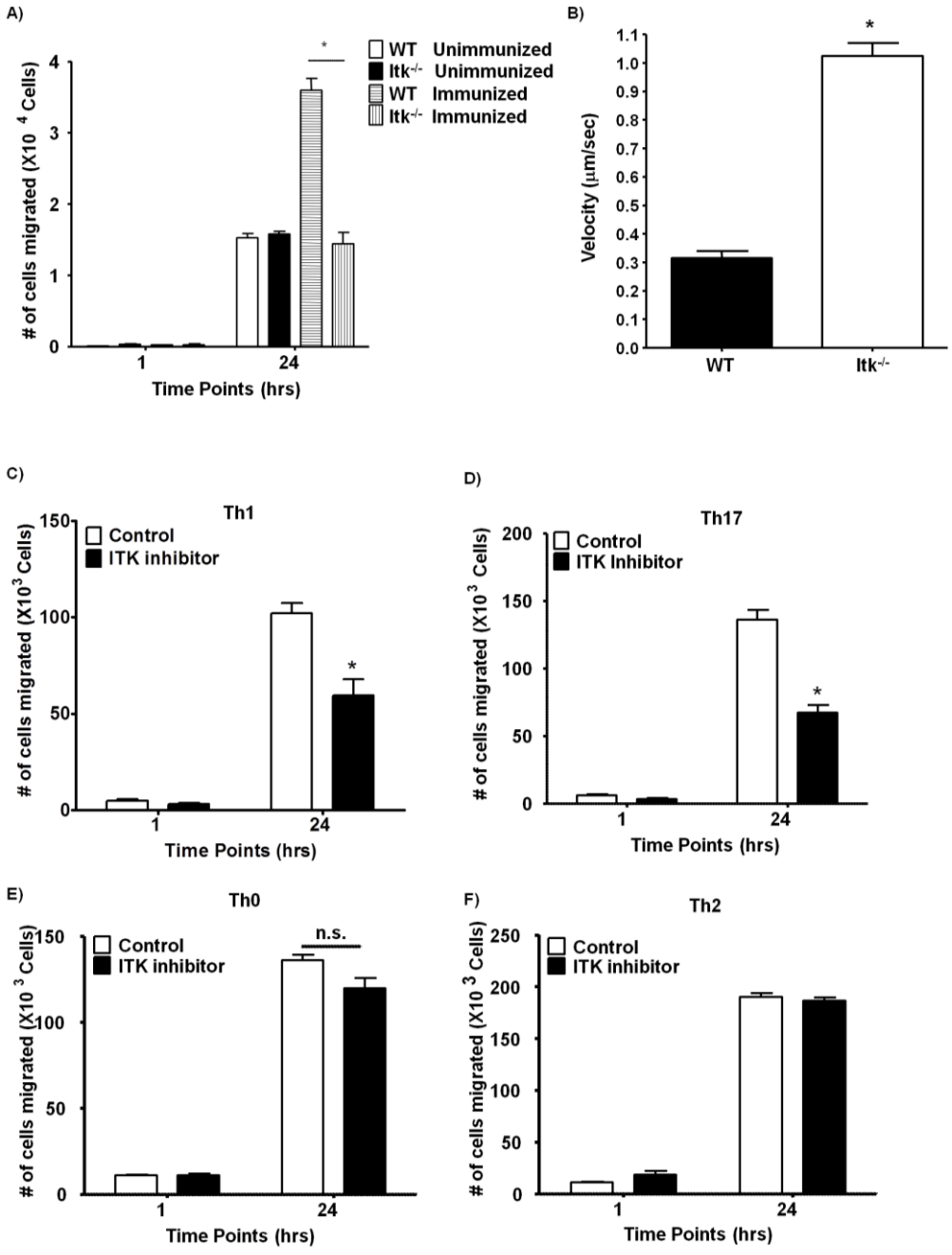
A)
WT Unimmunized
Itk-/- Unimmunized
WT Immunized
Itk-/- Immunized
# of cells migrated (X10 4 Cells)
Time Points (hrs)
B)
Velocity (μm/sec)
WT
Itk-/-
C)
Th1
Control
ITK inhibitor
# of cells migrated (X10 3 Cells)
Time Points (hrs)
D)
Th17
Control
ITK Inhibitor
# of cells migrated (X10 3 Cells)
Time Points (hrs)
E)
Th0
Control
ITK inhibitor
n.s.
# of cells migrated (X10 3 Cells)
Time Points (hrs)
F)
Th2
Control
ITK inhibitor
# of cells migrated (X10 3 Cells)
Time Points (hrs)

Figure A1. 5. Itk$^{-/-}$ mice show inefficient migration across the blood brain barrier during EAE and *in vitro*. **A)** 2.5x10^5 CD4$^+$ T cells isolated from MOG peptide-immunized WT and Itk$^{-/-}$mice were added to a layer of mouse brain endothelial cells (bEnd3) cultured as a model of the brain endothelial barrier and the number of cells migrating across the layer was determined at 1, 24 hrs post addition of T cells.*p<.05, means ± SEMs, by unpaired student t test. **B)** WT or Itk$^{-/-}$ CD4$^+$ T cells (1x10^5) were plated on cover glass and the movement of cells recorded by time lapse video microscopy. The time (t) to travel 100 μm (d) was measured and the velocity calculated based on the equation (v=d/t). **C and D)** CD4$^+$ T cells isolated from MOG-T cell receptor (TCR) transgenic mice (2D2-TCR-Tg) mice were stimulated with 5 μg/ml of MOG peptide for 72 hrs into Th1 and Th17 cells. 5 X 10^5 cells were loaded onto a layer of mouse brain endothelial cells (bEnd3) cultured as a model of the brain endothelial barrier and the number of Th1 **(B)** or Th17 **(C)** cells migrating across the layer was determined at 1 and 24 hrs post addition of T cells.*p<.05, means ± SEMs, by unpaired student t test (n=3).

We next determined whether inhibition of Itk signaling alters specifically the migration of MOG-specific Itk-sufficient effector T cells. We isolated T cells from MOG-T cell receptor (TCR) transgenic mice (2D2-TCR-Tg) and induced their differentiation to Th1 or Th17 *in vitro*. These Th1 and Th17 cells were treated with an Itk inhibitor evaluated for ability to migrate across our *in vitro* BBB. We found that significantly lower numbers of both Th1 and Th17 cells treated with the Itk inhibitor were recovered from the bottom of transwells at both early and later time points compared to vehicle controls (Fig. A1.5C and D). This confirms that inhibition of Itk signaling alters the migration of effector CD4 T cells across brain endothelial barrier cells. These results are consistent with the initial observation of reduced numbers of immune cells in the CNS and attenuated disease in $Itk^{-/-}$ mice and in recipients of $Itk^{-/-}$ CD4 T cells.

Displacement of F-actin in $Itk^{-/-}$ CD4 T cells occurs specifically under conditions of peptide/MHC Class ll:TCR interactions.

Cytoskeletal reorganization is necessary for cell movement, cell function and communication with other cells [26]. Our data indicate that Itk plays a role in both $CD4^+$ T cell response to myelin antigen (MOG) stimulation (Fig A1. 4), as well as in their ability to migrate across the BBB (Fig A1. 5). Previous studies have shown that T cells lacking Itk are defective in their ability to polymerize actin, to become polarized and to reorganize their cytoskeleton in response to TCR engagement, contributing to defective T cell activation [1, 27-28]. To further investigate the role of Itk in actin cytoskeletal reorganization in $CD4^+$ T cells during myelin antigen

restimulation, we isolated $CD4^+$ T cells from WT and $Itk^{-/-}$ mice previously immunized with MOG peptide, then stimulated them *in vitro* with MOG peptide (in the presence of APCs) and stained for F-actin and the CD4 co-receptor. We observed that MOG peptide stimulated $Itk^{-/-}$ $CD4^+$ T cells exhibit distinct displacement of actin away from the CD4

Figure A1. 6.

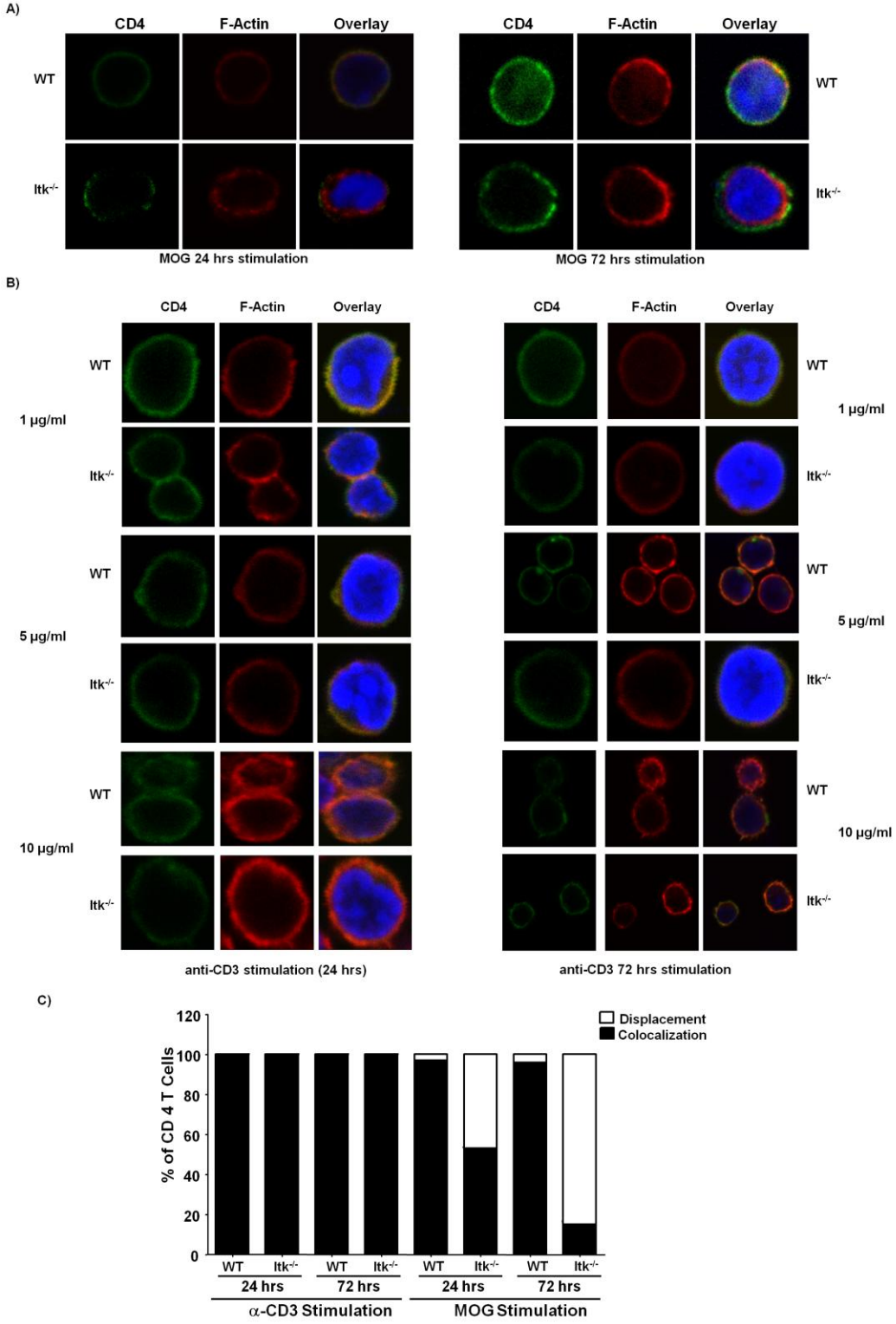
A)
CD4
F-Actin
Overlay
WT
Itk-/-
MOG 24 hrs stimulation
MOG 72 hrs stimulation
B)
1 µg/ml
5 µg/ml
10 µg/ml
anti-CD3 stimulation (24 hrs)
anti-CD3 72 hrs stimulation
C)
Displacement
Colocalization
% of CD 4 T Cells
120
100
80
60
40
20
0
24 hrs
72 hrs
α-CD3 Stimulation
MOG Stimulation

Figure A1. 6. Antigen specific defect in F-actin/CD4 colocalization in the absence of Itk. A) $CD4^+$ T cells isolated from WT or $Itk^{-/-}$ mice immunized with MOG peptide were stimulated with 5 μg/ml of MOG peptide, or **B)** plate bound α-CD3 (coated at 10 μg/mL of α-CD3 in PBS) for 24 or 72 hrs. Cells were fixed and stained with Alexa Fluor 488 α-CD4 and Alexa Fluor 568 phalloidin to visualize F-actin. Representative images taken from each group. **C**) Images from each treatment group were analyzed to quantify the co-localization or displacement of F-actin from CD4 co-receptor (n=100 per each group).

co-receptor (Fig A1. 6A). This is in stark contrast to MOG peptide-stimulated WT $CD4^+$ T cells, which showed complete co-localization between actin and the CD4 co-receptor (Fig. A1. 6A and B). Unstimulated WT or $Itk^{-/-}$ $CD4^+$ T cells, or stimulation with varying concentrations of anti-CD3 in the presence of APCs did not result in displacement of F-actin from the CD4 co-receptor at the time points examined (Fig A1. 6 C and D). These findings strongly suggest that Itk signaling induces actin co-localization with CD4 co-receptor specifically under conditions of antigen-MHC Class ll:TCR interactions. Put another way, actin displacement in $Itk^{-/-}$ $CD4^+$ T cells occurs maximally under conditions of peptide/MHC Class ll:TCR interaction.

Latrunculin B partially rescues migration of $Itk^{-/-}$ $CD4^+$ T cells across the BBB.

Cell migration strongly depends on the organization and degree of actin filament polymerization [26]. Latrunculin B (LatB) is a marine toxin which dose-dependently inhibits actin polymerization by sequestering G-actin and thus, prevents F-actin assembly [29]. In order for cells to migrate efficiently, the actin cytoskeleton needs to be dynamic, (i.e. polymerizing into F-actin and depolymerizing to G-actin). At high concentrations, LatB completely prevents F-actin assembly and disrupts actin polymerization, thus blocking cell migration. However, at the lower concentrations, LatB it allows more dynamic changes in F-actin polymerization. Thus low concentrations of LatB can enhance the dynamics of F-actin polymerization. We wanted to determine whether mild disruption of actin polymerization using low concentration of LatB, in $Itk^{-/-}$ cells would in part rescue signaling downstream of Itk and promote more efficient migration across brain endothelial cell monolayers. We

Figure A1. 7.

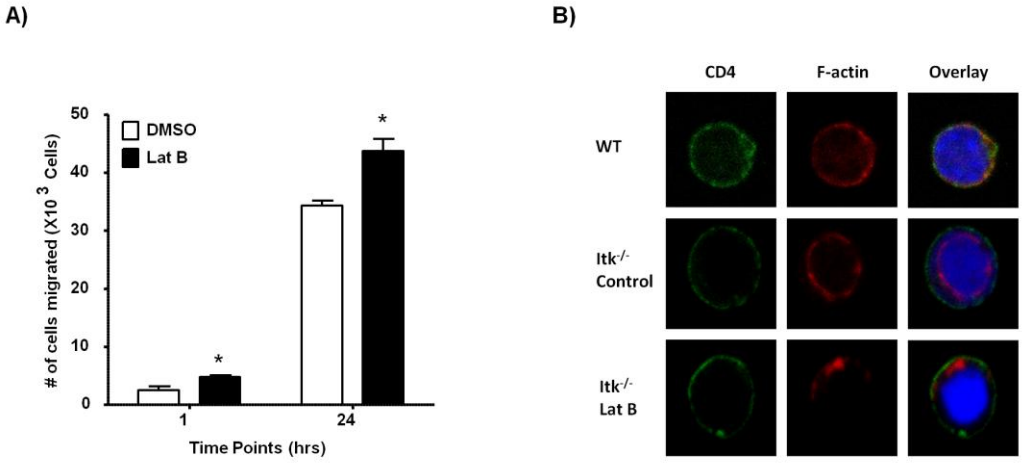
A)
B)
DMSO
Lat B
# of cells migrated (X10 3 Cells)
Time Points (hrs)
1
24
CD4
F-actin
Overlay
WT
Itk-/- Control
Itk-/- Lat B

Figure A1. 7. Latrunculin B partially rescues the transmigration capacity of CD4$^+$ T cells by actin-cytoskeletal reorganization. A) CD4$^+$ T cells isolated from Itk$^{-/-}$ mice immunized with MOG peptide were stimulated with 5 μg/ml of MOG peptide for 72 hrs and pretreated with DMSO or LatB (1 μM) for 1 hr. Cells were loaded onto mouse brain endothelial barrier and the number of cells migrating across the layer was determined at 1, 24 hrs post addition of T cells. *p<.05 means ± SEMs, by unpaired student *t* test (n=4). **B)** MOG peptide stimulated Itk$^{-/-}$ CD4$^+$ T cells were treated with DMSO or LatB (1 μM) for 1 hr and cells were fixed and stained with Alexa Fluor 488 α-CD4 and Alexa Fluor 568 phalloidin to visualize F-actin. MOG peptide stimulated WT CD4$^+$ T cells were also used as control.

treated MOG peptide-activated Itk$^{-/-}$ CD4^{+} T cells with a low concentration (1 μM) of LatB prior to their migration. We observed a significant increase in LatB-treated Itk$^{-/-}$ T cells recovered at the bottom of the transwell after their transmigration across the *in vitro* BBB (Fig A1. 7A). This is compared to lower numbers of vehicle treated cells. These results further confirm that the lack of Itk signaling, at least in large part, attenuated disease in Itk$^{-/-}$ mice by hampering the migration of pathogenic T cells into the CNS, thereby reducing the collateral tissue damage in the CNS.

We next determined whether LatB induces discernable changes in F-actin morphology. We observed that Itk$^{-/-}$ CD4^{+} T cells activated with MOG peptide and treated with LatB (as above), display a distinct change in expression and co-localization of F-actin in relation to the CD4 co-receptor, compared to LatB untreated Itk$^{-/-}$ CD4^{+} T cells (Fig. A1. 7B). There was less detectable actin in LatB-treated Itk$^{-/-}$ CD4^{+} T cells (**Fig A1. 7B**). Moreover, it appears that LatB sequestered F-actin in a dense area in the cell that is positioned in close proximity to the CD4 co-receptor (**Fig A1. 7B**). Thus, we hypothesize that Itk-regulated actin positioning in the proximity of CD4 is critical for the function of CD4^{+} T cells.

Itk signaling regulates Treg/ Th17 axis to exacerbate EAE

Foxp3^{+} Treg cells can suppress inflammation and ameliorate pathogenesis during EAE [30]. We wanted to determine if Treg cells played a role in the disease phenotype observed in Itk$^{-/-}$ mice. The number of Treg cells in brain and spinal cord of WT and Itk$^{-/-}$ mice at day 30 were not statistically significant (**Fig. A1. 8A**). However, while there were no differences in the number of Tregs, we found that the ratio of

Figure A1. 8.

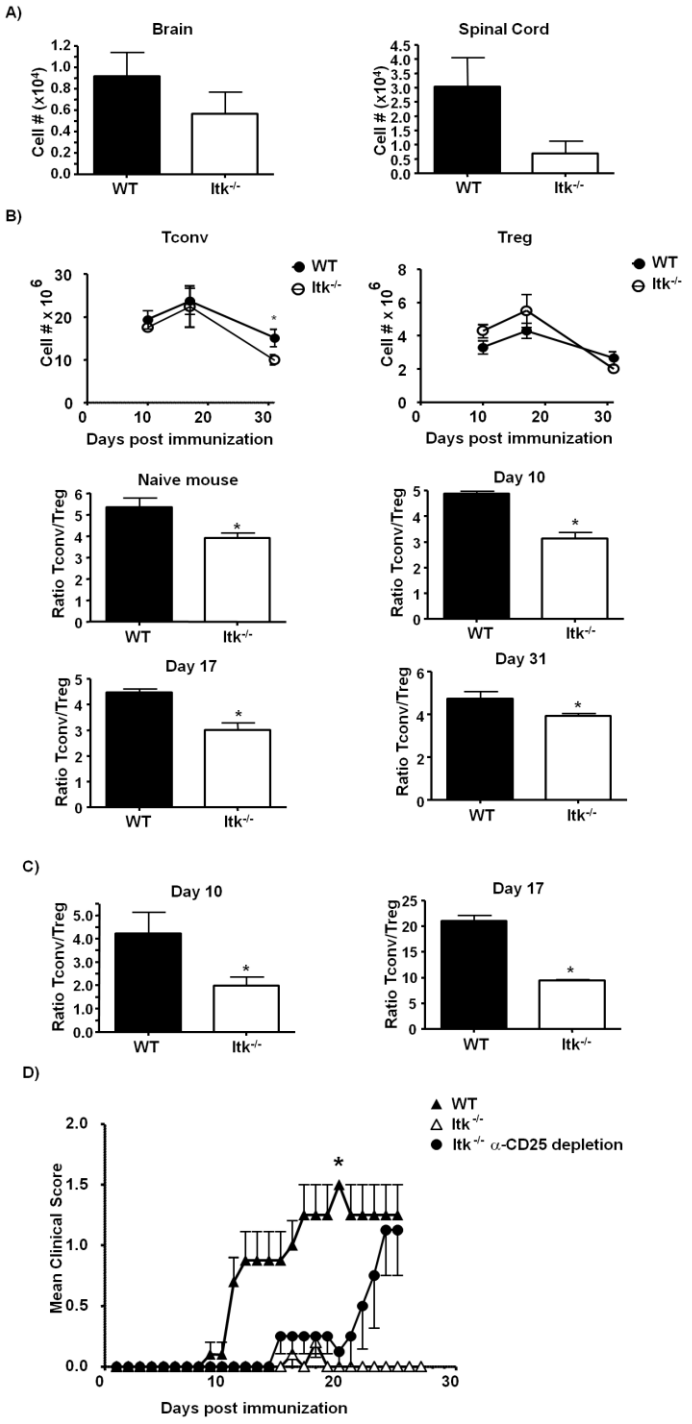
A)
Brain
Spinal Cord
Cell # (x10⁴)
WT
Itk-/-
B)
Tconv
Treg
Cell # x 10⁶
Days post immunization
Naive mouse
Day 10
Day 17
Day 31
Ratio Tconv/Treg
C)
D)
Mean Clinical Score
Itk-/- α-CD25 depletion

Figure A1. 8. Itk signaling regulates Treg/Th17 axis to exacerbate EAE. A) Cells were isolated from the brain and spinal cord of d31 immunized mice and analyzed for $CD4^+Foxp3^+$ Treg cells by FACS analysis, 3 mice/group. **B**) Splenocytes from the indicated WT and $Itk^{-/-}$ mice were analyzed for $CD4^+$ T cell (Tconv) and $CD4^+$ $Foxp3^+$ T cells (Treg) and the number and relative proportion of Tconv to Treg cells was calculated. **C**) Splenocytes of WT and $Itk^{-/-}$ mice isolated from d10 (left panel) and d17 (right panel) immunized mice were stimulated with 5 μg/mL MOG peptide for 72 hrs and analyzed for the ratio of Tconv to Treg cells as before. Values are means ± SEMs, by unpaired student *t* test. **D**) WT or $Itk^{-/-}$ mice were immunized to develop EAE and scored daily for clinical signs of EAE. $Itk^{-/-}$ mice were injected with either vehicle (PBS) or 200 μg α-CD25 (PC61 mAb) antibody every four days. Note that 4 of 5 mice injected with α-CD25 developed disease. Values are means ± SEMs, *$p < .05$ by 2-way ANOVA, n=5.

conventional T cells to Treg was perturbed in the periphery of naïve Itk$^{-/-}$ mice, and this altered ratio was maintained during the progression of EAE (Fig A1. 8B). Absence of Itk signaling also resulted in better expansion of Treg cells *ex vivo* in response to MOG peptide, with a significantly higher proportion of Treg cells in cultures of Itk$^{-/-}$splenocytes isolated either at day 10 or day 17 post EAE induction (Fig A1. 8C).

To determine whether this Tconv/Treg cell ratio contributed to the reduced susceptibility of Itk$^{-/-}$ mice to developing EAE, we depleted Treg cells *in vivo* by administration of α-CD25 and then induced EAE in Itk$^{-/-}$ mice. Interestingly, ablation of Treg cells resulted in increased disease severity in Itk$^{-/-}$ mice although the onset of EAE was still considerably delayed (Fig A1. 8D), suggesting that Itk regulates autoimmune pathologies during EAE in part by controlling the Treg/T effector balance.

A1.5. Discussion

In this study, we investigated the role of Itk in the $CD4^+$ T cell mediated neuroinflammatory disease, EAE, a murine model of MS. Both EAE and MS are characterized by invasion of inflammatory Th1 and Th17 autoreactive cells into the CNS that cause damage to myelin tissue, resulting in paralysis and neuronal damage and loss [12-14, 17]. Furthermore, defects in T regulatory cell numbers or function are also pathogenic for both EAE and MS [17, 30-32]. We found that the absence of Itk signaling is protective in EAE, suggesting that Itk plays an important role in the generation of autoreactive $CD4^+$ T cells that are pathogenic in EAE. This work supports and extends previous work by Gomez-Rodriguez et al, showing that Itk is essential for the production of IL17A by Th17 cells via activation and nuclear translocation of NFATc1 [4]. In addition to potentiating Th17 responses *in vivo*, we also show that Itk is essential for the elaboration of effector function of autoreactive Th1 cells, and that Itk signaling regulates the balance between Treg and T effector cells to exacerbate autoimmune pathologies during EAE. Furthermore, we show that Itk is important for the ability of effector $CD4^+$ T cells to migrate into the CNS, and critical for proper activation of $CD4^+$ T cells in part by regulating co-localization between CD4 and F-actin.

The progression of EAE follows an initial Th1 response, which transitions to an IL-17 driven response [16]. Our results suggest that Itk may play a more critical role in acute phase of EAE, since the clinical signs and number of $CD4^+$ T cells in the CNS of the $Itk^{-/-}$ mice eventually catch up with the WT animals at later stages of development of the disease. However, we also found that while $Itk^{-/-}$ T cells have the

capacity to become producers of IFNγ, they are less likely to migrate to the brain, hence the reduced numbers of these cells in the brain and spinal cord, and contribute to the pathology of the disease. We and others have suggested that $Itk^{-/-}$ $CD4^{+}$ T cells retain Th1 responses, and so we were also surprised that Itk was also required for Th1 responses and IFNγ secretion, since this has not been previously identified as a defect in these cells [3]. This could be secondary to Itk regulation of Ca^{2+} responses and activation of nuclear factors such as NFAT [33], both of which are critical for the rapid production of effector cytokines IFNγ and IL17A by differentiated T helper cells upon TCR stimulation [34]. It is also possible that Itk's role in the initial stimulation and differentiation of these cells to the Th1 lineage is different compared to its role in already differentiated Th1 cell. We are further investigating these roles of Itk in already differentiated cells. Nevertheless, our results suggest that $Itk^{-/-}$ T cells, either in $Itk^{-/-}$ mice or in the T cell transfer model, exhibit delayed induction of pathogenesis related to reduced IFNγ production, and the transition to IL-17A production does not occur.

EAE development is dependent on the ability of inflammatory $CD4^{+}$ T cells (and other immune cells) to migrate to the CNS where they mount inflammatory responses against myelin tissue resulting in tissue damage [24-25, 35-36]. We and others have previously shown that Itk signaling can promote migration of T cells via the chemokine SDF1α by driving actin rearrangements downstream of CXCR4 [37-38]. Consistent with this, we found reduced numbers of $Itk^{-/-}$ $CD4^{+}$ effector T cells in the CNS and spinal cord. Moreover, we demonstrated that $Itk^{-/-}$ $CD4^{+}$ T cells isolated from MOG-immunized mice were less efficient in migrating across brain endothelial

cells in an *in vitro* blood brain barrier model. We also observed that treatment of WT MOG-specific Th1 and Th17 cells with an Itk inhibitor led to a decrease in their migration of across brain endothelial cell monolayers. Furthermore, treatment of $Itk^{-/-}$ $CD4^+$ T cells with low concentrations of LatB, which enhances the turnover of actin and facilitates cell migration, led to enhanced migration, suggesting that regulation of the actin cytoskeleton by Itk in part regulates these events. This further confirms that Itk signaling potentiates and/or promotes $CD4^+$ T cell migration into the CNS and resultant neuroinflammation/neurodegeneration. We also found that activation of effector $CD4^+$ T cells in the absence of Itk is affected by alterations in the actin cytoskeleton. While the defects in actin cytoskeletal rearrangement downstream of the TCR is well established in the absence of Itk [39], what is not known is how these defects affect CD4 co-receptor localization. We observed disrupted interaction between CD4 and F-actin in the absence of Itk, and this is only observed in MOG-activated $CD4^+$ T cells but not under conditions of α-CD3 induced T cell activation. This antigen-specific defect may contribute to the defect in activation of $CD4^+$ effector T cells and could result in the reduced pathogenicity of these cells. This strongly suggests that Itk signaling can be a therapeutic target for pharmacological modulation to regulate inflammatory T cell entry into the CNS such as MS.

In this work we also observed that the ratio of Tconv:Treg cells is perturbed in naïve $Itk^{-/-}$ mice compared to WT controls. $Itk^{-/-}$ mice have fewer Tconv cells per Treg cell at the basal level and maintain this altered ratio throughout the progression of EAE. Gomez-Rodriguez et al have recently shown that Itk regulates the balance between Treg cells and Th17 cells [40], and we have also shown that the absence of

Itk signaling results in enhanced development of Tregs. Our data suggests that this regulation of Th17 vs. Tregs may control, in part, the ability to develop EAE. Thus in addition to dampening detrimental effector responses, absence of Itk signaling may also favor the expansion and/or survival of Treg cells to the detriment of Th17 cells. $Foxp3^+$ Treg cells have been shown to be critical for suppression and regulation of inflammation during EAE [17]. Consistent with this, we find that depletion of Treg cells during and post EAE immunization resulted in more severe disease pathophysiology in $Itk^{-/-}$ mice, albeit delayed. The fact that Treg depleted $Itk^{-/-}$ mice still exhibit delayed disease onset would suggest that the protection we see is primarily due to a defect in effector T cell function and that this is further enhanced by the presence of a lower ratio of Tconv:Treg cells. These results suggest that inhibiting Itk may tip the balance in favor of anti-inflammatory responses, which would be highly favorable in conditions such as inflammatory, autoimmune diseases and prevention of transplant rejection.

These results are interesting when taken in the context of published work on the regulation of T helper cell fate by mTOR signaling. Recent work has suggested that mTOR signaling can promote the differentiation of effector $CD4^+$ T cells while absence of mTOR signaling results in preferential expansion of Treg cells [41-42]. mTORC1 and mTORC2 promotes differentiation of Th1 and Th17 cells while mTORC2 potentiates Th2 responses [42-44]. mTORC1 and mTORC2 have been shown to inhibit induction of Foxp3 and subsequent differentiation of Treg cells [43-45]. Our work is also of interest given Gomez-Rodriguez et al's findings that Itk signals represses the expression of PTEN, which can control mTOR signaling

downstream of the TCR to affect the balance between effector Th17 $CD4^+$ T cell and Treg responses [40]. Our recent work also supports this conclusion since we have found that inhibition of the kinase activity of Itk enhances the development of Treg cells. However, while the function of inducible Tregs are not affected by Itk [40], we have shown that the function of natural or thymic derived Tregs is dependent on Itk. Note that it is not clear whether Tregs involved in regulating the development of EAE are inducible or thymic/natural Tregs, which may determine how effective the balance between suppressive and pathogenic T cells responses are in the $Itk^{-/-}$ mice developing EAE. Nevertheless, it is clear that absence of Itk signaling not only dampens effector $CD4^+$ T cell responses but also tips the balance in favor of anti-inflammatory responses by promoting the expansion of regulatory T cells.

CTLA-4 deficient mice spontaneously develop autoreactive T cells that infiltrate various organs, and Jain et al recently reported that the absence of Itk results in the accumulation of autoreactive CTLA-4 deficient T cells in secondary lymph nodes, alleviating the autoimmune destruction of pancreas in models of type I diabetes [46]. These data suggest that Itk may control the ability of activated T cells to leave the lymph nodes and access sites of auto antigen for pathogenic destruction of tissue. Our findings support these conclusions, but also indicate that Itk regulates other aspects of the T cell immune response and biology. We propose that the absence of Itk signaling protects against neuroinflammation during EAE through a number of mechanisms. First, signaling through Itk is essential for the generation of autoreactive effector Th1 and Th17 cells that are central to neuroinflammation. Second, Itk signaling regulates the balance between pathogenic Th1/Th17 and tolerogenic Treg

cells to exacerbate EAE. Finally, Itk signaling may also play a role in how antigen specific cells migrate across the blood brain barrier. This work therefore has implications for understanding Itk as a potential therapeutic target. In light of this, inhibitors of Itk could be attractive options for treatment of Th1/Th17 mediated autoimmune pathologies such as MS, and in treatment regimens where it would be beneficial to expand regulatory $CD4^+$ T cells.

References

1. Gomez-Rodriguez, J., et al., *Tec kinases, actin, and cell adhesion.* Immunol Rev, 2007. **218**: p. 45-64.
2. Andreotti, A.H., et al., *T-cell signaling regulated by the Tec family kinase, Itk.* Cold Spring Harb Perspect Biol, 2010. **2**(7): p. a002287.
3. Fowell, D.J., et al., *Impaired NFATc translocation and failure of Th2 development in Itk-deficient CD4+ T cells.* Immunity, 1999. **11**(4): p. 399-409.
4. Gomez-Rodriguez, J., et al., *Differential expression of interleukin-17A and -17F is coupled to T cell receptor signaling via inducible T cell kinase.* Immunity, 2009. **31**(4): p. 587-97.
5. Kannan, A.K., et al., *IL-2-inducible T-cell kinase modulates T2-mediated allergic airway inflammation by suppressing IFN-gamma in naive CD4 T cells.* J Allergy Clin Immunol, 2013.
6. Sahu, N. and A. August, *ITK inhibitors in inflammation and immune-mediated disorders.* Curr Top Med Chem, 2009. **9**(8): p. 690-703.
7. August, A. and M.J. Ragin, *Regulation of T-cell responses and disease by tec kinase Itk.* Int Rev Immunol, 2012. **31**(2): p. 155-65.
8. Ascherio, A. and K.L. Munger, *Environmental risk factors for multiple sclerosis. Part I: the role of infection.* Ann Neurol, 2007. **61**(4): p. 288-99.
9. Cantorna, M.T., *Vitamin D and its role in immunology: multiple sclerosis, and inflammatory bowel disease.* Prog Biophys Mol Biol, 2006. **92**(1): p. 60-4.
10. Whitacre, C.C., *Sex differences in autoimmune disease.* Nat Immunol, 2001. **2**(9): p. 777-80.

11. Navikas, V. and H. Link, *Review: cytokines and the pathogenesis of multiple sclerosis.* J Neurosci Res, 1996. **45**(4): p. 322-33.

12. Hemmer, B., et al., *Multiple sclerosis -- a coordinated immune attack across the blood brain barrier.* Curr Neurovasc Res, 2004. **1**(2): p. 141-50.

13. Keegan, B.M. and J.H. Noseworthy, *Multiple sclerosis.* Annu Rev Med, 2002. **53**: p. 285-302.

14. El-behi, M., A. Rostami, and B. Ciric, *Current views on the roles of Th1 and Th17 cells in experimental autoimmune encephalomyelitis.* J Neuroimmune Pharmacol, 2010. **5**(2): p. 189-97.

15. Wekerle, H., et al., *Animal models.* Ann Neurol, 1994. **36 Suppl**: p. S47-53.

16. Jager, A., et al., *Th1, Th17, and Th9 effector cells induce experimental autoimmune encephalomyelitis with different pathological phenotypes.* J Immunol, 2009. **183**(11): p. 7169-77.

17. Kohm, A.P., et al., *Cutting edge: CD4+CD25+ regulatory T cells suppress antigen-specific autoreactive immune responses and central nervous system inflammation during active experimental autoimmune encephalomyelitis.* J Immunol, 2002. **169**(9): p. 4712-6.

18. Bynoe, M.S., et al., *Epicutaneous immunization with autoantigenic peptides induces T suppressor cells that prevent experimental allergic encephalomyelitis.* Immunity, 2003. **19**(3): p. 317-28.

19. Wilhelm, I., C. Fazakas, and I.A. Krizbai, *In vitro models of the blood-brain barrier.* Acta Neurobiol Exp (Wars), 2011. **71**(1): p. 113-28.

20. Liao, X.C. and D.R. Littman, *Altered T cell receptor signaling and disrupted T cell development in mice lacking Itk.* Immunity, 1995. **3**(6): p. 757-69.

21. Korn, T., et al., *IL-17 and Th17 Cells.* Annu Rev Immunol, 2009. **27**: p. 485-517.

22. Hu, J. and A. August, *Naive and innate memory phenotype CD4+ T cells have different requirements for active Itk for their development.* J Immunol, 2008. **180**(10): p. 6544-52.

23. Kuchroo, V.K., et al., *T cell response in experimental autoimmune encephalomyelitis (EAE): role of self and cross-reactive antigens in shaping, tuning, and regulating the autopathogenic T cell repertoire.* Annu Rev Immunol, 2002. **20**: p. 101-23.

24. Mills, J.H., et al., *Extracellular adenosine signaling induces CX3CL1 expression in the brain to promote experimental autoimmune encephalomyelitis.* J Neuroinflammation, 2012. **9**: p. 193.

25. Mills, J.H., et al., *CD73 is required for efficient entry of lymphocytes into the central nervous system during experimental autoimmune encephalomyelitis.* Proc Natl Acad Sci U S A, 2008. **105**(27): p. 9325-30.

26. Lafouresse, F., et al., *Actin cytoskeleton control of the comings and goings of T lymphocytes.* Tissue Antigens, 2013. **82**(5): p. 301-11.

27. Singleton, K.L., et al., *Itk controls the spatiotemporal organization of T cell activation.* Sci Signal, 2011. **4**(193): p. ra66.

28. Labno, C.M., et al., *Itk functions to control actin polymerization at the immune synapse through localized activation of Cdc42 and WASP.* Curr Biol, 2003. **13**(18): p. 1619-24.

29. Wakatsuki, T., et al., *Effects of cytochalasin D and latrunculin B on mechanical properties of cells.* J Cell Sci, 2001. **114**(Pt 5): p. 1025-36.

30. Fletcher, J.M., et al., *CD39+Foxp3+ regulatory T Cells suppress pathogenic Th17 cells and are impaired in multiple sclerosis.* J Immunol, 2009. **183**(11): p. 7602-10.

31. Haas, J., et al., *Reduced suppressive effect of CD4+CD25high regulatory T cells on the T cell immune response against myelin oligodendrocyte glycoprotein in patients with multiple sclerosis.* Eur J Immunol, 2005. **35**(11): p. 3343-52.

32. Viglietta, V., et al., *Loss of functional suppression by CD4+CD25+ regulatory T cells in patients with multiple sclerosis.* J Exp Med, 2004. **199**(7): p. 971-9.

33. Schwartzberg, P.L., L.D. Finkelstein, and J.A. Readinger, *TEC-family kinases: regulators of T-helper-cell differentiation.* Nat Rev Immunol, 2005. **5**(4): p. 284-95.

34. Murphy, K.M. and S.L. Reiner, *The lineage decisions of helper T cells.* Nat Rev Immunol, 2002. **2**(12): p. 933-44.

35. Kurkowska-Jastrzebska, I., et al., *Neurodegeneration and inflammation in hippocampus in experimental autoimmune encephalomyelitis induced in rats by one--time administration of encephalitogenic T cells.* Neuroscience, 2013. **248**: p. 690-8.

36. Lin, M.H., et al., *T cell-specific BLIMP-1 deficiency exacerbates experimental autoimmune encephalomyelitis in nonobese diabetic mice by increasing Th1 and Th17 cells.* Clin Immunol, 2014. **151**(2): p. 101-13.

37. Fischer, A.M., et al., *Regulation of CXC chemokine receptor 4-mediated migration by the Tec family tyrosine kinase ITK.* J Biol Chem, 2004. **279**(28): p. 29816-20.

38. Takesono, A., et al., *Requirement for Tec kinases in chemokine-induced migration and activation of Cdc42 and Rac.* Curr Biol, 2004. **14**(10): p. 917-22.

39. Grasis, J.A. and C.D. Tsoukas, *Itk: the rheostat of the T cell response.* J Signal Transduct, 2011. **2011**: p. 297868.

40. Gomez-Rodriguez, J., et al., *Itk-mediated integration of T cell receptor and cytokine signaling regulates the balance between Th17 and regulatory T cells.* J Exp Med, 2014. **211**(3): p. 529-43.

41. Powell, J.D. and G.M. Delgoffe, *The mammalian target of rapamycin: linking T cell differentiation, function, and metabolism.* Immunity, 2010. **33**(3): p. 301-11.

42. Chi, H., *Regulation and function of mTOR signalling in T cell fate decisions.* Nat Rev Immunol, 2012. **12**(5): p. 325-38.

43. Delgoffe, G.M., et al., *The kinase mTOR regulates the differentiation of helper T cells through the selective activation of signaling by mTORC1 and mTORC2.* Nat Immunol, 2011. **12**(4): p. 295-303.

44. Lee, K., et al., *Mammalian target of rapamycin protein complex 2 regulates differentiation of Th1 and Th2 cell subsets via distinct signaling pathways.* Immunity, 2010. **32**(6): p. 743-53.

45. Delgoffe, G.M., et al., *The mTOR kinase differentially regulates effector and regulatory T cell lineage commitment.* Immunity, 2009. **30**(6): p. 832-44.

46. Jain, N., et al., *CD28 and ITK signals regulate autoreactive T cell trafficking.* Nat Med, 2013. **19**(12): p. 1632-7.

Appendix 2.

Non-alcoholic fatty liver disease induces Alzhimer's disease (AD) in wild type mice and accelerates AD in an AD model.

*This appendix was submitted to Journal of Immunology

A2.1. Abstract

Non-alcoholic fatty liver disease (NAFLD) is a chronic liver disease afflicting about one third of the world's population and 30% of the US population. It is induced by consumption of high lipid diets and is characterized by liver inflammation and subsequent liver pathology. Here, we investigated NAFLD-induced liver inflammation in the pathogenesis of Alzheimer's disease (AD). We fed AD-transgenic (APP-Tg) and wild-type (WT) mice with high fat/lipid diet or a control diet. Chronic NAFLD induced advanced AD in WT mice, accelerated advanced-AD in APP-Tg mice, induced neuronal apoptosis and decreased brain expression of low-density lipoprotein receptor-related protein-1, that is involved in beta-amyloid clearance, in both WT and APP-Tg mice. Removal of mice from HFD during acute disease reversed liver pathology, neuroinflammation and decreased beta-amyloid plaque load. These findings are highly translatable, as they indicate chronic inflammation induced outside the brain is sufficient to induce neurodegeneration in the absence of genetic predisposition.

A2.2. Introduction

Alzheimer's disease (AD) is a progressive neurodegenerative disease associated with decline in cognitive function, impairment in memory, language and visual-spatial coordination, eventually resulting in complete loss of basic function [1]. Dementia of all forms affects about 5% of the population older than 65. There are approximately 5.5 million cases of AD in the US alone and this number is estimated to nearly triple by the year 2040. Moreover, as the world population lives longer, AD and dementia are predicted to constitute a major global health problem in the aging population of the world [2].

Major pathological hallmarks of AD present as senile amyloid plaques that are composed of Amyloid β (Aβ) protein and intracellular neurofibrillary tangles with characteristic reactive microgliosis and astrogliosis. AD is characterized by dystrophic neuritis, neuronal loss, synaptic dysfunction and cerebral atrophy [1]. AD can be largely divided into early and late onset forms. Early onset AD is induced in patients carrying genetic mutation/s in amyloid precursor protein (APP) and/or Presenilin (PS1 or PS2) which induces formation of insoluble Aβ. Late onset AD, also known as sporadic AD, is believed to be induced by aberrant processing of Aβ resulting in pathological lesions. In general, APP is cleaved by α-secretase that generates soluble Aβ that has neuroprotective function [3]. However when APP is cleaved by beta-secretase-1 (BACE1) it produces $A\beta_{1\text{-}42}$ which is insoluble and forms amyloid plaques that are proapoptotic and neurodegenerative and is believed to induce cognitive impairment [4-5]**.** While the underlying cause of AD is not known, advancing age,

environmental stressors and genetic factors appear to be important precursors [6-7]. In addition to Aβ deposits, AD is characterized by neurofibrillary tangles which are neuronal deposits of hyperphosphorylated Tau, also referred to as tauapathies that are well correlated with cognitive impairment and advanced neurodegeneration [1, 8]. Due to this association, it is still debated whether the initiating factor for AD is Aβ plaque or tauopathy [9].

In the United States, diets high in fats/lipids which are commonly known as "fast foods," are prevalent in a significant proportion of the population and is becoming an important public health issue. High fat diets (HFD) are implicated in various metabolic syndromes leading to obesity, atherosclerosis, insulin resistance, dementia, cognitive decline and potentially, to AD [10-14]. HFD also induces liver pathology called non-alcoholic fatty liver disease (NAFLD) that is characterized by fatty liver, accumulation of lipids in hepatocytes and infiltration of inflammatory immune cells in the liver parenchyma and secretion of proinflammatory cytokines resulting in liver damage [11-12, 15-16]. NAFLD is the fourth largest cause of liver disease in the Western hemisphere. It afflicts about 30% of the US population and is the twelfth leading cause of death in the US amongst adults 45-54 years [17]. The increase in NAFLD has been linked to increased prevalence of obesity and metabolic diseases in the US and worldwide (7). NAFLD is associated with marked progressive inflammation, fat deposition and fibrosis of the liver (8,10). Also, a clear association exists between cardiovascular risk factors or carotid atherosclerosis and dementia progression leading to AD [18].

Cholesterol is an important building block of the brain [19], which is rich in cholesterol and produces over 20% of total cholesterol in the body. This high cholesterol content is needed for neuronal function, as the brain cannot access plasma cholesterol due to restrictions posed by the blood brain barrier [20]. For this reason, neuronal cells express high levels of cholesterol-uptake receptors such as LDLR, low-density lipoprotein receptor-related protein 1 (LRP1) and apoliprotein-E (ApoE). Up to 70% of the brain's cholesterol make up the myelin sheath of oligodendrocytes and the membrane of astrocytes, with the remainder contributing to neuronal function including the myelin sheath of neurons that relay synaptic signals. ApoE, and LRP1, are related to cholesterol metabolism and are important risk factors contributing to the prevalence of AD [21-23]. The ApoE variant, ApoE4, increases AD risk and accelerates AD onset (Bu, 2009; Liu et al., 2013). Multivariate analysis of metabolites in the blood of AD patients when compared to age-matched controls, showed that of the ten metabolites that distinguished AD from its age-matched cohorts, six of them were long chain cholesteryl esters that were reduced in AD [24]. Also, several large cohort studies showed that long-term treatment with statins, which lowers serum cholesterol levels, could alleviate AD symptoms, suggesting that alteration in lipid metabolism contributes to AD pathogenesis [25-26]. LRP1 is an endocytic receptor highly expressed in the liver, on neurons and on vascular smooth muscle and glial cells in the CNS vasculature and functions in the clearance of Aβ from the CNS. Aβ clearance is impaired in neurons from LRP1-defificient mice [27]. Binding of APP to LRP1 results in increased trafficking and clearance of APP. However, LRP1 is also involved in Aβ production. Hence, its involvement in Aβ synthesis and clearance

makes it a prime target in AD pathogenesis. Deletion of LRP1 exacerbated Aβ deposition and increased CAA [28]. It is speculated that ApoE may inhibit or facilitate LRP1 endocytosis of Aβ. Since ApoE4 is linked to both sporadic and familial AD and ApoE functions in the cellular transfer of lipids through LRP1 on the cell surface, it is presumed that LRP1, ApoE or both are involved in dysfunction of the lipid transport mechanism and Aβ clearance.

The increase in obesity and NAFLD prevalence in our society, both induced by diets high in fats/lipids (HFD) and their link to chronic inflammation and metabolic diseases, mirrors increase in AD and AD-like syndromes. We therefore decided to investigate the impact of NAFLD in AD pathogenesis in an AD transgenic mouse model (APP-Tg) and in C57BL/6, wild type (WT) mice.

To elucidate the effect of a diet with increased lipids, which we will refer to as HFD, that manifests as NAFLD in AD pathogenicity, compared to standard mouse diet (SD), we fed APP-Tg and WT mice with HFD for 2 months, 5 months and up to one year. HFD induced systemic and CNS inflammation that accelerated Aβ plaque deposition during acute NAFLD (2, 5 months) in APP-Tg mice and it induced neuroinflammation but did not induce Aβ plaques in WT mice compared to SD controls. Removal of APP-Tg mice from HFD after 2 months decreased Aβ plaque load and reversed signs of systemic and CNS inflammation in both WT and APP-Tg mice. APP-Tg and WT mice were kept on HFD for up to one year to determine the impact of chronic NAFLD in AD induction in WT mice and progression in APP-Tg mice. We observed advanced signs of AD, including accelerated cerebral amyloid angiopathy (CAA), and increased tauopathy, and neuronal loss in APP-Tg mice. More

importantly, long term HFD treatment induced plaque formation, CAA and tauopathy in WT mice. The advanced signs of AD was associated with a decrease in CNS expression of LRP1 during chronic disease. These studies indicate that HFD induced inflammation plus aging is sufficient to trigger neurodegeneration and accelerate the process of AD even in the absence of genetic predisposition.

A2.3. Materials and Methods

Mice and diet

The APP-Tg mouse [B6.Cg- Tg(APPswe,PSEN1dE9)85Dbo/J] was generated as previously described [29]. APP-Tg mice and their WT littermates were fed either a standard diet (SD) (Harlan Teklad TD.7912), or a high-fat diet (HFD) (1.0% cholesterol, 0.5% cholic acid, 18% triglyceride; Harlan Teklad TD.88051, "Paigen diet") [12] beginning at the age of 2 months. APP-tg and WT mice were fed for 2 months, 5 months, and 1 year either with HFD or SD or APP-Tg mice removed from HFD after 2 months and were put back on SD for 3 months. All animal work was done in accordance with PHS guidelines and was approved by Cornell's institutional animal care and use committee (Protocol # 2008–0092).

Tissue harvest and histology

Deeply anesthetized mice were weighed and transcardially perfused with ice cold PBS then brain, spleen, and liver were collected for analysis. After macroscopic photo documentation, all livers were weighed and used for leukocyte preparation, except two 30 mg tissue sections which were used for histopathology and RNA preparation. Approximately 30 mg of liver and one brain hemisphere were flash frozen in Tissue-Tek O.C.T. (Sakura Finetek) and stored at -80℃. 10µm thick frozen sections were affixed to Supefrost/Plus slides (Fisher), fixed in acetone, and stored at -80℃. For immunohistochemistry staining, slides were thawed and treated with 0.03% H_2O_2 in PBS to block endogenous peroxidase or fixed and permeabilized in acetone

for immunofluorescence staining, blocked with casein (Vector Laboratories) in normal goat serum (Zymed), and then incubated with anti- CD45, phospho Tau**,** ApoE, CD31, LRP-1, 6E10, GFAP or NeuN primary antibodies. For immunohistochemistry, slides were then incubated with biotinylated goat anti-rat Ig (Jackson ImmunoResearch) and streptavidin–HRP (Zymed) and developed with an AEC (Red) substrate kit (Zymed) and a hematoxylin counterstain then coverslips were mounted with Fluoromount-G. For immunofluorescence, slides were instead subjected to AF488, TexRed, or AF647 conjugated secondary antibody and coverslips were mounted with Vectastain containing DAPI (Vectorlabs). For TUNEL staining which was used for detecting cell death, reaction mixture supplied by Roche's In Situ Cell Death Detection Kit, AP (Cat. No. 11 684 809 910) was used following the protocol provided from Roche.

Standard or frozen histological tissue sections were formalin fixed and processed for hematoxylin and eosin (H&E) or Oil-Red-O staining and hematoxylin counterstaining respectively, then examined by light microscopy. For the green fluorescent Thioflavine S (ThioS) staining of plaques, frozen sections were incubated with 1% ThioS (Sigma-Aldrich) in distilled water for 5 min, differentiated in 70% ethanol for 5 min, washed three times for 5 min each with distilled water and cover-slipped with Vectastain containing DAPI (Vectorlabs). Images were captured using a Zeiss Axio Imager M1 microscope.

quantitative PCR

Brain and liver mRNA was extracted with TRIZOL (Invitrogen) and cDNA was synthesized using High-Capacity cDNA Reverse Transcription Kits (Applied

Biosystems) according to the protocols provided by the manufacturers. Quantification of expression levels of ApoE, LRP1, TLR1, TLR2, TLR6 and of pro-inflammatory cytokines (IL-6', TNFα, IL-17 and IL-1b) were performed using specific primers and KAPA SYBR FAST qPCR Kit (KAPA biosystems) and ran on CFX96 thermocycler (Bio-Rad). Relative mRNA expression levels of genes were analyzed using $2^{\wedge dCT}$ method, normalized with GAPDH as reference gene and fold change plotted was relative to the respective SD controls. Specificity of reaction was analyzed using melting curve analysis. Primer sequences can be viewed in supplemental table 1.

ELISA assay

Splenocytes were harvested from SD or HFD fed mice after 1 year and treated with either PBS or ConA for 48-72 hrs. Supernatant was collected and used for ELISA analysis using eBioscience Ready Set Go Kit. Briefly, plates were coated overnight at 4 ℃ with capture antibodies against IL-6, TNFα, IL-17 and then washed. Incubation was repeated with added standards and samples and washed then subsequently incubated with biotin conjugated detection antibodies. Plate was washed and developed with 1X TMB substrate solution (ebioscience) and the optical density (O.D.) was read at 450 nm using Biotek fluormetry (Biotek). O.D. values were converted into absolute concentration using the standard curve.

Statistical Analyses

Data were analyzed by one-way-ANOVA, followed by Bonferroni's Multiple Comparison test or student t-test (two-tailed, unpaired) using GraphPad Prism 5

software (Graphpad, La Jolla, CA). Plotted data shown represents mean ± s.e.m where significance is indicated by *, $P<0.05$; **, $P<0.01$; ***, $P<0.001$.

A2.4. Results

Acute stage NAFLD accelerated beta-amyloid plaque formation in APP-Tg mice.

It is becoming more and more evident that diets high in fats/lipids can cause metabolic diseases such as NAFLD. Metabolic diseases are emerging as significant contributors to dementia and cognitive decline [30-31]. To investigate the impact of acute NAFLD in AD pathogenesis we induced NAFLD in age- and gender-matched WT and APP-Tg mice, by feeding them a high fat/high cholesterol diet (HFD) (consisting of 1% cholesterol and 18% triglicerides) (Table A2.1) beginning at 2 months old. Mice were fed HFD for 2 months, 5 months, or removed from HFD after 2 months and were put back on standard diet (SD) for 3 months, while control mice (APP-Tg and WT mice) were fed SD for either 2 months or 5 months. To determine whether HFD increased beta-amyloid (Aβ) plaque burden in APP-Tg mice, or induced Aβ plaques in WT mice, we analyzed brain sections of APP-Tg mice on HFD for 2 and 5 months, and of mice that were removed from HFD after two months and were put back on SD, as well as of SD fed control mice (Fig A2.1). We observed a significant increase in Aβ plaque load in HFD fed APP-Tg mice at 2 and 5 months (Fig 1B and C) compared to SD fed controls (Fig A2.1.A) as visualized by Thioflavine S stained plaques. APP-Tg mice that were removed from HFD after two months have lower plaque burden than mice on HFD for 5 months (Fig A2.1.B-D). Not only was the plaque burden in HFD APP-Tg mice greater, the plaque sizes were larger in diameter than the average plaque size in control mice on SD and were

Table A2.1. Fat composition of standard diet (SD) and high fat diet (HFD).

Fat Composition (%)	SD	HFD
Total Fat	5.8	15.8
Cholesterol	0	1.0
Cholic acid	0	0
Triglyceride	0	18

Figure A2.1.

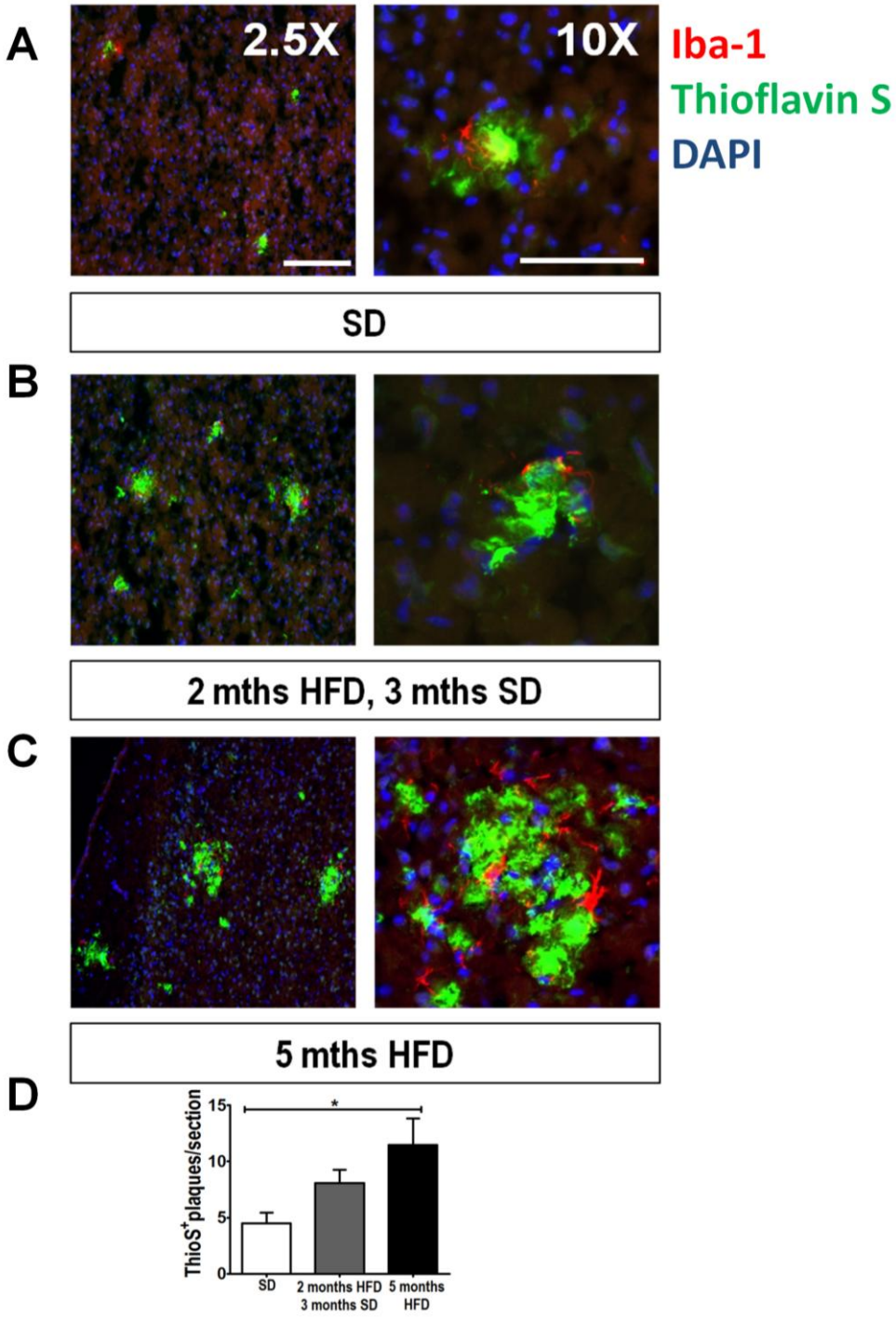
A
2.5X
10X
Iba-1
Thioflavin S
DAPI
SD
B
2 mths HFD, 3 mths SD
C
5 mths HFD
D
ThioS+ plaques/section
15
10
5
0
*
SD
2 months HFD
3 months SD
5 months
HFD

Figure A2.1. HFD accelerated beta amyloid plaque burden in APP-tg mice. Representative images of Thioflavin-S (green) and Iba-1 (red) stained cortical brain sections from age-matched APP-Tg mice fed with either SD for five months (A), kept two months on HFD then replaced with SD for three months (B), or kept on HFD for five months straight (C). Right panel images are at 10x magnification showing plaque cluster from lower 2.5x magnification of left panels. Bar = 100µm. (D) Quantification of plaque load in cortical sections of multiple fields (10 fields/mouse) from 5 mice /group in one representative experiment.

inundated with activated microglial cells (Fig A2.1.D). We did not observe Aβ plaques in WT mice on HFD either at two or five months (Supplementary Fig A2.1). We conclude that HFD accelerated Aβ plaque formation in APP-Tg mice but did not induce plaques in WT controls. Moreover, removal of APP-Tg mice from HFD to SD lessened plaque load compared to mice on HFD for five months duration. This suggests that if dietary intake is corrected early in disease (prior to advanced AD), that signs of AD can be reversed.

Both APP-Tg and WT mice are susceptible to HFD-induced NAFLD steatohepatitis and systemic inflammation

NAFLD induces severe liver inflammation and causes significant liver damage [16]. To confirm NAFLD induction we examined the livers of mice and observed that both APP-Tg and WT mice on HFD exhibited significant liver abnormality, characterized by severe hepatomegaly, fat accumulation and significant increase in liver size and weight in both APP-Tg and WT HFD fed mice (Fig A2.2.A and B). Interestingly, when both APP-Tg and WT mice were removed from HFD after 2 months and put back on normal chow (SD) for three months, the fatty liver resolved and the size of their livers was similar to control mice that were continuously on SD (Fig A2.2.A). Notably, HFD consumption did not lead to abnormal body weight gain in either APP-Tg or WT mice compared to control mice on SD (Fig A2. 2.B).

To further define the liver pathology in HFD fed mice, we performed immunohistochemistry to examine immune cell infiltration in the liver (hepatitis), as well as Oil-Red-O staining to evaluate fat deposition in the liver cells (steatosis) (Fig

Figure A2.2

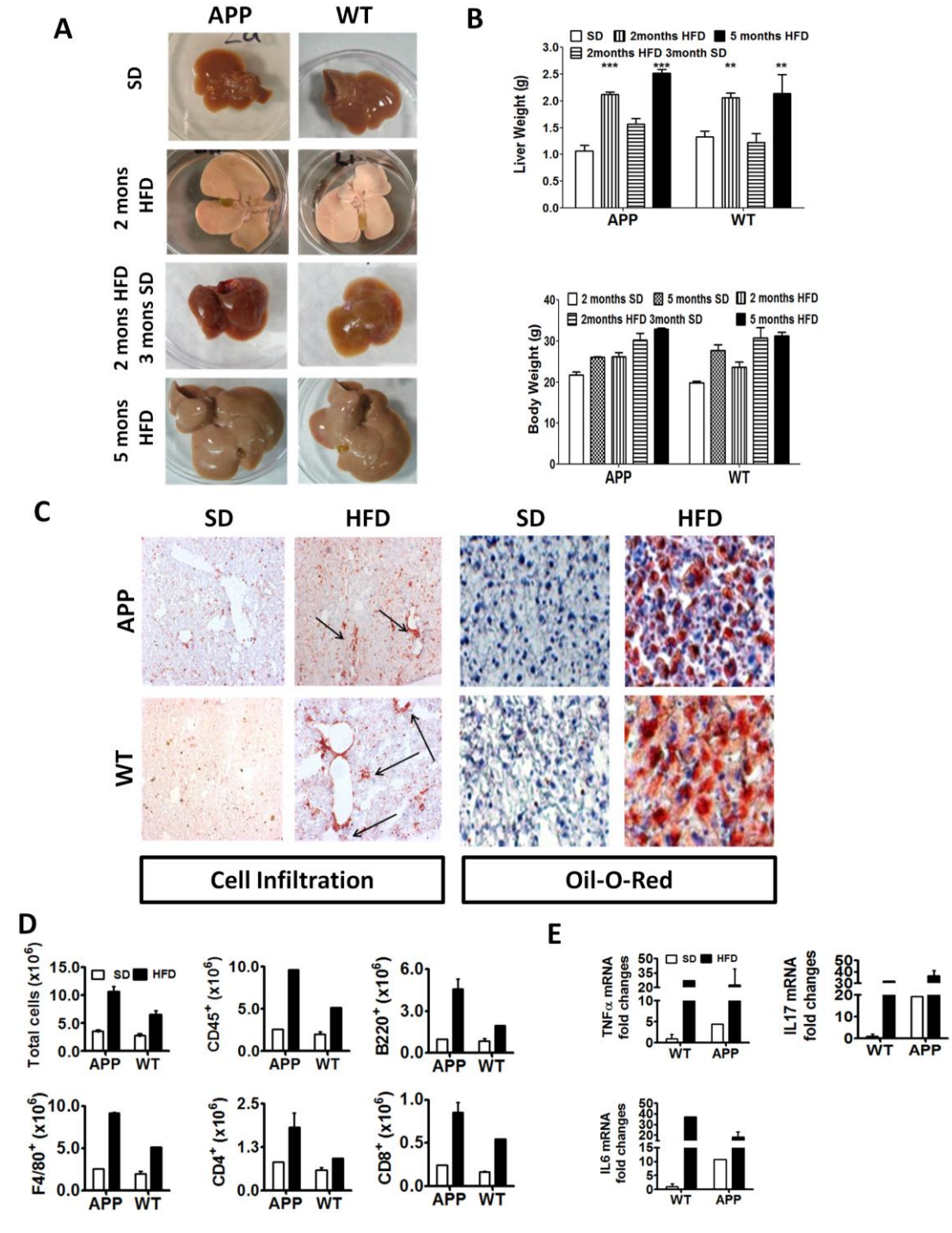
A
APP
WT
SD
2 mons HFD
2 mons HFD 3 mons SD
5 mons HFD
B
SD
2months HFD
5 months HFD
2months HFD 3month SD
Liver Weight (g)
APP
WT
2 months SD
5 months SD
2 months HFD
2months HFD 3month SD
5 months HFD
Body Weight (g)
C
SD
HFD
SD
HFD
APP
WT
Cell Infiltration
Oil-O-Red
D
Total cells (x10^6)
CD45+ (x10^6)
B220+ (x10^6)
F4/80+ (x10^6)
CD4+ (x10^6)
CD8+ (x10^6)
E
TNFα mRNA fold changes
IL17 mRNA fold changes
IL6 mRNA fold changes

Figure A2. 2. HFD induces acute liver pathology and inflammation in APP-tg and WT C57BL/6 mice. (A**)** Representative images of livers from SD and HFD fed WT or APP-tg mice, with corresponding liver and body weights of their respective age matched SD fed controls (B). (C) Representative frozen tissue sections of livers from either SD or HFD fed APP-tg and WT mice after two months: images depict leukocyte infiltration into the liver parenchyma (left panels) after CD45 antibody staining (red) (arrows indicate sites of lymphocyte infiltration); right panels depict Oil-red-O staining of liver sections showing lipid droplets and lipid accumulation in HFD fed APP-tg compared to WT mice, and SD controls. (D) Quantitative analysis of total leukocyte numbers (CD45+ and CD45- populations) isolated from livers of 2 month SD or HFD fed WT and APP-tg mice by flow cytometry. (E) Pro-inflammatory cytokines (TNF-α, IL-6 and IL-17) mRNA expression in livers from 2 month SD or HFD fed APP-Tg and WT mice.

A2.2.C). We observed multifocal hepatitis and substantial steatosis in HFD fed WT and APP-Tg mice, whereas livers of SD fed mice were devoid of hepatitis or steatosis (Fig A2.2.C). Although livers of both HFD fed WT and APP-Tg mice showed marked lipid droplet deposition, WT mice exhibited larger pockets of fat deposits than APP-Tg mice (Fig A2.2.C). Analysis of inflammatory leukocyte subpopulations revealed increase in $CD4^+$, $CD8^+$, $B220^+$, and $F4/80^+$ cells in livers of both HFD fed WT and APP-Tg mice compared to their respective SD fed controls (Fig A2.2.D). We next determined whether NAFLD induced a systemic proinflammatory state in HFD mice. We performed gene expression analysis of proinflammatory cytokines from livers of HFD and SD App-Tg and WT mice using quatitative PCR (qPCR). We observed increased expression of TNF-alpha, IL-6 and IL-17 in both APP-Tg and WT mice on HFD compared to SD controls (Fig A2.2.E). These findings indicate that HFD-induced NAFLD caused an acute inflammatory state, in the absence of increased weight gain in HFD APP-Tg and WT mice that accelerated the process of AD in APP-Tg mice.

HFD induces neuroinflammation in both APP-Tg and WT mice in acute stage NAFLD.

Peripheral inflammation, that is, inflammation induced outside the CNS, has long been associated with inducing CNS inflammation leading to neurodegeneration [10, 32]. To determine whether NAFLD-induced inflammation (which initially starts in the liver) induces CNS inflammation in HFD fed mice, that may account for the accelerated plaque burden in APP-Tg mice (Fig A2.1), we performed cytokine gene

expression analysis on brains of HFD and SD fed WT and APP-Tg mice. We observed higher levels of TNF-alpha and IL-6 mRNA in brains of APP-Tg mice on HFD compared to SD controls (Fig A2..3.A). Interestingly, we observed a different inflammatory profile in the CNS of WT mice on HFD that expressed higher levels of IL-1beta and IL-17 mRNA in the CNS compared to SD controls (Fig A2. 3B). This indicates that peripheral inflammation has a significant effect on induction of CNS inflammation (Fig A2.3.B).

Toll-like receptors (TLRs), which are innate immune receptors that recognize microbial components called PAMPS (pathogen-associated molecular patterns) or endogenous ligands released by necrotic or injured cells called DAMPS (damage-associated molecular patterns) and have been recently described in CNS inflammation [33]. TLR association with specific DAMPs lead to receptor activation, which subsequently leads to initiation of an inflammatory cascade such as we observed in Fig A2. 3A and B. We investigated whether TLRs were altered in the CNS of APP-Tg or WT mice on HFD compared to controls during acute NAFLD. We focused on TLRs 1, 2 and 6 as these TLRs are known to recognize lipoproteins and glycolipids among others [34]. We observed significant upregulation of TLR 1, 2 and 6 in the brains of HFD fed WT and APP-Tg mice compared to SD controls (Fig A2.3.C). This confirms that HFD induced a potent inflammatory cascade inducing TLRs and culminating in secretion of proinflammatory mediators in the CNS.

Microgliosis is characterized by an increase in the number and accumulation of activated microglial cells around CNS lesions or during CNS injury and are believed to contribute to CNS pathology in models of neuroinflammation [35-36]. We found

that HFD fed WT and APP-Tg mice showed markedly pronounced staining for the activated microglial marker Iba-1, in areas surrounding the choroid plexus and (Fig A2.3.D). Interestingly, despite the absence of plaques in WT mice on HFD, these mice showed intense Iba-1 staining and increased microglial cell numbers, suggesting that the CNS of these mice are being primed for a neuroinflammatory or pathological event (Fig A2.3.D and E). Quite interestingly, Iba-1 staining was significantly reduced in mice that were removed from HFD after two months and put back on SD, indicating HFD-induced systemic inflammation is the major factor contributing to CNS inflammation and microglial activation (Fig A2.3D and E). We also observed Iba-1 staining in SD fed APP-Tg mice, albeit to a lesser extent (Fig A2.3.D and E), suggesting preexisting pro-nflammatory conditions in the CNS of these mice as was previously reported [37].

Figure A2.3.

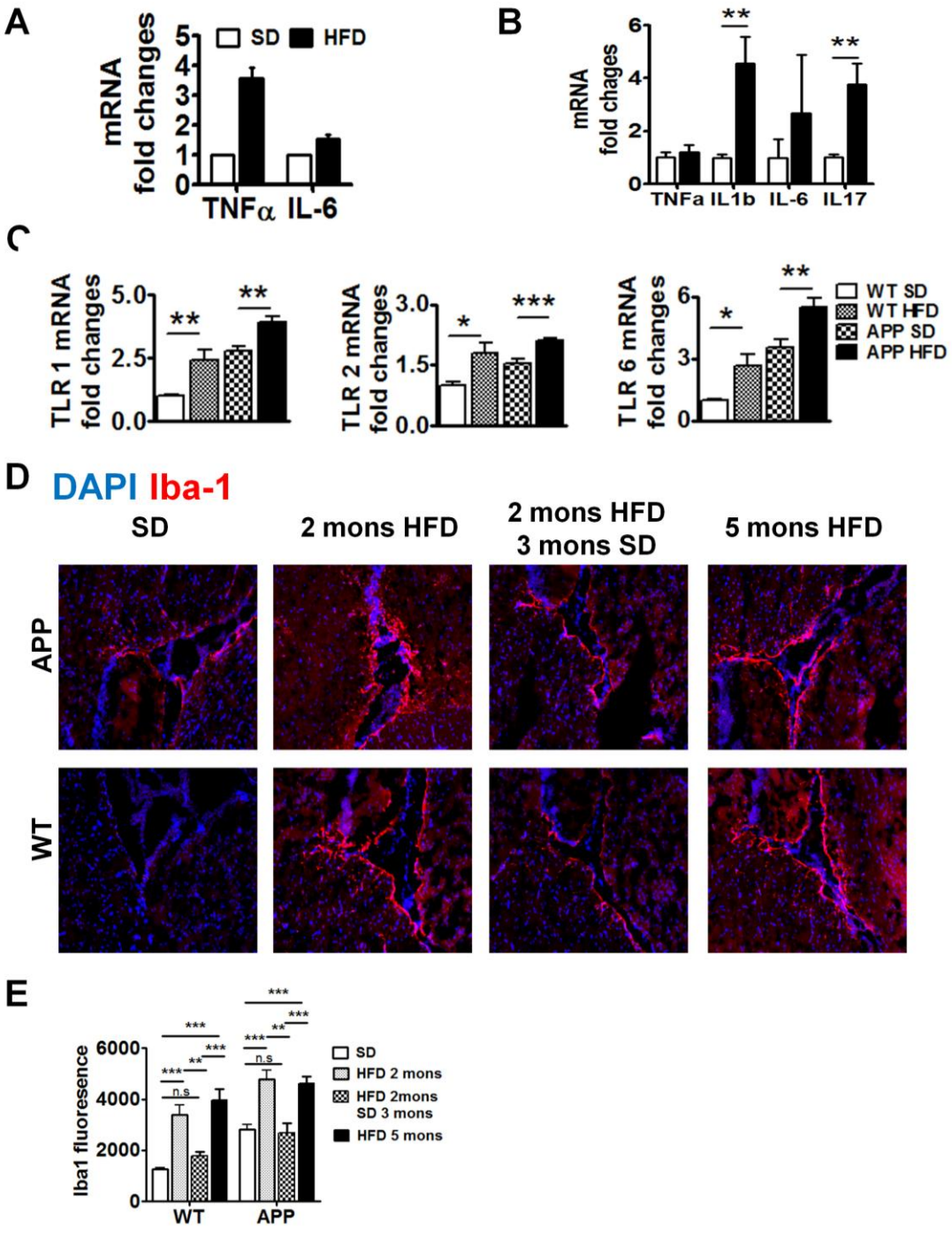
A
mRNA fold changes
SD
HFD
TNFα
IL-6
B
mRNA fold chages
TNFa
IL1b
IL-6
IL17
C
TLR 1 mRNA fold changes
TLR 2 mRNA fold changes
TLR 6 mRNA fold changes
WT SD
WT HFD
APP SD
APP HFD
D
DAPI Iba-1
SD
2 mons HFD
2 mons HFD 3 mons SD
5 mons HFD
APP
WT
E
Iba1 fluoresence
SD
HFD 2 mons
HFD 2mons SD 3 mons
HFD 5 mons
WT
APP

Figure A2. 3. Increased inflammation and microglial activation in brains of HFD fed mice. Pro-inflammatory cytokine mRNA expression in brains of APP-tg **(**A**)** and WT mice (B); brain mRNA expression of TLR1, TLR2 and TLR6 of APP-tg or WT mice after being on SD or HFD for two months (C). Representative immunofluorescent, Iba-1 stained brain images from APP-Tg and WT mice fed either SD or HFD for 2 or 5 months, or initially with HFD for 2 months and then put back on SD for 3 months (D) and quantification of Iba-1 expression intensity (E). Iba-1 expression (red) and DAPI nuclei staining (blue) near the choroid plexus.

Impact of HFD in chronic disease: NAFLD one year later caused advanced signs of AD in both WT and APP-Tg mice.

To mimic the life-long diet pattern in human, we kept APP-Tg and WT mice on HFD for up to one year to evaluate its impact on systemic as well as on brain inflammation and consequent AD pathogenesis. Because we observed accelerated plaque formation in APP-Tg mice at two and five months on HFD, that is comparable with the plaque loads and sizes seen in these mice around 18-24 months on SD, we anticipated an even greater plaque burden in APP-Tg mice on HFD after one year. Surprisingly, instead of increased plaques, we observed a significant decrease in overall plaque load in APP-Tg mice on HFD compared to those on SD (Fig A2.4.A). We hypothesized that the reduced plaque load may be a result of neuronal and/or glial cell death or due to increased plaque clearance by astrocytes, that can exert a protective response to fibrillar Aβ by removing/clearing it from the CNS [38]. We examined and enumerated Aβ plaque deposition in the entire brain (Fig A2.4.A and Supplementary Fig A2.2). We observed a dramatic reduction in both Aβ plaques in the midbrain, the hippocampus, the hypothalamus, the olfactory bulb and the cerebellum of HFD fed mice compared to mice on SD (Fig A2.4.A and Supplementary Fig A2.2). Moreover, when compared to SD fed aged APP-Tg mice (20 months old), APP-Tg mice on HFD for one year (and 14 months old) had significantly reduced astrocyte staining as shown in the hippocampus and is indicative of astrocyte loss (Fig A2. 4.B).

Figure A2.4.

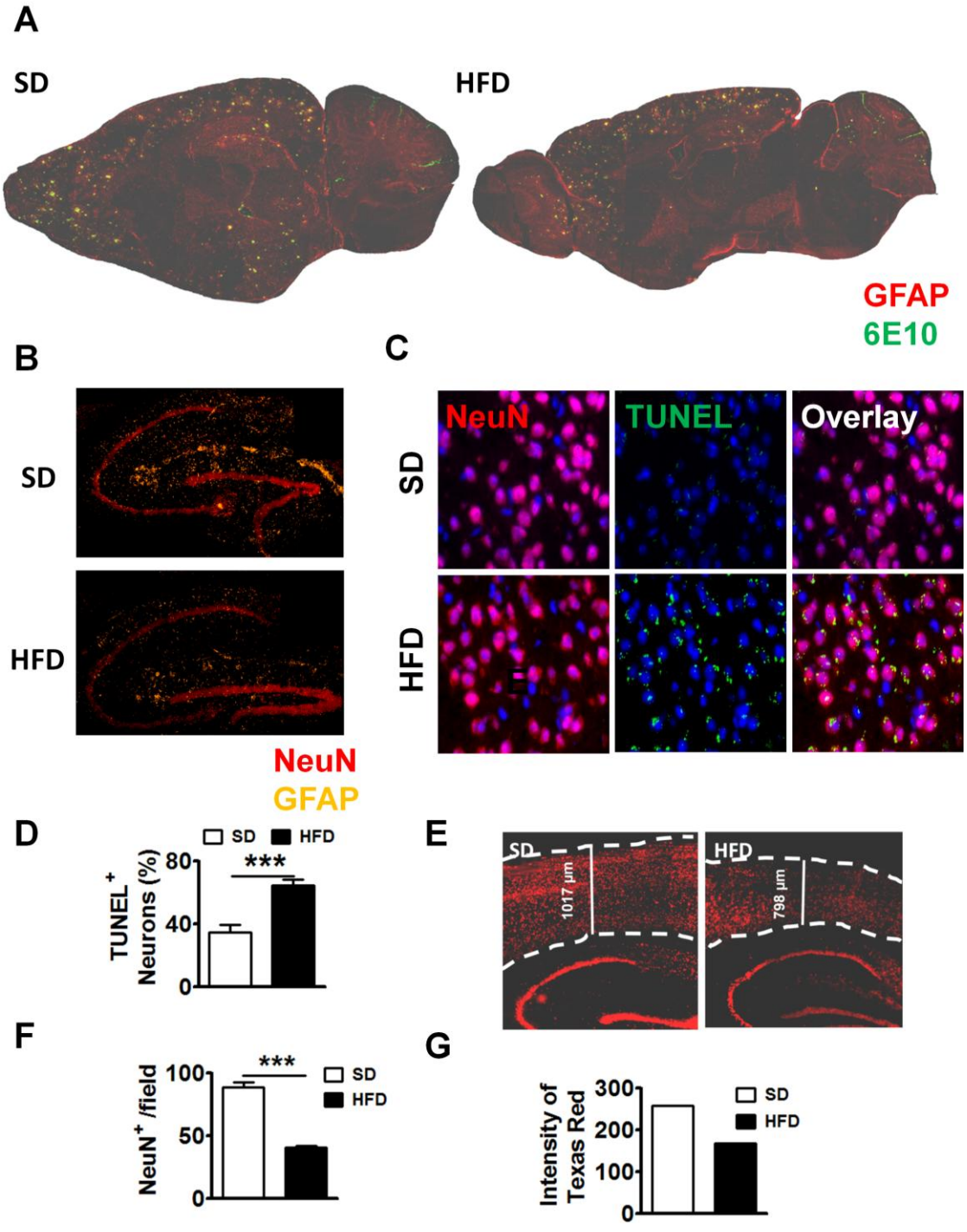
A
SD
HFD
GFAP
6E10
B
SD
HFD
NeuN
GFAP
C
NeuN
TUNEL
Overlay
SD
HFD
D
SD
HFD
***
TUNEL+ Neurons (%)
80
40
0
E
SD
HFD
1017 µm
798 µm
F
***
SD
HFD
NeuN+ /field
100
50
0
G
Intensity of Texas Red
300
200
100
0
SD
HFD

Figure A2.4. Long term HFD feeding (1 year) markedly decreased NeuN$^+$ cells, Aβ plaque load and astrocytes in brains of APP-tg mice. (**A**) Representative brain sections from 1 year SD or HFD fed APP-tg mice, stained with anti-6E10 anti-beta-amyloid antibody (green) or anti-GFAP (red) antibody showing Aβ plaque or astrocytes, respectively. (**B**) Immunofluorescence staining of representative frozen brain hippocampal sections from 1 year SD or HFD fed APP-tg mice, stained with anti-NeuN antibody that stain neurons (red), anti-GFAP antibody (gold), showing neuronal cells, astrocytes, respectively. Representative images (**C**) and quantitative analysis (**D**) of immunofluorescence in brain sections from SD or HFD fed APP-tg mice double stained with NeuN (red), or TUNEL (green) which is a marker for apoptosis. TUNEL/NeuN double positive cells were quantified as a percentage of total cell count. (**E**) Representative image of brain sections from SD or HFD fed APP-tg mice stained with anti-NeuN antibody (red). Dotted lines indicate the outline of NeuN positive signal of the mid brain. (**F**) Quantitative analysis of E, showing the number of NeuN positive cells from different fields of the brains from SD or HFD fed mice. (**G)** Quantitative analysis of E, showing intensity of NeuN positive signal in dentate gyrus of SD or HFD fed mice.

To determine whether the decreased plaque load in the CNS of APP-Tg mice was the result of neuronal death and consequently a decrease in Aβ production, thereby reducing plaque formation in HFD fed mice, we stained frozen brain sections with antibodies to TUNEL which stains DNA in dead or dying cells, and to NeuN which stains neurons. We observed higher incidence of TUNEL positive NeuN cells in HFD fed mice compared to SD fed APP-Tg mice (Fig A2.4.C and D). Further, enumeration of neuronal cells in the cortex showed they were significantly decreased in HFD APP-Tg mice compared to SD controls (Fig A2.4.E and F). Also, the thickness of the cortex was shrunken in HFD fed APP-Tg mice compared to SD controls. Moreover, the intensity of NeuN positive signal in the dentate gyrus was reduced in HFD fed APP-Tg mice compared to SD fed controls (Fig A2.4.E and G). Since astrocytes and neurons are major producers of Aβ, these findings suggest that reduction in neuronal cells and astrocytes may be responsible for the reduced plaque burden.

Figure A2.5.

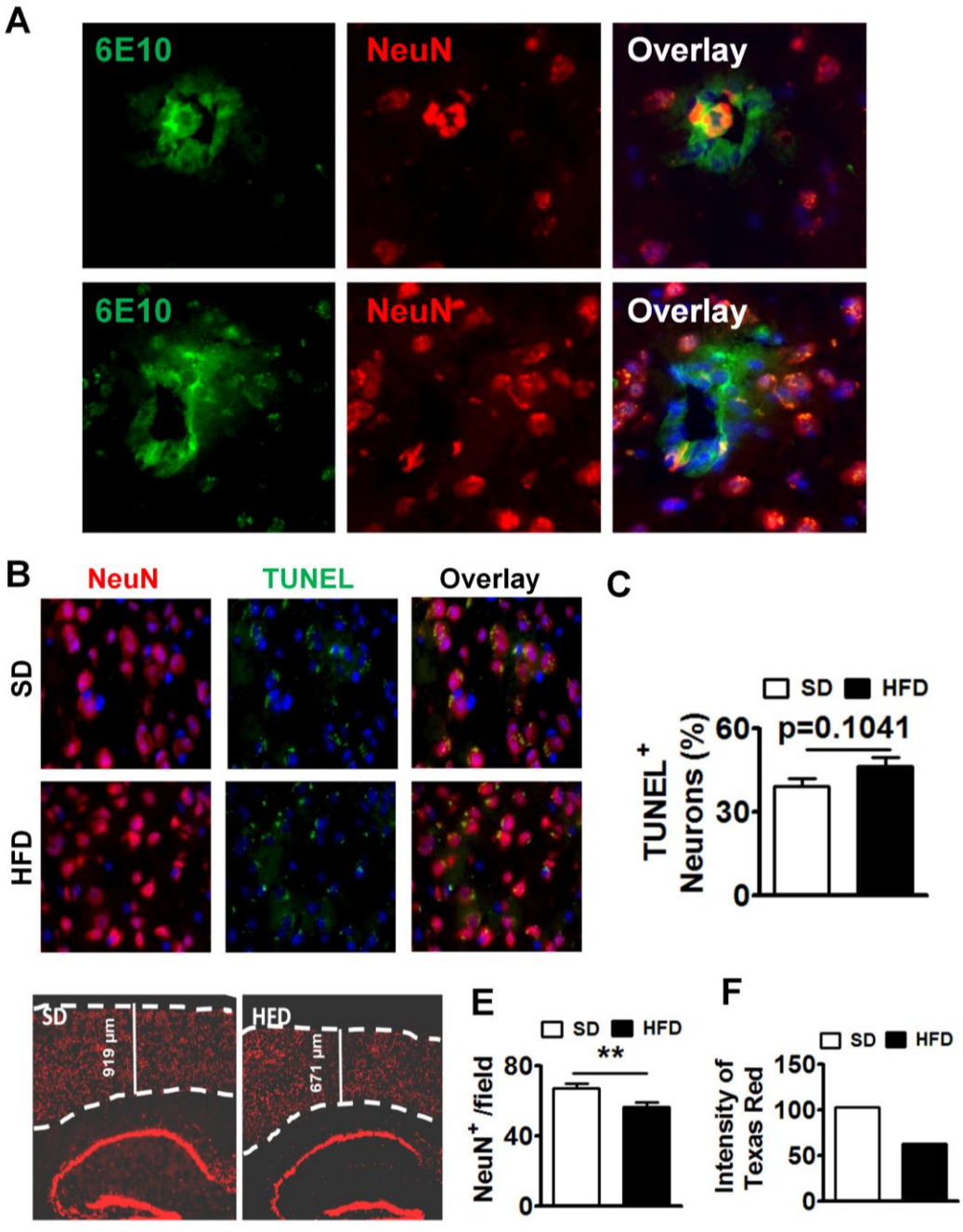
A
6E10
NeuN
Overlay
6E10
NeuN
Overlay
B
NeuN
TUNEL
Overlay
SD
HFD
C
SD
HFD
p=0.1041
TUNEL+ Neurons (%)
60
30
0
SD
HED
919 µm
671 µm
E
SD
HFD
**
NeuN+ /field
80
40
0
F
SD
HFD
Intensity of Texas Red
150
100
50
0

Figure A2.5. Long term HFD feeding (1 year) induced Aβ plaque formation in brains of WT mice and decreased NeuN$^+$ cells. (**A**) Representative images of brain sections from HFD or SD fed WT mice stained with anti-NeuN (red) and anti-6E10 (green), antibodies for neurons and Aβ plaque respectively. (**B**) Representative images of immunofluorescent stained brain sections from SD or HFD fed WT mice double stained with anti-NeuN (red) and TUNEL (green): double positive cells were quantified as a percentage of total cell count (**C**). (**D**) Representative image of Brain sections from SD or HFD fed WT mice stained with anti-NeuN antibody (red). Dotted lines indicate the margin of NeuN positive layer in the brain. (**E**) Quantitative analysis of D, showing numbers of NeuN positive cells from multiple fields of the brain from SD or HFD fed mice. (**F**) Quantitative analysis of D, capturing the intensity of NeuN positive signal in dentate gyrus from SD or HFD fed mice.

HFD induces AD plaques and neuronal cell loss in WT mice.

WT mice developed fulminant inflammation both in the periphery and in the CNS similar to and to some degree greater than APP-Tg mice in acute NAFLD (Fig A2.2 and 3). Brains of WT mice had increased numbers of activated microglial cells and high levels of proinflammatory mediators but no evidence of plaque induction during acute NAFLD. We examined brains of WT mice to determine whether aging, six months later, in the presence of HFD induced Aβ plaques. Indeed, we observed significant plaque burden in HFD fed WT mice compared to SD controls (Fig A2.5.A). This finding is significant, because it indicates, HFD-induced chronic inflammation, plus aging, is sufficient to induce signs of AD in mice lacking genetic predisposition to AD (Fig A2.5.A). To test whether WT mice also show increased neuronal apoptosis as was observed in APP-tg mice, we performed TUNEL/NeuN double staining. Similar to APP-Tg mice, we observed a higher incidence of TUNEL positive NeuN staining (not significant) in WT mice on HFD compared to SD (Fig A2.5.B and C). To test if HFD induced neuronal loss, we quantified the number of NeuN positive cells in different brain regions. Indeed, we observed statistically significant reduction of NeuN positive signal in the cortex of HFD fed WT mice compared to controls (Fig A2.5.D and E). Also, the intensity of NeuN positive signal in the dentate gyrus was reduced in HFD fed WT mice compared to SD controls (Fig A2.5.D and E). This suggests that long term HFD treatment in WT mice is sufficient to induce plaque formation and neuronal loss. Interestingly, we did not observe any decrease or reduction in astrocytes or Aβ plaque deposition in brains of WT mice on SD vs HFD as was observed in APP-Tg mice (Supplementary Fig A2. 3).

Long term high fat diet induces advanced signs of AD in WT and APP-Tg mice.

In addition to Aβ senile plaque deposits, aggregation of neurofibrillary tangles composed of hyperphosphorylated tau (pTau) is a prominent hallmark of advanced AD. Tau is the microtubule-associated protein (MAP) that is involved in the delivery of neurotransmitter signals through microtubule tracks in axons [39-40]. In its hyperphosphorylated state such as in AD, or Tauapathies, Tau is aggregated and unable to relay proper neurotransmission, leading to neuronal dysfunction [8-9, 41]. To test whether tauopathy is induced in APP-Tg mice one year after being on HFD, we stained the brains of HFD and SD control mice with an antibody that binds to pTau. We observed very intense pTau staining in the hipoccampus and cortex of APP-Tg mice but not in controls, indicating long-term HFD induced major advanced signs of neurodegeneration (Fig A2.6.A). We next determined whether WT mice on HFD also exhibit pTau staining. Indeed, similar to APP-Tg mice, WT mice exhibited intense pTau staining in the dentate gyrus that was not observed in SD fed mice (Fig A2.6.A). These findings strongly indicate that HFD induced major advanced signs of neurodegeneration, not only in animals predisposed to AD (APP-Tg mice) but was sufficient to induce them in WT mice as they age.

We next investigated whether Cerebral amyloid angiopathy (CAA), which is a sign of advanced AD that is characterized by accumulation of $A\beta_{1\text{-}40}$ in the brain vasculature and is believed to cause microinfarction leading to neurological dysfunction and neuronal death was induced by HFD [42-43]. Aβ deposition in cerebral vessels lowers the force of Aβ clearance, resulting in increased parenchymal

Figure A 2. 6.

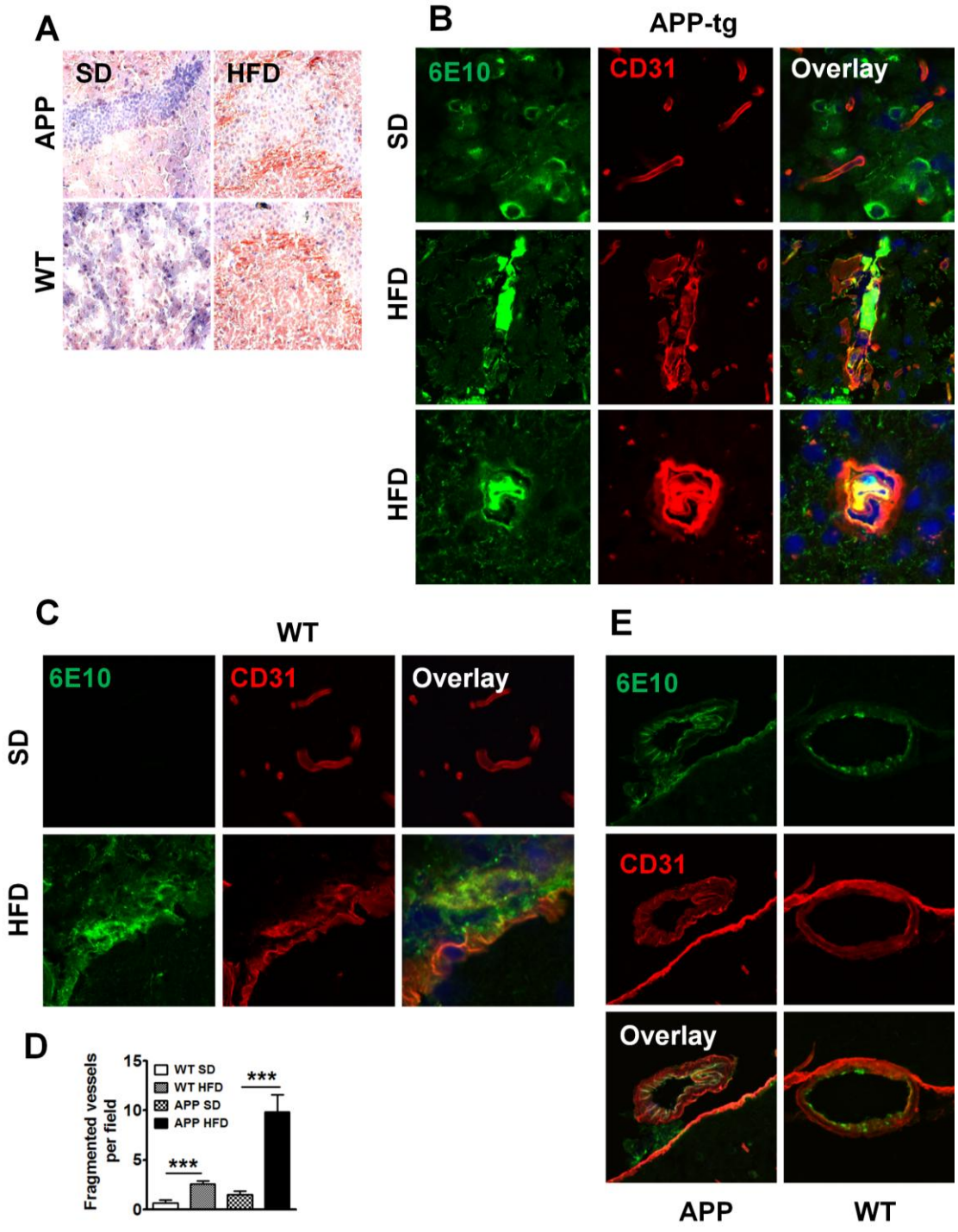
A
SD
HFD
APP
WT
B
APP-tg
6E10
CD31
Overlay
SD
HFD
HFD
C
WT
6E10
CD31
Overlay
SD
HFD
D
Fragmented vessels per field
15
10
5
0
WT SD
WT HFD
APP SD
APP HFD
***
***
E
6E10
CD31
Overlay
APP
WT

Figure A2.6. Long term HFD (1 year) induces advanced signs of AD in both APP-tg and WT mice. (**A**) Representative images of mouse hippocampal area, from SD or HFD fed (for 1 year) APP-Tg and WT mice stained with anti-phosphorylated-Tau (S396) antibody. (**B**) Representative brain sections from SD or HFD fed APP-Tg mice stained with anti-CD31 (red) and anti-beta amyloid antibody, 6E10 (green) to assess the degree of cerebral amyloid angiopathy (CAA) and vasculopathy; top three panels depict SD (controls), middle three panels show HFD induced CAA and bottom three panels depict double-barrell lumen of vessels in HFD fed APP-tg mice. (**C**) Representative brain images from WT mice double-stained with antibodies to beta-amyloid (6E10) and CD31 (vasculature) for SD (top three panels) or HFD (bottom three panels) to evaluate CAA. (**D**) Quantification of fragmented vessels taken over multiple microscopic fields throughout the brains of SD and HFD fed WT and APP-tg mice (10 field/mouse, N=3 mice/group). (**E**) Brains of WT or APP-tg mice were analyzed to determine the presence of leptomeningeal CAA (representative sections shown). .

Aβ build up. We examined brains of mice after double-staining with antibodies to Aβ and CD31 (marker for the endothelial vasculature). We observed intense and frequent signs of CAA, evidenced by Aβ accumulation in vessels of HFD fed APP-Tg and WT mice vasculature but not in SD controls (Fig A2.6.B). In addition, we observed vessel wall thickening, and double barreling of vessel lumen that is consistent with advanced and severe CAA (Fig A2.6.B). Throughout the brains of APP-Tg and WT mice, we observed what appears to be a high frequency of broken or fragmented vessels (Fig A2.6.C and D). Also, APP-Tg mice had a higher incidence of lepto-meningeal CAA deposition which is a more advanced form of CAA (Fig A2.6.E). These findings indicate that HFD can induce signs of advanced AD in WT mice and profoundly accelerate advance AD in HFD fed APP-Tg mice.

HFD decreased LRP1 and increased inflammatory profile in brains of WT and APP-Tg in chronic NAFLD

LRP1, is highly expressed in the liver, on neurons and on vascular smooth muscle and glial cells in the CNS and functions in the clearance and trafficking of Aβ from the CNS. However, studies show that LRP1 is also involved in Aβ production [44]. Thus, LRP1 involvement in Aβ synthesis and clearance makes it a prime target in AD pathogenesis. Deletion of LRP1 exacerbated Aβ deposition and increased CAA (Kanekiyo et al., 2012). We investigated whether LRP1 expression is altered in the CNS of HFD fed mice both at early (acute NAFLD, 2 months) and later-chronic NAFLD (after one year on HFD) compared to SD controls. We observed increased LRP1 expression in brains of HFD fed APP-Tg mice but not WT mice compared to

their respective SD controls (Fig A2.7.A). However, in chronic NAFLD, both HFD fed APP-Tg and WT mice expressed significantly lower levels of LRP1 in CNS tissue compared to SD controls (Fig A2.7.A). This decrease in LRP1 expression is consistent with the increased neurodegenerative changes observed in chronic disease and may reflect a protective role for LRP1 in AD [44].

ApoE is a known risk factor for AD. Its variant ApoE4 increases the risk of AD and accelerates AD onset (Bu, 2009; Liu et al., 2013). ApoE is a ligand for LRP1 and its main function is the cellular transfer of lipids through LRP1 on the cell surface. There is mixed evidence as to whether ApoE is involved in binding and/or clearance of Aβ [45]. It is speculated that ApoE may inhibit or facilitate LRP1 endocytosis of Aβ [46]. We therefore analyzed ApoE expression in both acute and chronic NAFLD and found no difference in ApoE expression in acute or chronic NAFLD in WT or APP-Tg (Fig A2.7.B). This indicates that ApoE expression/function remains relatively unchanged despite accelerated signs of neurodegeneration and neuronal loss. In contrast, LRP1 expression increased in acute/early phase of NAFLD in APP-Tg mice, but was unchanged in WT mice on HFD. LRP1 levels decreased significantly during chronic NAFLD in both APP-Tg mice and WT mice on HFD. This leaves us to speculate that decrease in LRP1 expression/function is linked to advanced signs of AD.

To determine whether systemic inflammation was maintained through the chronic phase of NAFLD, we examined the cytokine profiles of lymphocytes in peripheral lymphoid organs of APP-Tg mice after one year on SD or HFD. We observed increased TNF alpha, IL-6 and IL-17 in HFD fed APP-Tg mice compared to SD controls (Fig A2.7.C). Similarly, lymphocytes from HFD fed WT mice secreted

Figure A 2. 7.

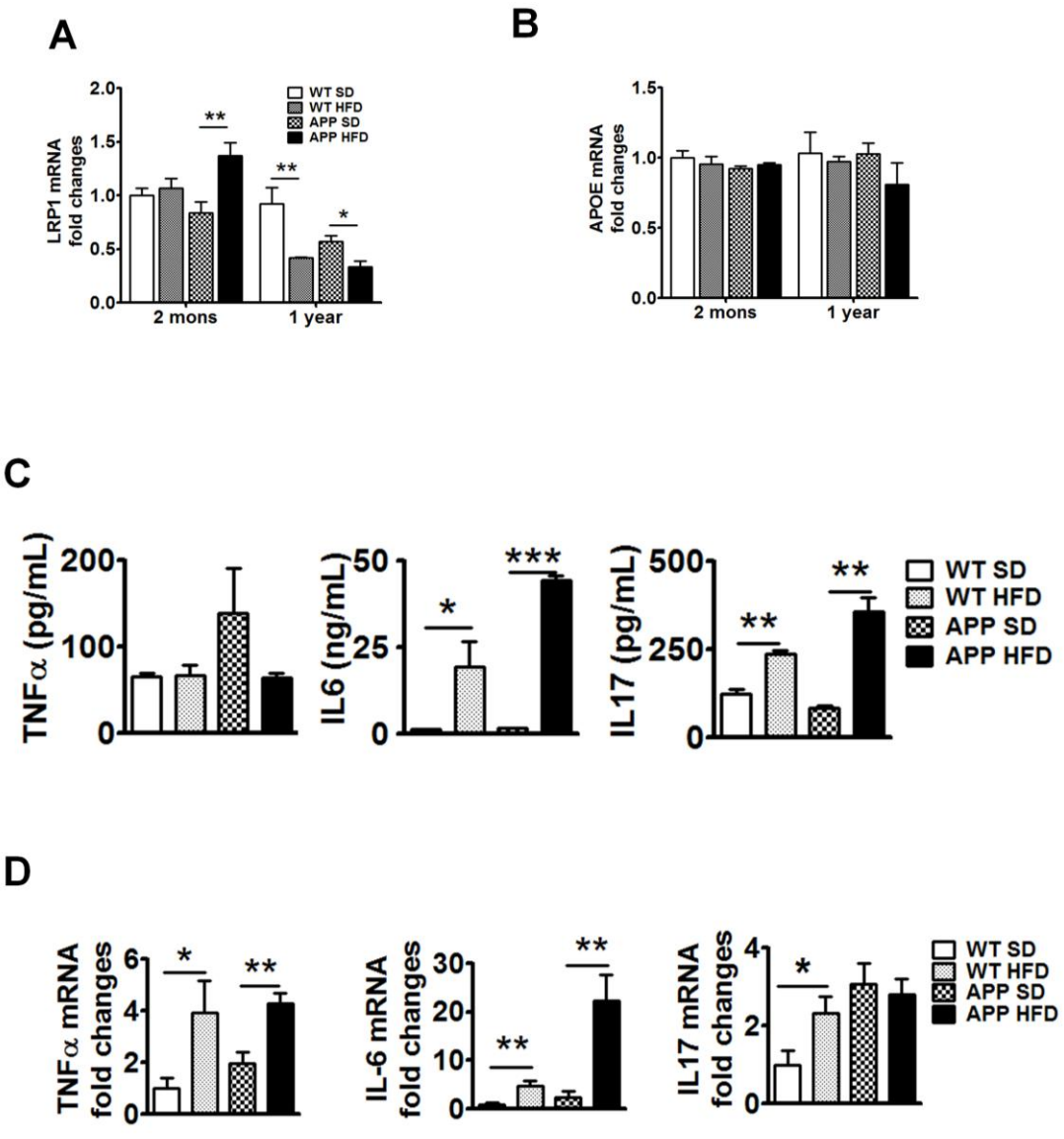
A
LRP1 mRNA fold changes
2.0
1.5
1.0
0.5
0.0
**
**
*
WT SD
WT HFD
APP SD
APP HFD
2 mons
1 year
B
APOE mRNA fold changes
1.5
1.0
0.5
0.0
2 mons
1 year
C
TNFα (pg/mL)
200
100
0
IL6 (ng/mL)
50
25
0
*
***
IL17 (pg/mL)
500
250
0
**
**
WT SD
WT HFD
APP SD
APP HFD
D
TNFα mRNA fold changes
6
4
2
0
*
**
IL-6 mRNA fold changes
30
20
10
0
**
**
IL17 mRNA fold changes
4
2
0
*
WT SD
WT HFD
APP SD
APP HFD

Figure A2. 7. Long term HFD treatment (1 year) decreased brain LRP1 and maintains a chronic inflammatory state in brains of WT and APP-Tg in chronic NAFLD. mRNA expression of LRP1 (A) or APOE (B) were analyzed in brains of SD or HFD fed (2 months or 1 year) mice by quantitative real-time PCR (n=2 experiments). (C) Splenocytes from 1 year SD or HFD fed mice were stimulated with PMA-ionomycin for 3 days, supernatants were collected and pro-inflammatory cytokines (TNF-α, IL-6, IL-17) were quantified by ELISA. (D) mRNA expression level of pro-inflammatory cytokines (TNF-α, IL-6, IL17) were analyzed in brains from mice on HFD or SD for 1 year by quantitative real-time PCR (n=2 experiments).

high levels of the pro-inflammatory cytokines TNF-a, IL-6 and IL-17 compared to their SD counterparts (Fig A2.7.C). To determine whether this chronic HFD induced systemic inflammatory profile is consistent with CNS inflammatory profile, we performed quantitative RT-PCR of these cytokines on brain samples. Indeed, we observed that these cytokines were highly upregualted in brains of HFD fed APP-Tg mice and WT mice compared to their SD counterparts (Fig A2.7.D). Together, these results suggest that augmented systemic immune responses induced by HFD have a sustained impact on increased brain inflammatory response and profoundly impact neurodegeneration (Fig A2.7.D).

A2.5. Discussion

In this study, we demonstrate that a modest increase in dietary lipids fed to WT or APP-Tg mice induced, first, acute inflammation of the liver, followed by a chronic inflammatory state.. This HFD-induced acute inflammation, was characterized by invasion of inflammatory immune cells into the liver parenchyma, and production of increased levels of proinflammatory cytokines by immune cells locally (liver) and systemically (lymphoid organs). Concomitant with this increased peripheral inflammatory state, we observed profound acceleration in neurodegenerative signs and increased neuroinflammation in APP-Tg mice compared to mice that remained on SD. We observed acceleration in beta-amyloid plaque formation leading to higher plaque loads, larger plaque size, and increased microgliosis and astroglyosis in APP-Tg mice. In AD patients' brain, activated microglial cells were observed around plaques and were initially thought to be a clearance mechanism to remove Aβ plaques from the CNS. However, it turned out that these activated microglial cells did not reduce plaque burden [37], but instead they induced neuronal damage. In our study, APP-Tg mice on SD exhibit activated microglial cell accumulation in the midbrain that is consistent with previous report of a proinflammatory state in these mice. Compared to SD fed mice, microglial cell accumulation were about 4-fold increased in HFD fed mice, and this correlated with increased pro-inflammatory cytokine expression in HFD fed mice. This increase in both CNS and peripheral inflammation is reversed when mice are removed from HFD and put back on SD: we observed decreased activated microglial cell numbers, decreased liver pathology and CNS proinflammatory cytokines. This

reversal in inflammation was consistent with reduced Aβ plaque burden. This indicates that the accelerated signs of AD observed in APP-Tg mice were directly linked to induction of NAFLD in the liver.

Interestingly, WT mice on HFD exhibit similar increase in activated microglial cells accumulation even though they did not exhibit signs of Aβ plaque deposition at two or five months on HFD. WT mice on HFD exhibited more pronounced hepatitis and lipid deposits in liver cells than APP-Tg mice but they did not develop signs of AD in the acute phase of NAFLD. HFD fed WT mice showed increased proinflammatory cytokine gene expression (TNF-alpha, Il-6 and IL-17) in liver and in peripheral lymphoid organs, and liver pathology was more pronounced in WT mice, with higher immune cell infiltration in the liver parenchyma. Both IL-6 and Il-17 proinflammatory cytokines were highly pronounced in WT mice but were almost absent in SD controls. Il-6 and Il-17 play pathogenic roles in the neuroinflammatory disease, multiple sclerosis. The profound increase in these cytokine gene expression levels strictly coincides with increased activated microglial cells in the CNS, potentially setting the stage for the neurodegeneration we observed in WT mice on HFD one year later. Moreover, when WT mice were removed from HFD diet and placed on SD, inflammation ceased, liver pathology was reverted, and activated microglial cells were absent. Of interest, was the absence of plaques in these WT mice despite showing all other signs of inflammation observed in APP-Tg mice. This indicates that HFD-induced systemic inflammation was primed the CNS for the neurodegeneration which we later observed. These studies suggest that AD can be induced and driven by acute-chronic systemic inflammation in individuals that are not

otherwise genetically predisposed. It also indicates that early intervention can reverse the process.

Brains of APP-Tg mice on long term HFD had significantly less plaques compared to SD fed mice. APP-Tg mice showed dramatic decrease in Aβ plaques in the hippocampus, the olfactory bulb, and mid brain. Also striking was the absence of astrocytic tracks in brain areas where Aβ plaques were absent or diminished such as the hippocampus and midbrain. Moreover, we observed neuronal loss and increased apoptotic neurons in hippocampus and mid brain. This was not the case for older mice (15-24 months) on SD, indicating that aging alone is not responsible for the loss of astrocytes. As discussed above, removal from HFD reduced plaque load and decreased inflammatory signals. Thus, astrocytic loss may be a result of accelerated AD pathology resulting in CNS toxicity leading to astrocyte death. Astrocyte death can lead to neuronal neglect and subsequent death because of the critical role they play in neuronal function [38]. Increased neuronal death may also explain the decreased plaque load in chronic AD due to decreased APP production. Based on these studies we conclude that inflammation induced outside the CNS (in the liver) is sufficient to induce AD in the absence of predisposing genetic factors.

Signs of CAA and hyperphosphorylated tau (pTau) expression are representative of advanced AD. pTauu aggregates and is unable to signal proper neurotransmission, leading to neuronal dysfunction; and CAA results in a lack of Aβ clearance from the CNS. We observed strong expression of pTau and evidence of CAA in both WT and APP-Tg mice on HFD but not in SD controls. pTau was expressed as strongly in WT as in APP-Tg mice, even though Aβ was induced much

later in WT mice. Thus, if CAA and tauapathy represents advanced AD, one may argue that AD accelerated more dramatically in WT mice than APP-Tg mice, and it may be regulated differently in genetically predisposed (APP-Tg) versus non-predisposed individuals (WT). CAA involves deposition of amyloid in cerebral vasculature and is a hallmark of advanced AD resulting in pathological changes in cerebral blood vessels referred to as vasculopathies. Signs of CAA were more extensive in APP-Tg mice compared to WT mice on HFD. We observed vessel wall thickening and a high number of CNS vessels exhibit doube-barrel lumen (Ref). One of the most striking observations was the increase appearance of fragmented or broken vessels in APP-Tg mice but not in WT mice on HFD and not in SD controls. This clearly indicates that HFD-induced inflammation can result in massive CNS destruction and pathology over a life time.

Low-density lipoprotein receptor-1 (LRP1) is involved in a number of pathways linked to AD pathogenesis and has multiple functions. It is most highly expressed in brain, liver and lungs. In the brain, it is highly expressed in glial cells, neurons and cells of the cerebral vasculature. LRP1 can directly regulate gene expression through its intracellular domain and it regulates the endocytosis of many diverse ligands including ApoE, APP and Aβ. LRP1 appears to have bimodal opposing functions linked to AD pathogenesis. It is involved in Aβ clearance and Aβ production. It mediates Aβ clearance by cellular uptake followed by lysosomal degradation and/or transcytosis of intact Aβ across the BBB to the circulation and consequent peripheral clearance [46]. We observed increased LRP1 expression in APP-Tg mice on HFD, but not in WT mice, during the acute phase of NAFLD.

Increased LRP1 expression may represent its increased function in clearance of Aβ from the CNS in APP-Tg mice during accelerated Aβ production. Maybe the reason LRP1 did not increase in WT mice on HFD is due to the absence of Aβ in the CNS of these mice during acute NAFLD. However, during chronic NAFLD, we then observed a significant decrease in LRP1 in CNS of both APP-Tg and WT mice on HFD. This decrease coincides with advanced signs of AD, including reduced Aβ plaque load, reduced number of neurons and astrocytes and increased vascular destruction, suggesting that LRP1 plays a protective role in AD. It is possible that the reduction in LRP1 expression during chronic NAFLD may be a result of glial and neuronal cell loss and vascular destruction, as these cells abundantly express LRP1. Alternatively, advanced AD may have rendered LRP1 defective in clearing Aβ from the CNS.

It is interesting that no change in ApoE expression was observed during acute or chronic stages of NAFLD, despite significant neuronal and glial cell loss. The major function of ApoE is to transport cholesterol and other lipids in plasma and brain through a variety of cell surface receptors including LRP1. Astrocytes are the main source of ApoE. Since cholesterol is a critical component of glial and neuronal cell membrane including myelin sheath, it is possible that destruction of astrocytes resulted in limited cholesterol production needed for membrane synthesis and CNS repair. However, this is unlikely since such a reduction may have resulted in decreased ApoE. Other likely scenarios for no change in ApoE include its function in cholesterol trafficking was unhindered, whereas its function in Aβ trafficking was defective, or that the reduced plaque burden in chronic NAFLD is the result of increased Aβ trafficking by ApoE. Obviously, the involvement of Aβ, LRP1 and ApoE in

neurodegeneration and AD pathogenesis is quite complex and needs further investigation beyond these studies.

Our studies address a growing problem in our society that relates to metabolic syndromes due to diets high in fat/lipid consumption and its impact in neurodegeneration. NAFLD is prevalent in as much as a third of the world's population. Similarly, AD frequency is rapidly growing. We showed that a modest increase in dietary lipid content caused increased systemic inflammation followed by increased neuroinflammation and accelerated AD signs in APP-Tg mice. More importantly, we showed that WT mice become susceptible to developing AD after long term HFD intake and developed advanced signs of AD. Moreover, APP-Tg mice on HFD exhibit irreversible CNS damage stemming from the effects of chronic HFD. These findings highlight a growing problem in our society whereby consumption of foods high in lipids over a life time can have detrimental consequences such as accelerating AD in potentially susceptible individuals or inducing it in those that are not susceptible. An important and critical finding of these studies is that change from HFD to SD, before irreversible CNS damage sets in, completely reversed signs of AD. This suggest, that life style changes such as reducing one's lipid/fat intake can have profound impact on disease outcome. We strongly believe this study will benefit millions of people who are in danger of developing AD or people currently suffering from early signs of AD or dementia. Future studies hinges on elucidating the fine changes conferred upon neuronal function resulting in their loss or dysfunction and defining the cerebral vasculopathies resulting from these events.

References

1. Serrano-Pozo, A., et al., *Neuropathological alterations in Alzheimer disease.* Cold Spring Harb Perspect Med, 2011. **1**(1): p. a006189.
2. Thies, W. and L. Bleiler, *2013 Alzheimer's disease facts and figures.* Alzheimers Dement, 2013. **9**(2): p. 208-45.
3. Saura, C.A., E. Servian-Morilla, and F.G. Scholl, *Presenilin/gamma-secretase regulates neurexin processing at synapses.* PLoS One, 2011. **6**(4): p. e19430.
4. Koedam, E.L., et al., *Early-versus late-onset Alzheimer's disease: more than age alone.* J Alzheimers Dis, 2010. **19**(4): p. 1401-8.
5. Moreno-Grau, S., et al., *Evaluation of Candidate Genes Related to Neuronal Apoptosis in Late-Onset Alzheimer's Disease.* J Alzheimers Dis, 2015.
6. Benilova, I., E. Karran, and B. De Strooper, *The toxic Abeta oligomer and Alzheimer's disease: an emperor in need of clothes.* Nat Neurosci, 2012. **15**(3): p. 349-57.
7. Suh, J., et al., *ADAM10 missense mutations potentiate beta-amyloid accumulation by impairing prodomain chaperone function.* Neuron, 2013. **80**(2): p. 385-401.
8. Iba, M., et al., *Synthetic tau fibrils mediate transmission of neurofibrillary tangles in a transgenic mouse model of Alzheimer's-like tauopathy.* J Neurosci, 2013. **33**(3): p. 1024-37.
9. Roberson, E.D., et al., *Reducing endogenous tau ameliorates amyloid beta-induced deficits in an Alzheimer's disease mouse model.* Science, 2007. **316**(5825): p. 750-4.

10. Ghareeb, D.A., et al., *Non-alcoholic fatty liver induces insulin resistance and metabolic disorders with development of brain damage and dysfunction.* Metab Brain Dis, 2011. **26**(4): p. 253-67.

11. Tojima, H., et al., *Hepatocyte growth factor overexpression ameliorates liver inflammation and fibrosis in a mouse model of nonalcoholic steatohepatitis.* Hepatol Int, 2011.

12. Daugherity, E.K., et al., *The DNA damage checkpoint protein ATM promotes hepatocellular apoptosis and fibrosis in a mouse model of non-alcoholic fatty liver disease.* Cell Cycle, 2012. **11**(10): p. 1918-28.

13. Zeb, I., et al., *Relation of nonalcoholic fatty liver disease to the metabolic syndrome: the Multi-Ethnic Study of Atherosclerosis.* J Cardiovasc Comput Tomogr, 2013. **7**(5): p. 311-8.

14. Kahn, B.B. and J.S. Flier, *Obesity and insulin resistance.* J Clin Invest, 2000. **106**(4): p. 473-81.

15. Starley, B.Q., C.J. Calcagno, and S.A. Harrison, *Nonalcoholic fatty liver disease and hepatocellular carcinoma: a weighty connection.* Hepatology, 2010. **51**(5): p. 1820-32.

16. Egan, C.E., et al., *CCR2 and CD44 promote inflammatory cell recruitment during fatty liver formation in a lithogenic diet fed mouse model.* PLoS One, 2013. **8**(6): p. e65247.

17. Than, N.N. and P.N. Newsome, *A concise review of non-alcoholic fatty liver disease.* Atherosclerosis, 2015. **239**(1): p. 192-202.

18. Harmon, R.C., D.G. Tiniakos, and C.K. Argo, *Inflammation in nonalcoholic steatohepatitis.* Expert Rev Gastroenterol Hepatol, 2011. **5**(2): p. 189-200.

19. Vance, J.E., *Dysregulation of cholesterol balance in the brain: contribution to neurodegenerative diseases.* Dis Model Mech, 2012. **5**(6): p. 746-55.

20. Chen, X., et al., *Altered Cholesterol Intracellular Trafficking and the Development of Pathological Hallmarks of Sporadic AD.* J Parkinsons Dis Alzheimers Dis, 2014. **1**(1).

21. Puglielli, L., R.E. Tanzi, and D.M. Kovacs, *Alzheimer's disease: the cholesterol connection.* Nat Neurosci, 2003. **6**(4): p. 345-51.

22. Canevari, L. and J.B. Clark, *Alzheimer's disease and cholesterol: the fat connection.* Neurochem Res, 2007. **32**(4-5): p. 739-50.

23. Mahley, R.W. and S.C. Rall, Jr., *Apolipoprotein E: far more than a lipid transport protein.* Annu Rev Genomics Hum Genet, 2000. **1**: p. 507-37.

24. Proitsi, P., et al., *Plasma lipidomics analysis finds long chain cholesteryl esters to be associated with Alzheimer's disease.* Transl Psychiatry, 2015. **5**: p. e494.

25. Shepardson, N.E., G.M. Shankar, and D.J. Selkoe, *Cholesterol level and statin use in Alzheimer disease: I. Review of epidemiological and preclinical studies.* Arch Neurol, 2011. **68**(10): p. 1239-44.

26. Shepardson, N.E., G.M. Shankar, and D.J. Selkoe, *Cholesterol level and statin use in Alzheimer disease: II. Review of human trials and recommendations.* Arch Neurol, 2011. **68**(11): p. 1385-92.

27. Kanekiyo, T., et al., *Neuronal clearance of amyloid-beta by endocytic receptor LRP1.* J Neurosci, 2013. **33**(49): p. 19276-83.

28. Kanekiyo, T., et al., *LRP1 in brain vascular smooth muscle cells mediates local clearance of Alzheimer's amyloid-beta.* J Neurosci, 2012. **32**(46): p. 16458-65.

29. Jankowsky, J.L., et al., *Mutant presenilins specifically elevate the levels of the 42 residue beta-amyloid peptide in vivo: evidence for augmentation of a 42-specific gamma secretase.* Hum Mol Genet, 2004. **13**(2): p. 159-70.

30. Azizi, G. and A. Mirshafiey, *The potential role of proinflammatory and antiinflammatory cytokines in Alzheimer disease pathogenesis.* Immunopharmacol Immunotoxicol, 2012. **34**(6): p. 881-95.

31. Holmes, C., et al., *Proinflammatory cytokines, sickness behavior, and Alzheimer disease.* Neurology, 2011. **77**(3): p. 212-8.

32. D'Mello, C. and M.G. Swain, *Liver-brain inflammation axis.* Am J Physiol Gastrointest Liver Physiol, 2011. **301**(5): p. G749-61.

33. Paschon, V., et al., *Interplay Between Exosomes, microRNAs and Toll-Like Receptors in Brain Disorders.* Mol Neurobiol, 2015.

34. De Nardo, D., *Toll-like receptors: Activation, signalling and transcriptional modulation.* Cytokine, 2015.

35. de Kloet, A.D., et al., *Obesity induces neuroinflammation mediated by altered expression of the renin-angiotensin system in mouse forebrain nuclei.* Physiol Behav, 2014.

36. Tucsek, Z., et al., *Obesity in aging exacerbates blood-brain barrier disruption, neuroinflammation, and oxidative stress in the mouse hippocampus: effects on*

expression of genes involved in Beta-amyloid generation and Alzheimer's disease. J Gerontol A Biol Sci Med Sci, 2014. **69**(10): p. 1212-26.

37. Simard, A.R., et al., *Bone marrow-derived microglia play a critical role in restricting senile plaque formation in Alzheimer's disease.* Neuron, 2006. **49**(4): p. 489-502.

38. Wegiel, J., et al., *The role of microglial cells and astrocytes in fibrillar plaque evolution in transgenic APP(SW) mice.* Neurobiol Aging, 2001. **22**(1): p. 49-61.

39. Spillantini, M.G. and M. Goedert, *Tau pathology and neurodegeneration.* Lancet Neurol, 2013. **12**(6): p. 609-22.

40. Ballatore, C., V.M. Lee, and J.Q. Trojanowski, *Tau-mediated neurodegeneration in Alzheimer's disease and related disorders.* Nat Rev Neurosci, 2007. **8**(9): p. 663-72.

41. Winton, M.J., et al., *Intraneuronal APP, not free Abeta peptides in 3xTg-AD mice: implications for tau versus Abeta-mediated Alzheimer neurodegeneration.* J Neurosci, 2011. **31**(21): p. 7691-9.

42. Fryer, J.D., et al., *Apolipoprotein E markedly facilitates age-dependent cerebral amyloid angiopathy and spontaneous hemorrhage in amyloid precursor protein transgenic mice.* J Neurosci, 2003. **23**(21): p. 7889-96.

43. Thal, D.R., et al., *Capillary cerebral amyloid angiopathy is associated with vessel occlusion and cerebral blood flow disturbances.* Neurobiol Aging, 2009. **30**(12): p. 1936-48.

44. Goto, J.J. and R.E. Tanzi, *The role of the low-density lipoprotein receptor-related protein (LRP1) in Alzheimer's A beta generation: development of a cell-based model system.* J Mol Neurosci, 2002. **19**(1-2): p. 37-41.

45. Poirier, J., et al., *Apolipoprotein E and lipid homeostasis in the etiology and treatment of sporadic Alzheimer's disease.* Neurobiol Aging, 2014. **35 Suppl 2**: p. S3-10.

46. Martiskainen, H., et al., *Targeting ApoE4/ApoE receptor LRP1 in Alzheimer's disease.* Expert Opin Ther Targets, 2013. **17**(7): p. 781-94.

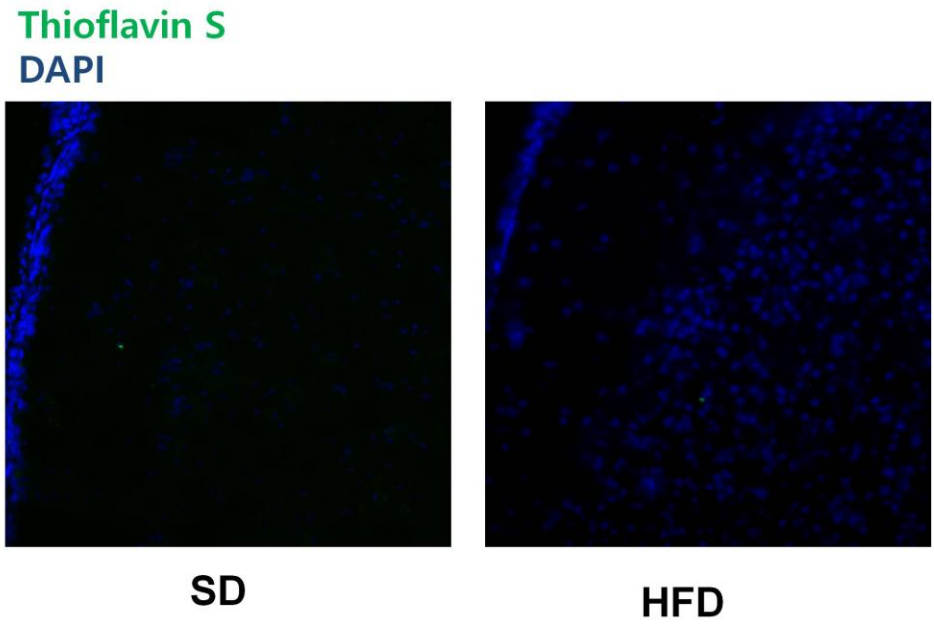

Supplementary Figure A2.1. Thioflavin S staining of brain section from WT mice fed with SD and HFD for five months. Brain sections from SD and HFD fed WT mice stained with thioflavin S (Green). Sections were counter stained with DAPI to visualize nucleus.

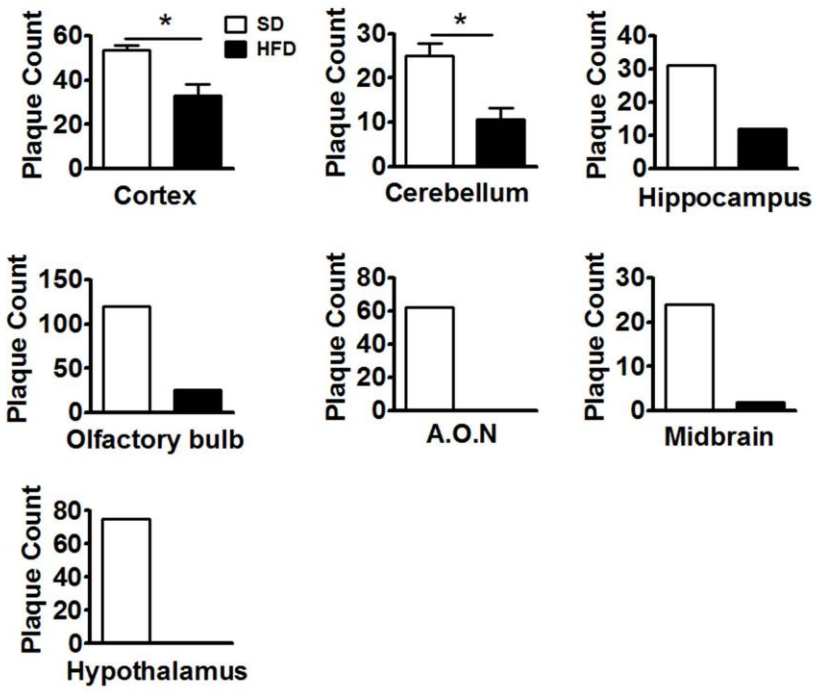

Supplementary Figure A2.2. Quantification of the Aβ plaques from different area of the brain sections of SD and HFD fed APP-Tg mice (1 year) from Figure A2.4.A.

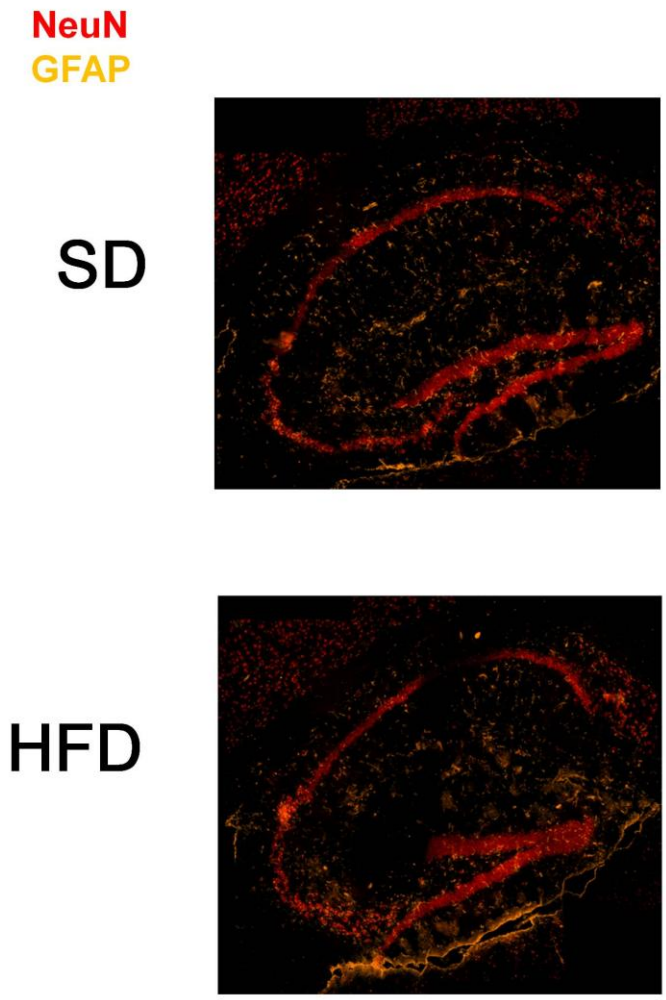

Supplementary Figure 3. Long term (1 year) HFD intake induces loss of astrocytes and neuronal cells in the hippocampal area of WT mice. Immunofluorescence staining of representative frozen brain hippocampal sections from 1 year SD or HFD fed WT mice. Brain sections were stained with anti-NeuN (Red), GFAP (Gold), DAPI (Blue) showing neuronal cells, astrocytes, nuclei, respectively.